

Preface

First of all, I want to thank Hasselt University and KULeuven for giving me the opportunity to do my dissertation. Throughout the entire education, I have learned the all necessary skills to help me bring this project to a successful conclusion.

I would also want to thank MidSim and the University of Wolverhampton for giving me the opportunity to participate in the Erasmus project. All fellow researcher of both MidSim and Cel Kunststoffen, with whom I came in contact, were all very helpful. This Erasmus study has really been a great learning experience both professionally and personally.

I especially would like to thank my promoters Mr. Van Bael, Mr. Spence and Mr. Emekwuru for their support and expert knowledge and who I could always ask for advice and information.

Finally, I would like to thank Mrs. Raymaekers for helping me to apply for this Erasmus study and all my friends and family for the support and advice they have given me.

Table of Contents

List of tables	7
List of figures	9
Abstract	11
Abstract in Dutch	13
1 Introduction	15
1.1 Background	15
1.2 The premise	16
1.3 Objectives	16
1.4 Materials and methods	17
2 Review of the literature	19
2.1 Process intensification	19
2.1.1 What is process intensification?	19
2.1.2 Design possibilities	19
2.1.3 Process intensification with the use of polymers	20
2.2 Diffusion bonding of metals	21
2.2.1 Mechanism behind diffusion bonding	21
2.2.2 Solid-state diffusion bonding	21
2.2.3 Liquid-state diffusion bonding	22
2.2.4 Surface cleanliness	23
2.2.5 Diffusion bonding with superplastic forming (SPF/DB).....	23
2.2.5.1 Superplasticity	24
2.2.5.2 Stop-off.....	24
2.2.5.3 Combining diffusion bonding with superplastic forming.....	24
2.3 Diffusion bonding of polymers	26
2.3.1 Issues	26
2.3.2 Possible solutions	26
2.4 Other possible bonding techniques for polymers	28
2.4.1 Solvent bonding.....	28

2.4.1.1	Mechanism behind solvent bonding.....	28
2.4.1.2	Issues	28
2.4.2	Adhesive bonding.....	29
2.4.2.1	Mechanism of adhesive bonding.....	29
2.4.2.2	Issues and possible solutions	29
Channel clogging.....	29	
Wettability.....	31	
Introduction of a different material	31	
2.5	Materials	32
2.5.1	Thermoplastic – thermoset – elastomer?.....	32
2.5.2	Which thermoplastic polymer to choose?.....	32
2.5.3	Diffusion bonding parameters.....	33
2.5.3.1	Polymethylmethacrylate	33
2.5.3.2	Cyclic olefin copolymer.....	34
2.5.3.3	Polystyrene.....	35
2.5.3.4	Polycarbonate.....	35
2.5.4	Choice of material with its bonding parameters	35
3	Methodology	37
3.1	Base material	37
3.1.1	Material properties according to the manufacturers specification	37
3.2	Size and geometry of the test samples	37
3.3	The bonding process	38
3.3.1	Heat source	39
3.3.2	Applying pressure	39
3.3.3	Time	40
3.4	Strength test	41
3.4.1	General setup.....	41
3.4.2	Machine parameters.....	42
3.5	Preliminary tests	43
3.5.1	Fine-tune test setup	43
3.5.2	Determination of the rough bonding parameters.....	45
3.6	Bonding tests	47

3.6.1	Control test.....	47
3.6.2	Bonding parameters.....	48
3.6.3	Modelling the strength test.....	49
3.6.3.1	The model.....	49
3.7	The effect of post-annealing	51
3.7.1	Test setup and parameters.....	51
3.8	The effect of polishing	53
3.9	Creating a cellular structure	54
3.9.1	Substances.....	54
3.9.1.1	Stop-off 1: chalk powder.....	54
3.9.1.2	Stop-off 2: silicone spray.....	54
3.9.1.3	Stop-off 3: surface roughening.....	55
3.9.2	Tests.....	55
3.9.2.1	Stop-off test 1: Chalk powder and silicone spray.....	55
3.9.2.2	Stop-off test 2: chalk powder.....	56
3.9.2.3	Stop-off test 3: Roughening the surface in order to inhibit bonding.....	57
3.10	Surface analysis of bonded area	59
3.10.1	Test equipment.....	59
3.10.2	Tests.....	59
4	Presentation of findings	61
4.1	Determination of the rough bonding parameters	61
4.2	Bonding tests	63
4.2.1	Control test.....	63
4.2.2	Bonding tests with a bond time of 30 minutes.....	65
4.2.3	Bonding tests with a bond time of 60 minutes.....	68
4.2.4	Combined.....	71
4.3	The effect of post-annealing	73
4.4	The effect of polishing	75
4.5	The results of the modelling	77
4.5.1	The contact status throughout the strength test.....	77
4.5.2	Deformation of the sample.....	79
4.5.3	The forces, which the tools exhibit on the sample.....	80

4.5.4	The stress distribution throughout the strength test.....	81
4.5.5	History plot of the load.....	83
4.6	Creating a cellular structure	85
4.6.1	Stop-off Test 1: Chalk powder and Silicone spray.....	85
4.6.2	Stop-off test 2: Chalk powder.....	86
4.6.3	Stop-off test 3: Surface roughening	86
4.7	Surface analysis of bonded area	87
4.7.1	Sample with a good bond	87
4.7.2	Sample with an incomplete bond	88
5	Discussion and implications of the findings	89
	Reference list	91
	Appendices	93

List of tables

- TABLE 1: THE GLASS-TRANSITION TEMPERATURE OF THE MOST COMMON THERMOPLASTIC POLYMERS 26
- TABLE 2: BONDING PARAMETERS TO POST-ANNEALING TEST 51
- TABLE 3: BONDING PARAMETERS TO TEST THE EFFECT OF POLISHING 53
- TABLE 4: BONDING PARAMETERS FOR STOP-OFF TEST 1 56
- TABLE 5: BONDING PARAMETERS FOR STOP-OFF TEST 2 57
- TABLE 6: BONDING PARAMETERS FOR STOP-OFF TEST 3 58
- TABLE 7: BOND STRENGTH RESULTS FOR THE CONTROL TEST 63
- TABLE 8: BOND STRENGTH RESULTS FOR THE BONDING PARAMETERS WITH A FIXED BONDING TIME OF 30 MINUTES 65
- TABLE 9: COMPARISON OF THE RESULTS FROM TWO BONDING TESTS WITH A BONDING TIME OF 30 MINUTES 67
- TABLE 10: BOND STRENGTH RESULTS FOR THE BONDING PARAMETERS WITH A FIXED BONDING TIME OF 60 MINUTES 68
- TABLE 11: RESULT FROM THE STRENGTH TEST FOR THE SAMPLES WHICH WERE POST-ANNEALED 73
- TABLE 12: RESULT FROM THE STRENGTH TEST FOR THE SAMPLE WHICH WERE BONDED USING THE SAME PARAMETERS 74
- TABLE 13: RESULT FROM THE STRENGTH TEST FOR THE SAMPLE WHICH WERE POLISHED PRIOR TO BONDING 76
- TABLE 14: RESULT FROM THE STRENGTH TEST FOR THE SAMPLE WHICH WERE BONDED USING THE SAME PARAMETERS 76

List of figures

FIGURE 1: MICRO HEAT EXCHANGER CONSTRUCTED FROM RECTANGULAR CHANNELS MACHINED IN METAL.....	20
FIGURE 2: 5 STAGES OF LIQUID STATE DIFFUSION BONDING	22
FIGURE 3: ROLLS-ROYCE TRENT 900, HIGH BYPASS TURBOFAN AIRCRAFT ENGINES UTILIZING DIFFUSION BONDING TO CREATE HOLLOW FAN BLADES	23
FIGURE 4: CROSS SECTION OF A HOLLOW FAN BLADE.....	23
FIGURE 5: BASIC SHAPES OF SUPERPLASTICALLY FORMED, DIFFUSION-BONDED STRUCTURES. A) REINFORCED SHEET; ONE SHEET. B) INTEGRALLY STIFFENED STRUCTURE; TWO SHEETS. C) SANDWICH; MULTIPLE SHEETS.	25
FIGURE 6: BOND STRENGTH OF PMMA AND COC SUBSTRATES FOLLOWING 24 MIN UV TREATMENT, COMPARED WITH NATIVE POLYMER SURFACES.	27
FIGURE 7: THEORIES OF ADHESION	29
FIGURE 8: ADHESIVE BONDING THROUGH A CAPILLARY PROCESS	30
FIGURE 9: THE VARIATION OF THE PARAMETERS OF THE THERMAL BONDING PROCESS.....	34
FIGURE 10: ONE OF TWO POLYMERS PLATES WITH ITS DIMENSIONS.....	38
FIGURE 11: THE CROSS-SHAPED GEOMETRY OF THE BONDING SAMPLES.....	38
FIGURE 12: HERAEUS SERIES 6000 HEATING OVEN/AIR-CIRCULATION OVEN.....	39
FIGURE 13: THE TEST SETUP WITH THE STACK OF WEIGHT ACTING AS PRESSURE	39
FIGURE 14: ZWICK-ROELL Z020 20 kN MATERIAL TEST MACHINE	41
FIGURE 15: CLOSE-UP OF THE TOOLS OF THE MATERIAL TEST MACHINE	41
FIGURE 16: CLOSE-UP OF THE TOOLS OF THE MATERIAL TEST MACHINE WITH A TEST SAMPLE.....	41
FIGURE 17: IMPROVED SETUP FOR THE BONDING PROCESS.	43
FIGURE 18: 3D-REPRESENTATION OF THE IMPROVED TEST SAMPLE WHICH INCLUDES THE SMALL SUPPORTS ON EITHER SIDE.....	44
FIGURE 19: FRONTAL VIEW OF THE IMPROVED TEST SAMPLE.....	44
FIGURE 20: FRONTAL VIEW OF THE IMPROVED TEST SETUP. THE ARROWS REPRESENT THE PRESSURE. THE DETAIL VIEW SHOWS THE DIFFERENT LAYERS OF THE TEST SETUP	44
FIGURE 21: FLOWCHART TO DETERMINE THE PARAMETERS FOR THE FOLLOWING TESTS.....	46
FIGURE 22: CONTROL TEST TO DETERMINE STRENGTH OF THE MATERIAL.	47
FIGURE 23: PARAMETERS FOR THE BONDING TESTS. EACH SET OF PARAMETERS IS TESTED TWICE.....	48
FIGURE 24: THE 3D REPRESENTATION OF THE MODEL. THE PINK AND PURPLE OBJECTS REPRESENT THE UPPER AND LOWER PMMA SHEETS. THE YELLOW AND GREEN OBJECTS DISPLAY THE LOWER AND UPPER TOOL RESPECTIVELY.....	49
FIGURE 25: ANNOTATING THE DIFFERENCE IN THE MESH SIZE	50
FIGURE 26: THE OVEN WHICH WILL BE USED TO PERFORM THE ANNEALING.....	52
FIGURE 27: THE SETUP FOR THE ANNEALING PROCESS	52
FIGURE 28: THE GEOMETRY OF THE SAMPLES FOR THE STOP-OFF TEST 1	56
FIGURE 29: THE GEOMETRY OF THE SAMPLES FOR THE STOP-OFF TEST 2	57
FIGURE 30: RESULTING FLOWCHART TO DETERMINE THE PARAMETERS FOR THE FOLLOWING TESTS. THE UNCOLOURED BALLOONS REPRESENT THE TESTS WHICH WERE NOT CONDUCTED. THE GREEN BALLOONS REPRESENT THE TESTS, WHICH WERE SUCCESSFUL. THE ONES WERE UNSUCCESSFUL.	61
FIGURE 31: COMPRESSION CURVE FOR THE CONTROL TEST	63
FIGURE 32: GRAPH SHOWING THE RESULTS FROM THE BOND STRENGTH TESTS WITH THEIR BONDING PARAMETERS (FIXED BOND TIME OF 30 MINUTES).....	66
FIGURE 33: GRAPH SHOWING THE BOND STATE AFTER THE BOND STRENGTH TESTS WITH THEIR BONDING PARAMETERS (FIXED BOND TIME OF 30 MINUTES)	67
FIGURE 34: GRAPH SHOWING THE RESULTS FROM THE BOND STRENGTH TESTS WITH THEIR BONDING PARAMETERS (PRESSURES OF 0.256 AND 0.313 MPA AND TEMPERATURES OF 115 AND 120 °C, FIXED BOND TIME OF 60 MINUTES).....	69
FIGURE 35: GRAPH SHOWING THE BOND STATE AFTER THE BOND STRENGTH TESTS WITH THEIR BONDING PARAMETERS (PRESSURES OF 0.256 AND 0.313 MPA AND TEMPERATURES OF 115 AND 120 °C, FIXED BOND TIME OF 60 MINUTES).....	70

FIGURE 36: COMPARISON OF THE EFFECT OF DIFFERENT BONDING TIMES ON THE BOND STRENGTH (PRESSURES OF 0.256 AND 0.313 MPa AND TEMPERATURES OF 115 AND 120 °C).....	71
FIGURE 37: COMPARISON OF THE EFFECT OF DIFFERENT BONDING TIMES ON THE BOND STATE (PRESSURES OF 0.256 AND 0.313 MPa AND TEMPERATURES OF 115 AND 120 °C).....	72
FIGURE 38: GRAPH SHOWING THE RESULTS FOR THE EXPERIMENTS WHICH LOOK AT THE EFFECT OF POST-ANNEALING.....	73
FIGURE 39: GRAPH SHOWING THE RESULTS FOR THE EXPERIMENTS WHICH LOOK AT THE EFFECT OF POLISHING. BOTH CURVES REPRESENT THE SAMPLES WHICH WERE POLISHED.....	75
FIGURE 40: THE BOND STATUS OF SAMPLE, WHICH IS BEING TESTED.....	77
FIGURE 41: THE BOND STATUS FOR DIFFERENT INCREMENTS THROUGHOUT THE SIMULATION. THE YELLOW COLOURED AREAS REPRESENT THE SECTIONS WHICH ARE STILL BONDED WHILE THE BLUE COLOUR INDICATES THE UNBONDED SECTIONS. THE RED COLOUR SHOWS THE AREAS WHERE THE BOND IS FAILING.....	78
FIGURE 42: THE MAXIMUM DEFORMATION OF THE SAMPLE.	79
FIGURE 43: THE AMOUNT OF DEFORMATION FOR EVERY SECTION OF THE SAMPLE.....	79
FIGURE 44: THE CONTACT NORMAL FORCES IN THE Z-DIRECTION ON THE SAMPLE. THE FORCES IN LEFT SAMPLE ARE ILLUSTRATED USING CONTOUR BANDS WHILE THE FORCES IN THE RIGHT SAMPLE ARE ILLUSTRATED USING CONTOUR LINES.	81
FIGURE 45: THE COMP 11 STRESSES FOR CERTAIN INCREMENTS.	82
FIGURE 46: LOAD CURVE FOR THE BONDING TEST (120 °C - 0.31 MPa - 30 MIN.)	83
FIGURE 47: THE SIMULATED LOAD CURVE	84
FIGURE 48: THE RESULT OF STOP-OFFTEST 1. THE SAMPLES DEFORMED HEAVILY DURING BONDING	85
FIGURE 49: THE RESULT FROM STOP-OFF TEST 2. THE RIGHT PICTURE SHOWS THAT THE K-SAMPLE WAS NOT BONDED.....	86
FIGURE 50: A MICROSCOPIC IMAGE OF THE SURFACE OF A SHEET. THE LEFT SIDE OF THE IMAGE SHOWS THE BOND AREA. THE RIGHT SIDE SHOWS AN UNBONDED AREA. (MAGNIFICATION: 5x).....	87
FIGURE 51: A MICROSCOPIC IMAGE OF THE SURFACE OF A SHEET WHICH WAS BONDED WITH SIGNIFICANT STRENGTH (MAGNIFICATION: 10x).....	88
FIGURE 52: A MICROSCOPIC IMAGE OF THE SURFACE OF INCOMPLETE BOND (MAGNIFICATION: 5x).....	88
FIGURE 53: THE TWO SHEETS WHICH DEFORMED HEAVILY AFTER A BONDING TEST USING A U-CLAMP TO PROVIDE THE BONDING PRESSURE.....	107
FIGURE 54: THE NEW SETUP SHOWING THE NEW GROUND SURFACE	108
FIGURE 55: THE DIMENSIONS OF THE TEST SAMPLES IN CENTIMETRES ACCORDING TO ASTM D638-03	111
FIGURE 56: THE RESULTING STRESS-STRAIN CURVE FOR THE MATERIAL PMMA IN DELIVERY CONDITIONS.....	112
FIGURE 57: THE RESULTING STRESS-STRAIN CURVE WITH THE ELASTIC PART HIGHLIGHTED IN ORDER TO DETERMINE THE YOUNG'S MODULUS	113
FIGURE 58: THE TECHNICAL SPECIFICATIONS OF THE OLYMPUS LEXT CONFOCAL LASER SCANNING MICROSCOPE	117

Abstract

Improving resource efficiency and effectiveness of materials is becoming very important in itself in the current economy. Though some of the manufacturing of structured components has been undertaken with polymeric materials, there has been little use of sheet polymeric materials in order to develop micro-channel devices. These micro-channel devices could, for example, be used in efficient heat exchangers and chemical reactors. The purpose of this master's thesis is to research selective diffusion bonding as part of the manufacturing process of these micro-channels in polymeric materials, in particular to further improve diffusion bonding and to find an effective way to inhibit bonding at predetermined places in order to achieve a selective bond.

In order to determine the quality of the bond a novel testing method was developed and verified using finite element modelling. The design of experiments methodology was used to determine the ideal bonding parameters, to test the effect of different surface modification techniques and to discover new stop-off substances. PMMA was used as a base material.

The results from strength tests showed that the following bonding parameters resulted in the best bond: 120 °C – 0.31 MPa – 60 min. Post-annealing did not improve bonding while polishing did show a noticeable improvement in repeatability. Chalk powder proved to be an excellent stop-off. The simulations of the strength test showed similar results as in the real-life experiments.

Abstract in Dutch

Het verbeteren van het verwerkingsrendement en -effectiviteit van materialen wordt steeds belangrijker in de huidige economie. Hoewel er al wat productie van gestructureerde componenten, gebruikmakende van polymeren, is ondernomen, blijft de implementatie van polymeren in de vervaardiging van deze microkanalen echter beperkt. Deze microkanalen kunnen bijvoorbeeld gebruikt worden efficiënte warmtewisselaars en reactoren. Het doel van dit eindwerk is onderzoek voeren naar het selectief diffusiebinden als onderdeel van het productieproces van deze microkanalen in polymeren. Meer specifiek het verbeteren van dit proces en een effectieve manier vinden om het binden te stoppen op welbepaalde plaatsen om zo een selectieve binding te verkrijgen.

Om de kwaliteit van de binding te bepalen werd een nieuwe testtechniek ontwikkeld en geverifieerd gebruikmakend van een eindige elementen modellering. De experimentele ontwerpmethode werd gebruikt om de ideale bindingsparameters te bepalen, het effect van verschillende oppervlakte aanpassingen te testen en voor het ontdekken van nieuwe *stop-off*-materialen. PMMA werd gebruikt als basismateriaal

The resultaten van de sterktetesten toonde aan dat de volgende bindingsparameters resulteerde in de beste binding: 120 °C – 0.31 MPa – 60 min. Het nagloeien van het proefstuk had geen invloed op binden terwijl het polijsten een merkbare verbetering in de herhaalbaarheid tot gevolg had. De simulaties van de sterktetest toonde vergelijkbare resultaten als de experimenten

1 Introduction

1.1 Background

Midlands Simulation Group or MidSim is research group that is part of the University of Wolverhampton. The group performs high quality research and development primarily focused at the aerospace and high value manufacturing sectors. For solving complex problems, which arise in their projects, they make use of numerical modelling and simulation. MidSim offers two main services: product design and development and manufacturing development. Their expertise and experience relates to:

- simulation, manufacturing and design of structured materials for lightweighting and ballistic performance;
- improved forming of thin materials by better heat management and design of die-tooling;
- improved heat transfer and coolant flow and possibilities for micro channel flow;
- vacuum insulation and robust design;
- diffusion bonding and joining of thin materials from titanium to plastic. ("Midland Simulation Group | Industry Expertise," n.d.)

This master's thesis researches the manufacturing process of lightweight (structured cellular) polymeric parts more specifically the bonding process.

Improving the resource efficiency and effectiveness of materials is becoming very important in itself, as well as making it more lightweight and/or improving impact/blast energy absorption.

Cellular materials are very efficient materials and often have a self-similar or fractal structure (such as in bone) which enables extreme efficiency of material usage. For example, the Eiffel Tower is a manmade hierarchical structure – with an exceptional efficiency.

Manufacturing difficulties have, until recently, inhibited the evolution of such efficient materials. Manufacturing improvements are driving the technology forward coupled with an increased interest in more sophisticated structured material design for armour design. This leads to an increased interest in the development and the design of homogeneous and heterogeneous cellular structured materials in which the geometry of the cellular structure is as important as the constituent materials (or the mismatch of materials if a heterogeneous cellular structure is required).

Though some of the manufacturing of structured components has been undertaken with polymeric materials, there has been little use of sheet polymeric materials in order to develop micro-channel devices. These micro-channel devices could, for example, be used in efficient heat exchangers (in spite of their bad thermal conductivity, see 2.1.3) and chemical reactors.

The application will ultimately determine the constraints. The two main groups of applications are:

- structural or thermal light-weighting;
- microfluidic devices.

There are companies who, already, diffusion bond polymeric materials (such as acrylics) but little account is taken of the opportunities for material efficiency and making lightweight structures that could compete with polymeric injected material – due to low tooling/die costs.

1.2 The premise

The aim of my research is to look whether we can use similar techniques, as already been done with metals, to create lightweight and structured materials out of thermoplastic polymers? There are multiple reasons why this approach would be useful.

One of the main reasons for creating structured parts is to be more material efficient. The goal is to keep the same stiffness while using less material, thus creating a more lightweight part.

In the past fabricating structured/cellular parts has proven to be extremely difficult if not impossible. The cost of making these parts has always been the biggest disincentive for implementing this technique in mass production. However, if the same techniques can be utilised as used with metals; we might overcome this issue.

The main advantage of using polymers is the superior formability when compared to metals. Forming at lower temperature results in a much easier development of the manufacturing processes.

Another advantage is the transparent nature of most polymers. This property is very useful for conducting a visual analysis during the bonding/forming process. Observing the behaviour during the bonding/forming will help future research in the manufacturing of structured parts. In the future these techniques might even be utilised as a rapid prototyping process before moving to a more costly manufacturing process of a comparable metal part – due to the higher forming temperature of metals.

1.3 Objectives

The bonding of polymer sheets can be achieved through various processes, however, the scope of this thesis will be limited to two main ways.

The first approach is to selectively bond two polymer sheets, followed by inflation. The main issues lay in the bonding of the sheets. If these sheets bond very easily, methods that can be used to stop the bonding at appropriate places will be investigated. This can be accomplished with the use of a “stop-off”. If, on the contrary, the sheets do not adequately bond, research will be carried out to ascertain ways to activate them to bond more easily.

The second method is to bond two pre-cut sheets. One of the issues with this approach is the potential damage to the micro channels due to high temperature and/or high pressure. If the aim is to reduce the required pressure to bond these sheets, the temperature would have to be increased accordingly. If, on the other hand, the objective is to lower the required temperature, the pressure would have to be increased. Improving the smoothness and flatness of the sheets will permit us to lower both the temperature and pressure without having to compromise on bond strength.

The first objective is to bond two polymer sheets with sufficient bond strength while keeping the deformation to a minimum. The bonding of just two sheets is generally of limited use in the industry. The bonding process should, therefore, be easily scalable to a larger number of sheets.

The second objective is to make bonding selective, i.e. through the use of a “stop-off”. Selecting the correct “stop off” is the main part of this objective. A good “stop-off” should effectively stop the bonding process at the places where it is applied and shouldn’t affect the surrounding areas. The “stop-off” should also be easily removable.

1.4 Materials and methods

The research is mainly focused on the implementation of polymers, more specifically thermoplastic polymers. The first step is to conduct a literature review on the properties of the different polymers. The bonding and forming parameters will be the basis for choosing the optimum polymer for this application. Likely candidates are polymethylmethacrylate (PMMA), polycarbonate (PC), cyclic olefin copolymer (COC) and polystyrene (PS).

The various bonding techniques will be examined, through a literature review, to select the best technique. The study will look at the cost of the equipment, ease of bonding and the effects it has on the sheets. The main goal is to produce a homogeneous bond, which will have the same properties as the bulk material. The possible issues, inherent in the different bonding techniques, will be investigated. Issues which might arise are for example: the buckling of the sheets under high pressure, clogging of the microchannel, etc...

Choosing the right “stop off” will be essential to achieve selective bonding. The method of using a “stop-off” is widely used in the metal industry. This is, however, not the case in the plastic industry. Selecting a good “stop-off” will likely take place through trial and error.

To determine the ideal bonding parameters, practical tests will be carried out. The main focal points of these tests will be to achieve adequate bond strength while keeping the geometry of the channels intact. This will inevitably become a balancing act between bond

strength and deformation of the sheets. Another point to investigate is the effect of surface modification on these parameters. The goal of the first test is to create a simple bond of two polymer sheets. The objective of the second test is research different substances that could be used as a stop-off.

The next step is to model this complex entity with a finite element programme to determine the behaviour of the sheets. A finite element model on its own is worthless without relating it to the real world, in this case the practical tests. When we establish a descriptive model, we can expand to ever more complex geometries of both the channels and the interface between different layers.

2 Review of the literature

This literature review will first outline a background for this thesis. The applications will also be discussed. After this the various bonding techniques will be explained, using the same process with metals, with the emphasis on diffusion bonding. The next step is to search the literature for examples, where this technique already has been used with polymers and what issues might arise. Another part of this literature review is to select which materials could be used. There will probably be a lot of candidates but the final selection criterion will be the availability of information regarding these materials in relation to the chosen bonding technique. The final step will be to look for bonding parameters for diffusion bonding which other people have used.

2.1 Process intensification

2.1.1 What is process intensification?

Stankiewicz and Moulijn (2000) describe process intensification as follows.

Process intensification consists of the development of novel apparatuses and techniques that, compared to those commonly used today, are expected to bring dramatic improvements in manufacturing and processing, substantially decreasing equipment-size/production-capacity ratio, energy consumption, or waste production, and ultimately resulting in cheaper, sustainable technologies.

Process intensification can be applied in many areas of engineering. This thesis will, however, look at process-intensifying equipment more specifically heat-transfer devices and novel reactors. Other examples are intensive mixing and mass-transfer devices. Both novel reactors and heat-transfer devices share –at least one – common constituent, which is the use of microchannels.

2.1.2 Design possibilities

The manufacturing process of structured cellular devices can be split in two main methods. The first technique uses pre-cut microchannels which are bonded to make a structured cellular device. A micro heat exchanger can be seen on the picture below. This heat exchanger is made up of thousands of microchannels. Every row of microchannels is essentially one sheet with multiple grooves. These grooves can range from 1 μm to 1 mm across and are milled beforehand. These pre-cut sheets will then be bonded to effectively seal the channels.

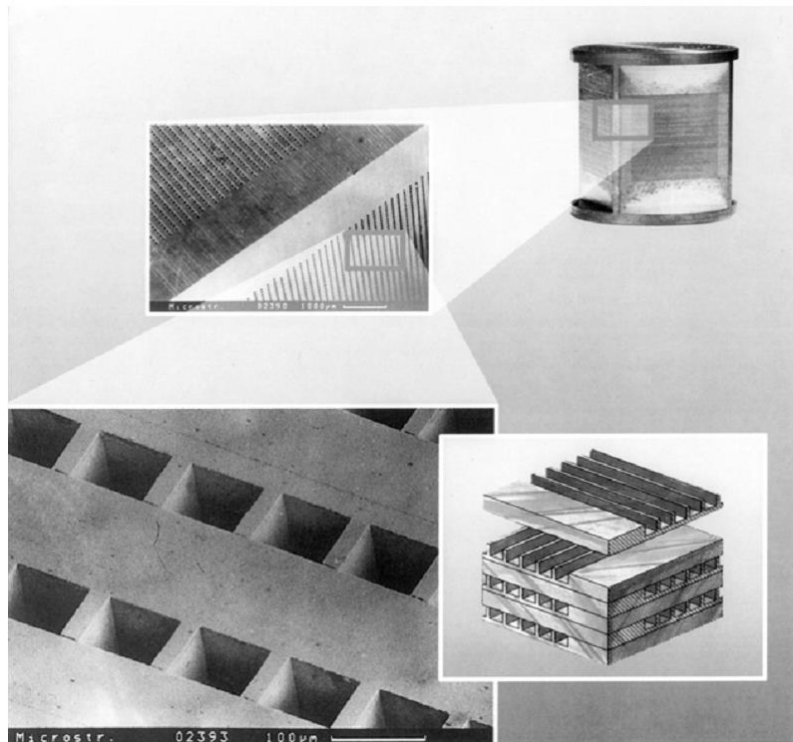


Figure 1: Micro heat exchanger constructed from rectangular channels machined in metal. (source: sharp et al., n.d.)

This technique will not be discussed further. The second method selectively bonds multiple sheets together. These sheets are afterwards inflated to make microchannels. This technique will be explained using metals and will be discussed later in more detail. In either technique the sheets need to be bonded. Bonding can be achieved with numerous techniques such as diffusion bonding, adhesive bonding or solvent bonding.

2.1.3 Process intensification with the use of polymers

The manufacturing process of these microchannels have proved extremely difficult and expensive due to the special equipment. Microchannels made using selective diffusion bonding followed by inflation can possibly overcome this issue.

The use of polymer microchannels will, however, have its drawbacks. The main disadvantage is the large pressure drop of the liquid. This is due to high shear rates which develop as a result of the microscopic dimensions of the microchannels. Liquids which are Newtonian at normal shear rates can become non-Newtonian at very high shear rates.

Polymers inherently have a bad thermal conductivity. This would implicate that polymer heat-exchangers would not be any good. The thin sidewalls, usually around 20 µm thick, will eradicate the negative effect of the bad thermal conductivity. Polymer heat exchanger will, more or the less, have the same thermal performance as their metal counterparts (T'joen et al., 2009). An added benefit of using polymers is the excellent corrosion resistance.

2.2 Diffusion bonding of metals

Diffusion bonding (DB), often inaccurately referred to as *diffusion welding*, is a manufacturing process for joining two surfaces by diffusion of material across the interface. This process is particularly interesting because it provides a good metallurgical bond with excellent mechanical properties. Unlike brazing, where a third material is introduced at the interface, mechanical properties of a diffusion bonded interface can match these of the bulk material. Because of all these reasons, diffusion bonding has become an attractive bonding technique in aerospace applications when using titanium and aluminium.

2.2.1 Mechanism behind diffusion bonding

Kazakov (1985) describes the bonding process as follows.

Diffusion bonding of materials in the solid state is a process for making a monolithic joint through the formation of bonds at atomic level, as a result of closure of the mating surfaces due to the local plastic deformation at elevated temperature which aids interdiffusion at the surface layers of the materials being joined.

Diffusion bonding can be achieved by applying a relatively small pressure while heating the material to a certain temperature, which depends on the material. For example when diffusion bonding titanium a temperature of 950 °C is required, which is higher than half its melting temperature. Pressures, on the other hand, do not exceed to a few MPa's. Bonding times are usually in the range of a few hours, but this strongly depends on the composition of the alloy and in particular on the grain size. (Partridge, 1987)

2.2.2 Solid-state diffusion bonding

Shirzadi (1997) describes the two stage process of solid-state diffusion bonding in more detail.

In the first stage, the contacting surface asperities undergo a plastic deformation as result of the applied pressure. These asperities originate from the grinding and polishing marks, produced during the surface finishing stage. The microplastic deformation continues until the localised effective stress at the contacting area becomes less than the yield strength of the material at the bonding temperature. In fact, the oxide layers, covering the faying surfaces, make up the initial contact. Due to local disruption, more metal-to-metal contact is achieved, as deformation of asperities continues. These local disruption are a result of brittle oxide, which usually fracture relatively easy. A bonded area of less than 10% and a large volume of voids and oxide remains between localised bonded regions are the result at the end of the first stage.

In the second stage of bonding, thermally activated mechanisms lead to void shrinkage and this increases further the bonded areas.

2.2.3 Liquid-state diffusion bonding

Liquid-state diffusion bonding, in relation with solid-state diffusion bonding, uses an interlayer between the faying surfaces which is made up of a different material. The material, used as an interlayer, has a lower melting point than the bulk material. During the bonding process the interlayer melts, which essentially forms a liquid at the interface. This liquid will subsequently diffuse in the adherent layers. MacDonald and Eagar (1992), based on findings of Tuah-Poku et al. (1988), divides the bonding process in four stages:

1. dissolution, the interlayer and parent material undergo interdiffusion to form a liquid phase when heated to the bonding temperature;
2. widening, the widening of the interlayer drives the composition into alpha rich liquidus;
3. isothermal solidification, diffusion of the melting point depressant in the parent material;
4. homogenisation, controlled by solid-state diffusion rate and depends on the time at temperature.

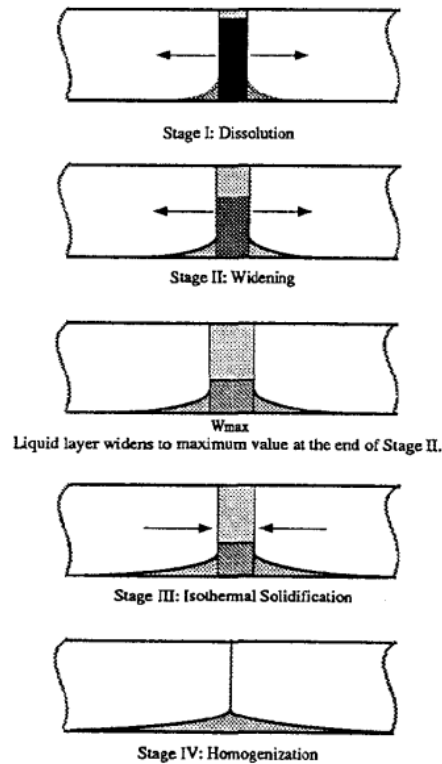


Figure 2: 5 stages of liquid state diffusion bonding

This method is also referred to as *diffusion brazing*. The main advantage of this method is that the required temperature and pressure to form a bond can be lowered. Dissimilar materials can also be bonded, using this technique.

2.2.4 Surface cleanliness

Creating a diffusion bond with the same strength as its parent metal puts high demands on the surface cleanliness. Surface oxides and absorbed gasses at the interface are some of the barriers which can interfere with the atomic bonding. Oxide-free conditions would be optimal but only exist for a limited amount of materials. Real-life conditions, however, do impede the diffusion bonding to some extent. The solubility of interstitial contaminants determines the amount of interference of the formation of the bond. Metals, who have a high solubility of interstitial contaminants, include titanium, tungsten, copper, etc. The solubility is, therefore, a measure for the ease of bonding.(Campbell, 2011)

2.2.5 Diffusion bonding with superplastic forming (SPF/DB)

An interesting development for creating a structured material out of titanium is using a combination of diffusion bonding with superplastic forming. These SPF/DB structures have numerous advantages over traditional manufacturing like a considerable weight saving and a reduction in the number of parts used. An example, where this techniques is being used, is in the aerospace industry to create hollow fan blades in aero-engines. (Fitzpatrick and Lloyd, 1998) Other applications are titanium compact heat exchangers.

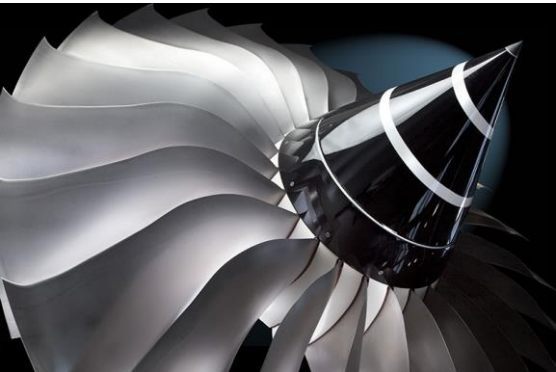


Figure 3: Rolls-Royce Trent 900, high bypass turbofan aircraft engines utilizing diffusion bonding to create hollow fan blades (source: http://www.rolls-royce.com/civil/products/largeaircraft/trent_900/)

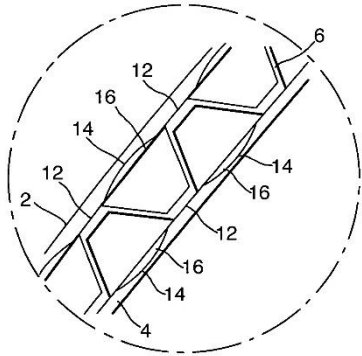


Figure 4: Cross section of a hollow fan blade (source: Hollow component with internal damping US20040191069 A1)

2.2.5.1 *Superplasticity*

Superplasticity is a phenomenon in which materials can achieve a high tensile elongation, in excess of several thousand percent, by using the right process parameters. Controlling the temperature and the strain rate are essential to achieve this increased formability. An added benefit is the fact that components, manufactured with this technique, are dimensionally stable and free of residual stress. This is due to the relative high forming temperatures, which are higher than the annealing temperature of the material.

2.2.5.2 *Stop-off*

To achieve selective bonding, there has to be a way to inhibit the bonding at certain, predetermined areas. Achieving this requires the use of a stop-off. A stop-off agent prohibits bonding on areas, even when subjected to bonding pressures and temperatures. To create structured material, the stop-off is applied in a predetermined pattern. Popular stop-off's are for example Yttria, boron nitride, graphite or alumina, all used to selectively bond titanium. (Weisert et al., 1988)

Selective bonding of polymers, using a stop-off, has not been done according to the literature. There are no proven examples where researchers used this technique to achieve selective bonding of polymers. This means that selecting a good stop-off, will be through trial and error.

2.2.5.3 *Combining diffusion bonding with superplastic forming*

The SPF/DB combines diffusion bonding with a forming process, where two or more sheets are used to create structured material. Creating a good diffusion bond, which is selective to predetermined areas, is essential in this process. Combining these two processes is possible due to the fact that the required parameters, of both processes, are similar. This technique also makes it possible to make a structured material constructed out of more than two sheets, thus making it possible to fabricate complex geometries.

The first step in SPF/DB-process is diffusion bonding of select areas, utilising the beforehand mentioned stop-off. Once a good bond is created, the second part can commence. A pressure, via an inert gas, is used to form the sheets in to the desired shape. This pressure is predetermined to achieve the desired strain rate, which is essential when superplastic forming. The sheets will start to deform until it makes contact with the die surface.

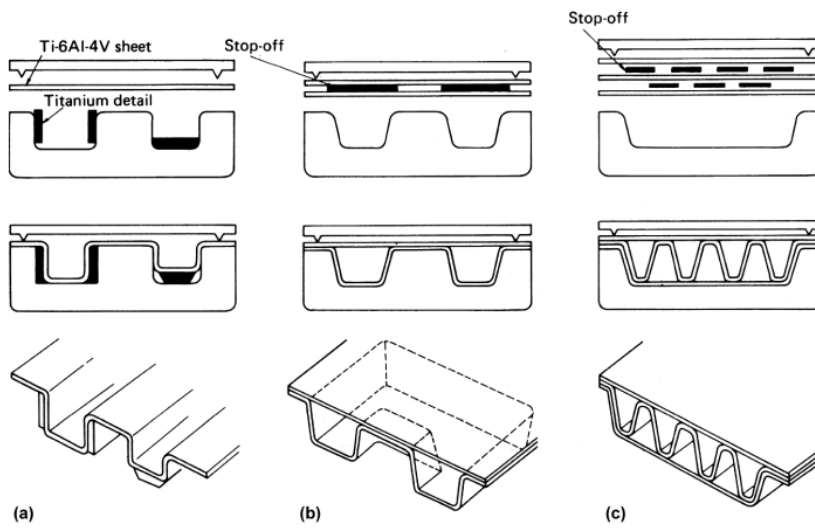


Figure 5: Basic shapes of superplastically formed, diffusion-bonded structures. A) Reinforced sheet; one sheet. B) Integrally stiffened structure; two sheets. C) Sandwich; multiple sheets. (Titanium: A Technical Guide, fig.9.14, p.77)

2.3 Diffusion bonding of polymers

To diffusion bond polymers, the substrates have to be heated near or above the glass-transition temperature, while applying pressure to increase contact forces. The glass-transition temperature is not high, compared to metals, which could be used as an advantage to fabricate microfluidic devices.

The glass-transition temperature of the most common thermoplastic polymers are listed in the table below.

polymer	glass-transition temperature [°C]
COC	151-169
PC	142-158
PET	60-84
PMMA	96-104
PS	90-100
PVC	74-88

Table 1: The glass-transition temperature of the most common thermoplastic polymers (CES EduPack 2013)

2.3.1 Issues

With standard diffusion bonding, the microstructures deform very easily with risk of clogging the microchannels. This is inherently the result of the bonding temperatures and pressures required to form a bond. Direct thermal bonding of polymers is driven by bonding pressure (forced flow), temperature and time. However, the deformation of the microchannel is also driven by the same three factors. (NG et al., 2008)

Zhu et al. (2007), among others, reported channel collapse when diffusion bonding PMMA with a temperature higher than 100 C. The article also mentions draping of the sidewalls of microchannels, with a cross section of 50 μm by 50 μm , when applying a temperature of 97 °C. When lowering the temperature, the microchannels retained their original shape.

2.3.2 Possible solutions

Sun et al. (2006) used an elevated temperature (165 °C) combined with a low pressure (20 kPA) to successfully bond two PMMA substrates. The low pressure ensures a good structural integrity, with no signs of deformation. The elevated temperature, on the other hand, results in high bond strength.

Another method was developed by Ahn et al. (2004). They come up with another novel technique to achieve diffusion bonding without deformation of the microchannels. Instead of elevating the bonding temperature, they increased the bonding pressure to tens of MPa. The bonding temperature was kept 20 to 40 °C below the glass-transition temperature of COC. It has to be noted that the surfaces of the samples were modified using a plasma pretreatment prior to bonding.

Lee et al. (2003) proposed a new low temperature bonding technique using X-ray irradiation. This irradiation decreases the molecular weight of the PMMA substrates. This will, as a result of, decrease the glass transition temperature. A lower T_g will allow to bond these substrates at a lower temperature without the damaging the geometry of the microstructures.

Tsao et al. (2007) used a UV/ozone surface treatment to achieve low temperature bonding of both PMMA and COC. A comparison was made between treated and untreated samples to see effect of the surface treatment. The tests were performed for temperatures between 25 and 110 °C. The graph below shows there results when looking at the bond strength as a function of the bond temperature. The graph shows a sharp increase in bond strength even in the lower temperature-range. The untreated samples do not show signs of bonding at temperature below 90°C. The treated samples, on the other hand, show relative high bond strengths even at low temperature. The bond strength of treated samples at 90 °C is more or less the same as the bond strength of the untreated samples at 110 °C. 110 °C is, however, too high when we want to use this technique with, for example, microfluidic devices because of the chance of channel deformation or even channel collapse.

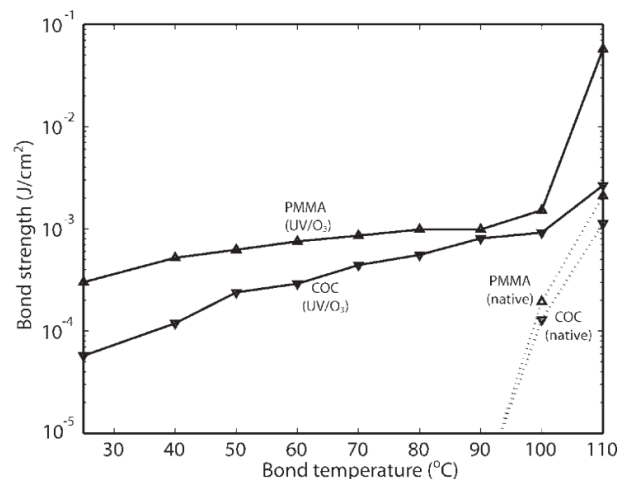


Figure 6: Bond strength of PMMA and COC substrates following 24 min UV treatment, compared with native polymer surfaces.

2.4 Other possible bonding techniques for polymers

2.4.1 Solvent bonding

Solvent bonding of metals is inherently impossible due to its mechanism. Nevertheless is this technique a viable option for bonding polymers because it can achieve high bond strengths without introducing a foreign material. Mechanisms behind this process are, to some extent, similar to ones used in, the previously mentioned, liquid state diffusion bonding. This technique also uses an interlayer to achieve bonding.

2.4.1.1 *Mechanism behind solvent bonding*

Solvent bonding is a process which uses a solvent to bond two substrates. The absorption of the solvent by the polymer causes the glass transition temperature to drop. The solvent essentially softens the surface of the substrate, increasing the mobility of the polymer chains. When two solvent-softened substrates are pressed together, polymer chains will start to diffuse across the interface.

Thermal activated solvent bonding differs from regular solvent bonding because it depends on the temperature. This type of solvent bonding uses a liquid which is not a solvent of the base material at room temperature. It is not until a certain temperature is reached that the liquid will become a solvent to the base material. This gives extra control over the bonding process.

2.4.1.2 *Issues*

Using solvent bonding is not as straightforward as it might seem. It has been reported that extra care has to be taken when applying the solvent since it can destroy the microchannels. Shah et al. (2006) experimented with utilising the capillary effect to help bond two sheets of PMMA. The solvent, in this case acetone, was pumped through the microchannels and relying on the capillary effect to draw some solvent in the interface. It was, however, reported that if the acetone would remain longer than two to three seconds in the microchannels, the channels would deform.

2.4.2 Adhesive bonding

One of the simplest ways of bonding two polymer sheets is through the use of an adhesive. This adhesive is usually a different material than the bulk material of the sheets, hence the reason why this technique is an indirect bonding technique. Adhesives come in different states, liquid or solid. Some require a form of activation depending on the type of glue. Activation can be through visible light, heat and/or pressure, etc...

2.4.2.1 Mechanism of adhesive bonding

The mechanism behind adhesives is adhesion. Adhesion is combination of different mechanisms, which work on different scales. The theory of adhesion can accurately be summarized in the following table.

Traditional	Recent	Scale of Action
Mechanical interlocking	Mechanical interlocking	Microscopic
Electrostatic	Electrostatic	Macroscopic
Diffusion	Diffusion	Molecular
Adsorption/surface reaction	Wettability	Molecular
	Chemical bonding	Atomic
	Weak boundary layer	Molecular

Figure 7: Theories of adhesion (Source: adhesives technology handbook)

2.4.2.2 Issues and possible solutions

Channel clogging

One of the issues experienced when bonding two sheets using an adhesive is the clogging of microchannels when going to submillimetre dimensions.

Riegger et al. (2010) suggests a number of possible solutions to reduce the risk of channel clogging. The first parameter, they discuss, is the layer thickness. They reported good result when applying an adhesive with a layer thickness of 2.5 μm . This is, however, different for each adhesive but it shows the significance of the layer thickness. The second technique, which yields good results, is with the use of capture channels. These channels capture any excess adhesive thus preventing it from clogging the

microchannels. The final parameter, they investigated, is the influence of increasing the viscosity of the adhesive. The results with this approach were especially good because it showed that an increase of viscosity will yield “perfect” results, and this without the use of capture channels.

Dang et al. (2005) as cited by Tsao and DeVoe (2009), described a different technique to prevent channel clogging. This technique utilises a contact printing process to apply an adhesive layer, which can be precisely controlled by the stainless steel pate hollow. To remove air bubbles and excessive adhesive, assuring that the adhesive cannot enter the microchannels, the author used a sacrificial channel network.

Lu et al. (2008) on the other hand, utilises the capillary action to fill the interstitial space between the microfluidic chip with a resin, without clogging the microchannels. It is worth noting that the microchannels must be clean, for the capillary process to work effectively. The resin is afterwards cured with UV-light. This process is shown in the following figure.

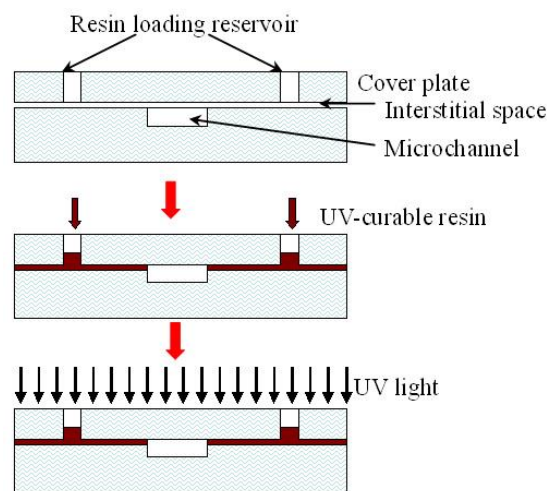


Figure 8: adhesive bonding through a capillary process (source: Lu et al., 2008)

Wettability

Achieving continuous contact between the sheets of the microfluidic devices is very important, as mentioned before. The process for achieving continuous contact is called wetting. "Wetting is the displacement of air (or other gases) present on the surface of adherents by a liquid phase. The result of good wetting is greater contact area between the adherents and the adhesive over which the forces of adhesion may act." (Satas and Tracton, 2001) To ensure a good wettability, the adhesive should have a lower surface tension than the critical surface tension of the adherent. The adhesive is in most cases a fixed given, thus making the surface tension a fixed value. As a result, the only variable which can be modified is the critical surface tension of the adherent. To vary this surface tension a number of techniques can be used.

To increase the surface tension of a polymer sheet, and thus improving wettability, a corona discharge method can be used. A corona discharge method utilises a single-phase, high frequency, power source. This power is applied, through electrodes on different potentials, to material. The side, subjected to high power potential, will experience an increase in surface tension. (Wolf, 2014)

Hansen and Schonhorn (1966) as reported by Ebnesajjad (2008) describes the use of plasma treatment as a viable technique for the preparation of low surface energy polymers for adhesive bonding. This technique describes the process of generating an inert gas-plasma, at reduced pressure, with the use of electrodeless glow discharge and subsequently exposing the polymer to this gas.

Introduction of a different material

Adhesive bonding introduces a different material to the interface. This can lead to numerous issues, depending on the combination of adherent and adhesive used. Because a different material is introduced, there will be a step change in the thermal and optical properties. Thermal mismatch can result in delamination at the interface. An optical change can, depending on the application, be unacceptable because a lot of microfluidic applications depend on optical-based observation, thus making an accurate observation impossible. (NG et al., 2008)

2.5 Materials

2.5.1 Thermoplastic – thermoset – elastomer?

Polymers can be categorised in many ways but its physical state and reaction to heat are the most important factors in relation with his thesis. When grouping these polymers, according to these factors, three categories can be made: thermoplastics, thermosets and elastomers.

A thermoset is a material that sets or cures in predetermined shape when subjected to heat. Curing is an irreversible process chemical in which crosslinks are made between the molecular chains, meaning that the shape is fixed. The cured polymers has three-dimensional shape, with high rigidity, due to these cross-links.

A thermoplastic, on the other hand, does not cure or set but it softens when subjected to heat and hardens when subsequently cooled down. The hardening process does not create chemical bonds but it merely relies on physical changes. This process can, therefore, be repeated many cycles until the polymer degrades.

Elastomers have rubber-like properties. There are two types of elastomers: thermoplastic and thermoset elastomers. Thermoplastic elastomers, like the name suggests, have the processing characteristics of a thermoplastic.

For applications, like microfluidic devices or efficient heat exchangers, an elastomer is not an option, due to its rubber-like properties. Thermosets are only option when combined with adhesive bonding because bonding “existing” sheets is not possible. However, due to numerous reasons, diffusion bonding was chosen as bonding technique of choice and thus eliminating thermosets as a viable option. This leaves thermoplastic polymers as the only possible solution when combined with diffusion bonding

2.5.2 Which thermoplastic polymer to choose?

Polymers come in all shapes and sizes, each having different material properties. However this thesis will limit the possible thermoplastic polymers to the group of the commodity plastics because we target implementation in the industry and thus making exotic plastics not a viable option.

Temperature, pressure and time are the key parameters to achieve a good diffusion bond. The required pressure is largely dependent on the state of the sheets, more specifically the flatness and roughness of the sheet. The temperature and time, on the other hand, are determined by the material itself. Choosing a good material will ultimately make the bonding process easier, by lowering the required temperature, time or both.

To choose a good test material, it is necessary to look in the literature to find examples where people have successfully diffusion bonded a specific material. When looking to the literature, it is notable that the vast majority of microfluidic devices are built using a limited amount of thermoplastic polymers. PMMA, PS, COC and PC are the most commonly used materials.

2.5.3 Diffusion bonding parameters

2.5.3.1 *Polymethylmethacrylate*

Zhu et al. (2007) investigated the effect of surface modification on the bonding strength, while changing the bonding temperature and pressure. The surface of PMMA is modified with its monomer (MMA) before bonding. In the first test, the effect of the bonding temperature on the bond strength is examined. It is noted that an increase of the bond temperature will result in a higher bond strength but this will also increase the chance of damaging the microchannels. The microchannels collapsed when using a temperature of 100°C. At 97°C, the sidewalls of the microchannels draped. The microchannels stayed intact when reducing the temperature below 97°C. The bond strength of the surface modified PMMA showed, however, a considerable increase. The second experiment looked at the bonding pressure. This test was performed at a bond temperature of 95°C. This test showed that the sidewalls draped when using a pressure of 3 bar (0.3 MPa). Using a lower pressure showed no visual damage to microchannels. The effect of surface modification again showed a considerable increase in bond strength. The final test examined the effect of post-annealing on the bond strength. It was reported that this process significantly increased the bond strength in both materials. The bonding time was kept constant during the tests at 3 minutes. Appendix 1 shows an extra graph which illustrates the influence of this surface modification.

Sood (2007) reported that the bonding temperature should stay below the glass transition temperature (105°C) to avoid the polymer from reaching a vicious state and prevent excessive degradation of the microchannels. The article specifically mentions 95°C as the optimal bonding temperature when bonding sheets, which contain microchannels. To avoid severe degradation, the bonding pressure was kept at a minimum (1-3 bar or 0.1 – 0.3 MPa). To achieve an acceptable bonding pressure, the bonding time to 10 to 30 min, to compensate for the reduced bonding temperature and pressure.

Sun et al. (2006) used a novel technique to achieve high bond strength. Instead of keeping the bond temperature below the glass transition temperature, the experiments were conducted using a temperature of 165°C while keeping the bond pressure very low (20kPa). The argumentation, behind the use of the high temperature, is the fact that PMMA does not massively depolymerize until 180°C. A time of 2 hours was reported for

the entire bonding process. It has to be noted that this process also contains an annealing process, which might explain the relative high bond strength (2.15MPa).

Du et al. (2012) described a new method to improve the bonding rate (effective bond area) when performing a novel water pretreatment. His pretreatment consist of an ultrasonic cleaning process, followed by submersing the PMMA substrates in deionized water for period of 1 hour. Afterwards the substrates are dried using nitrogen gas. The results show an average increase of 30% in effective bond area. The journal article also lists an interesting figure, showing the relation between the bond parameters mutually. The bonding process was done with the following parameters: a pressure ranging from 1.4 to 1.9 MPa, a temperature ranging from 91 to 93 °C and a bonding time of 6 minutes. The following figure illustrates the relationship between the bonding pressure and bonding temperature in relation to the bonding time.

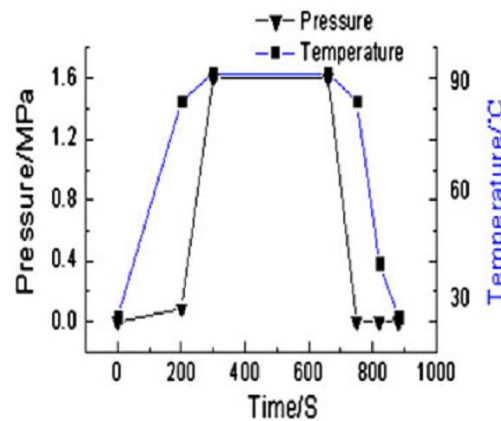


Figure 9: The variation of the parameters of the thermal bonding process (source: Du et al., 2012)

2.5.3.2 Cyclic olefin copolymer

Ahn et al. (2004) achieved diffusion bonding without significant deformation of the microchannels. Instead of elevating the bonding temperature, they increased the bonding pressure to tens of MPa. The bonding temperature was kept 20 to 40°C below the glass-transition temperature of COC. Prior to bonding the samples were pre-treated with a plasma treatment. Bonding was done with following parameters: a bonding temperature of 120 °C and a bonding pressure of 10 MPa. A bond time, however, was not mentioned. A bond strength of 20 MPa was measured.

2.5.3.3 Polystyrene

The parameters used to diffusion bond polystyrene substrates are very similar to ones used for PMMA, except for the required bonding time. Li et al. (2012) heated the substrates to 102°C while applying a pressure of 4MPa. A bonding time of 120 min was reported.

Young et al. (2011) successfully bonded two PS substrates using the following parameters. A bonding temperature of 90°C while applying a pressure of 3.45MPa. Unlike Li et al. (2012), who reported a bonding time of 120 minutes, Young et al. (2011) concluded that a bonding time 30 min provide the highest bond strength, while minimizing channel deformation.

2.5.3.4 Polycarbonate

Yi et al. (2010) used polycarbonate for the fabrication of a microfluidic chip. To create a satisfying bond, the substrates were heated to a temperature of 135 °C. A pressure of just 0.5 MPa was applied. Time required to achieving bonding was noted at 15 min.

Liu et al. (2001) conducted a similar test but used slightly different parameters. In this test, the substrates were heated to 134 °C while a pressure of 4 metric tons was applied. The test pieces measured 9 inch². This translates in a pressure of 6.75 MPa, when converted to SI-units. 10 minutes was reported as the required bonding time.

Wang et al. (2008) used an air plasma treatment, to clean the surface of the polycarbonate substrate, before bonding. The bonding itself was performed at a bonding temperature of 128°C and a pressure 0.1 MPa for 2-3 minutes.

2.5.4 Choice of material with its bonding parameters

Polycarbonate is, as mentioned in the literature, very hard to diffusion bond with taking extra measures such as, for example, a surface treatment/modification. Another reason is the wide range of bonding pressures, which were used in these journal articles. For these reasons, polycarbonate will not be tested in the practical tests.

COC will also be precluded as a possible test material because of the wide range bonding temperatures, found in the literature. This is due to the fact that COC is available in many different compositions, each with a different glass transition temperature. This would require extra tests, such as a glass transition temperature measurement using a differential scanning calorimeter or DSC. COC also has a reasonable high glass-transition temperature ranging from 151 to 169 °C (*CES EduPack 2013*, n.d.).

Polystyrene has, according to the literature, a relative low bonding temperature and pressure. This makes PS a likely candidate for conducting bonding tests.

PMMA might be the most researched polymer when used in microfluidic devices. This material has, just like polystyrene, a low bonding temperature and pressure. Another advantage of this material is the fact that a lot of research has already been devoted to improve bonding quality.

In the end, PMMA is chosen as test material because of the abundance of information available regarding every aspect of diffusion bonding this material.

3 Methodology

3.1 Base material

As mentioned in the literature review PMMA is chosen as base material, more specifically Plexiglas® XT sheets. The thickness of these sheets is 2 mm. Plexiglas® XT is the PMMA variant manufactured using an extrusion process.

3.1.1 Material properties according to the manufacturers specification

The most relevant material properties for this application are:

- Young's modulus: 3.3 GPa;
- Poisson's ratio: 0.37;
- Tensile strength (23 °C): 72 MPa
- Vicat softening temperature: 103 °C (the glass transition temperature was not listed);
- Forming temperature: 150 – 160 °C.

More material properties of PMMA can be found in appendix 2.

3.2 Size and geometry of the test samples

The size and geometry of the test samples are both very important for the further progress of the bond tests. The size has a direct effect on the test parameters. During the bond process, these sample will be put under pressure. The size of the samples will ultimately determine the contact area. Choosing dimensions too big will result in a large contact area. If we aim for a certain pressure, we will have to increase the applied force to compensate for the increased contact area. Smaller dimensions, on the other hand, could result in instabilities.

The test sample consists of the polymer plates, which have the following dimensions:

- Length: 75 mm
- Width: 25 mm
- Thickness: 2 mm

The geometry of these two polymer plates can be seen in picture 10.

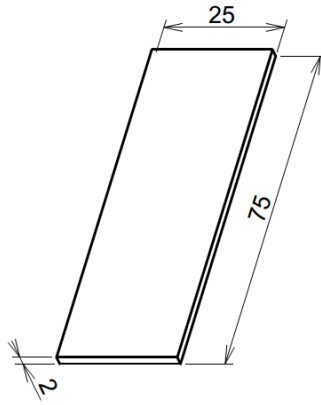


Figure 10: one of two polymers plates with its dimensions

These two polymer plates will be put together to create a cross-like geometry. This can be seen in the following picture.

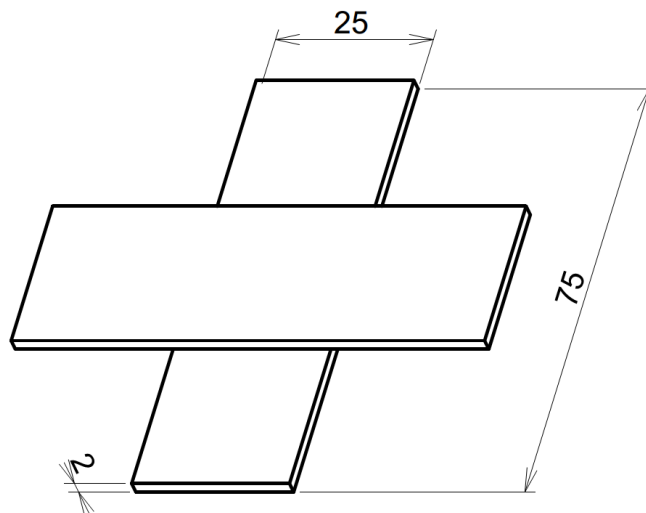


Figure 11: The cross-shaped geometry of the bonding samples

3.3 The bonding process

The diffusion bonding process of polymers is driven by temperature, bonding pressure and time. There are different methods to achieve a certain pressure or heat.

3.3.1 Heat source

The heat source, which will be used for these tests, is a conventional convection oven. This oven is a Heraeus series 6000 heating ovens / air-circulation ovens and has a range from 40°C to 300°C, which will be sufficient. The trays of the oven are stiff enough to hold the weight without bowing too much. The reason for using this oven is because of the relative quick heat-up time and good accuracy. The built-in thermometer was just off by 1 °C when tested. This difference is negligible in this application. A picture of this oven can be seen below.



Figure 12: Heraeus series 6000 heating oven/air-circulation oven

3.3.2 Applying pressure

Applying a certain pressure will be done using cast-iron weights. The total weight will depend on the surface area. The setup can be seen in the picture below.



Figure 13: the test setup with the stack of weight acting as pressure

3.3.3 Time

The time will be monitored with a simple stopwatch. For the regular bonding tests, these time will be in the order of 10 minutes to possibly two hours. The stop-off tests, on the other hand, will be tested for a time of at least 10 hours.

3.4 Strength test

3.4.1 General setup

To test the bond strength, a tensile-compression test machine (Zwick-Roell Z020 20 kN Material Test Machine) is used. The two crossheads can be interchanged with different ones. The tools, that were used, are normally used to conduct bending test. In this test two of these tools are used, albeit 90° rotated from each other.



Figure 14: Zwick-Roell Z020 20 kN Material test machine



Figure 15: close-up of the tools of the material test machine

A test sample installed in this setup can be seen in the picture below.

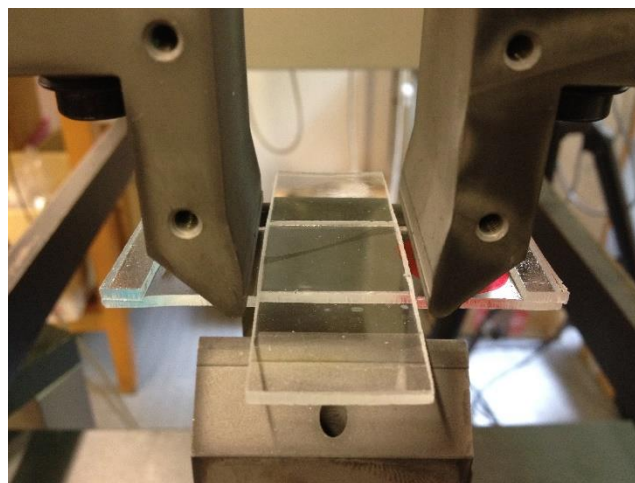


Figure 16: close-up of the tools of the material test machine with a test sample

3.4.2 Machine parameters

Grip to grip separation: 575 mm

LE speed: 100 mm/min

(Speed by which the crosshead travels from the current position to the start position)

Pre-load: 2N

(Test begins after reaching this pre-load value)

Pre-load speed: 10 mm/min

(Speed by which the crosshead travels to Pre-Load value)

Test speed: 0.5 mm/min

Force shutdown threshold: 80% F_{MAX}

(Test will be terminated when the force decreases below this value)

Force threshold for break investigation: 0.1% F_{NOM}

(Break detection will be activated after force value is reached)

Maximum extension LE channel: 10 mm

(Test will be terminated once this extension value is reached)

3.5 Preliminary tests

3.5.1 Fine-tune test setup

To come up with a good setup, which gives accurate results, preliminary tests have been done to uncover any issues regarding the use of the equipment. These preliminary tests also give an indication about the range of the parameters. A full report of the findings and an overview of the used parameters can be found in appendix 3.

The oven, which was used, has steel grills similar to the grills used in common household ovens. These grills, although quite rigid, did bend slightly under the weight of the weights. This causes instability to the setup. The preliminary tests showed that using the grill did not give reliable results. Often the stack of weights tilted to one side, causing the samples to be bonded on only one side. In the bond tests, the grill was not used. The entirety of weights and acrylic samples was put on the bottom of the oven.

In order to provide a solid base, thick steel plates were used. These plates do not bend under the weight. A downside of these plates is the slow heat-up time. To accommodate the possibility of a rapid temperature change, a thin aluminium plate was used. In earlier tests, a thick steel plate was used. In later tests, an aluminium plate was put between the thick steel plate and acrylic samples. The thin aluminium plate had the added benefit of being really smooth and flat. This also improved the bonding process.

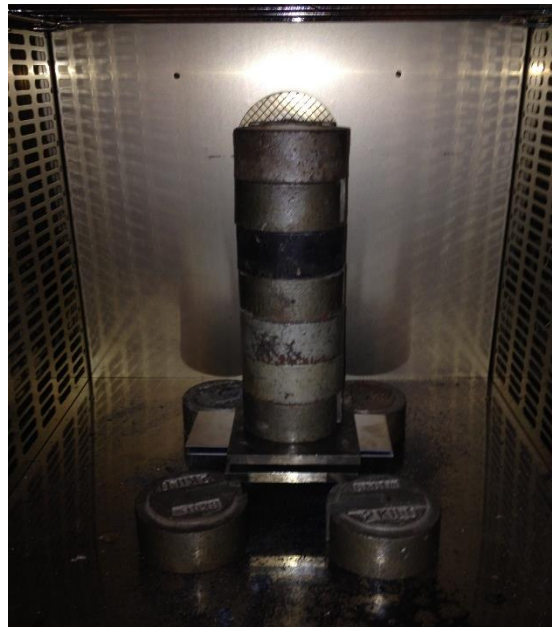


Figure 17: Improved setup for the bonding process.

The acrylic samples were bonded in cross shape. This made it easier to test its bond strength. This cross shape, on the other hand, did introduce a disadvantage to the stability of the setup. In the earlier tests, the stack of weights would often tilt to one side when the weights were placed slightly off-centre. This caused the samples to only bond on one side. To improve the stability, small supports were added to the overhanging sides. This did increase the surface area, which lowers the pressure because the weight is more distributed over a larger area. This means that the weight has to be increased in order to have the same pressure.

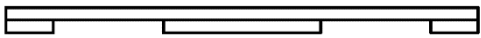
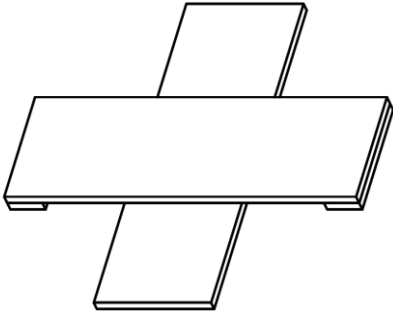


Figure 18: 3D-representation of the improved test sample which includes the small supports on either side.

Figure 19: Frontal view of the improved test sample.

The full setup with the added steel and aluminium plates can be seen below.

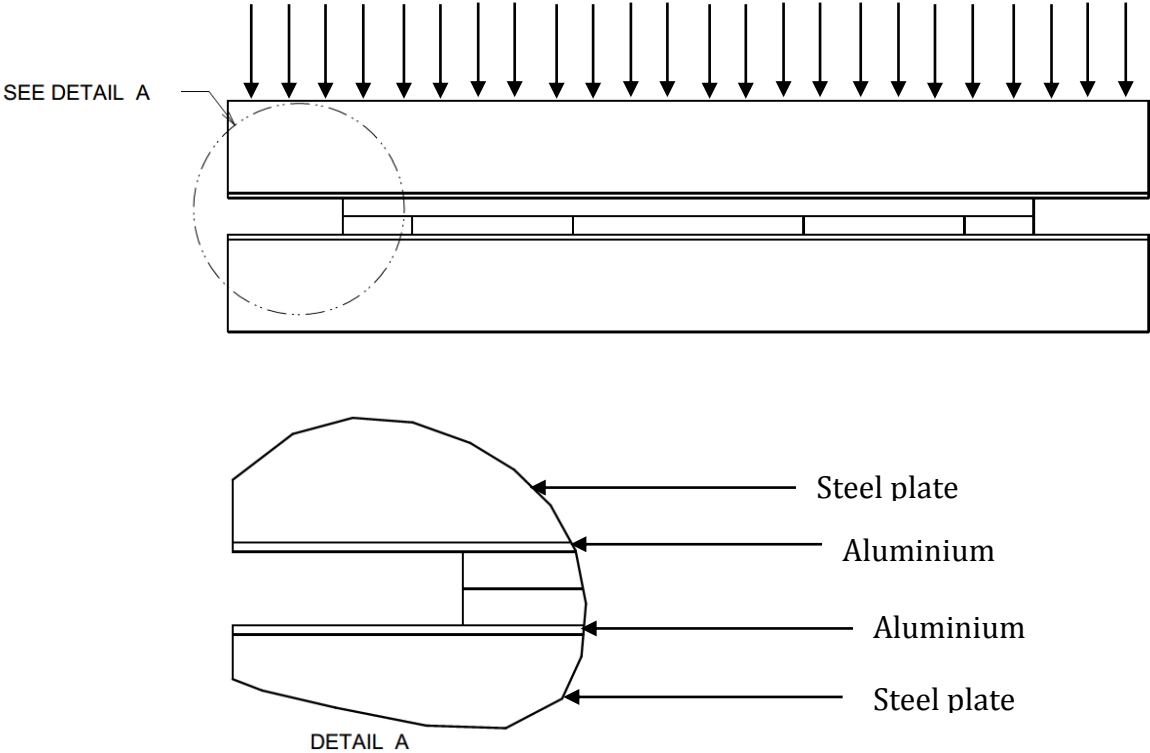


Figure 20: Frontal view of the improved test setup. The arrows represent the pressure. The detail view shows the different layers of the test setup

3.5.2 Determination of the rough bonding parameters

The preliminary tests provided a rough estimation of the process parameters. To determine the actual process limits, further tests have to be conducted. The most important parameter, when looking at implementation in the industry, is the time. A time reduction will result in the greatest saving. To do this in a logical manner, a flow chart was made to reflect the sequence in which the practical tests will be conducted.

This flow chart consists of parameters, which will be tested. From the preliminary tests, it was remarked that a temperature higher than 120 °C results in significant deformation. This is, therefore, taken as the upper temperature limit. The dimension of the oven and the amount of available weights give an upper limit in pressure. These weights have considerable dimension. The oven, on the other hand, has limited interior dimensions. This makes the amount of weight, corresponding with a pressure of 0.31 MPa, the maximum. Time is the only parameter which can be tested more freely. As noted above, this is also the most decisive parameter. The tests will, therefore, look at lowering the time required for bonding.

The results of each test will determine the next set of parameters. The flow chart can be seen in the following picture. The results of each tests will not be tested on strength. Failure or success of the bond is determined with a manual tests. If the bond has some strength, the test will be considered a success, in the flow chart marked with a "yes". If the test did not produce a bond, the result will be seen as a failure, in the flow chart marked with a "No".

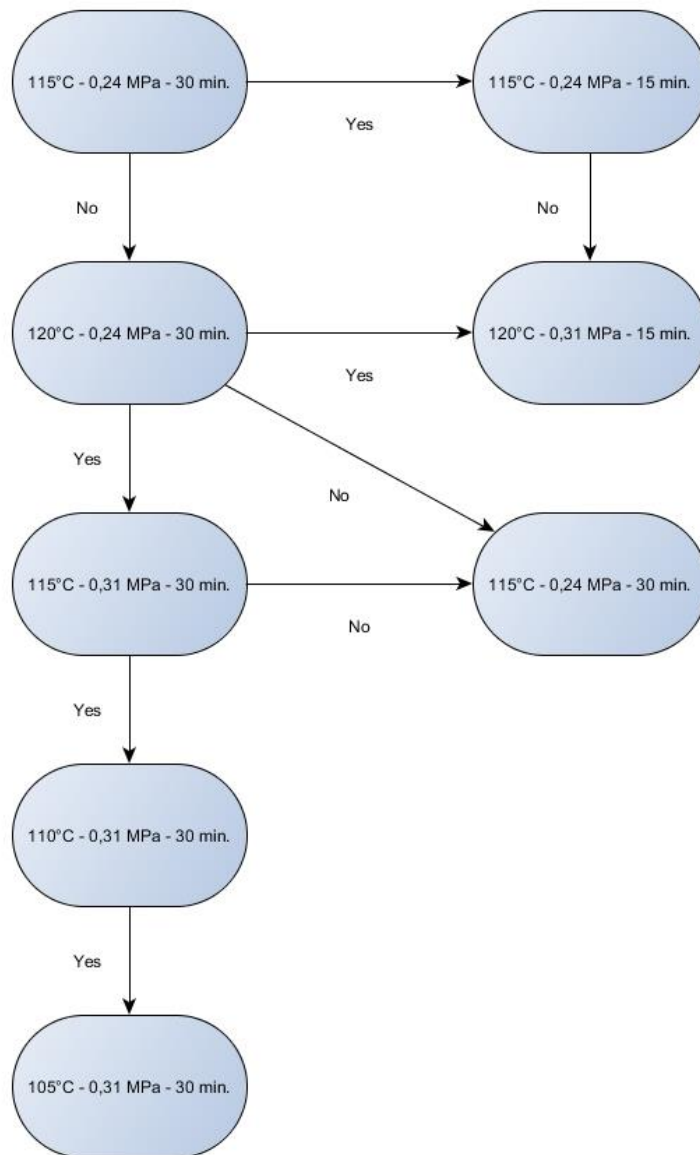


Figure 21: Flowchart to determine the parameters for the following tests

3.6 Bonding tests

To give more definitive results, more tests will have been conducted.

3.6.1 Control test

To identify the strength of the material in this application, a control test was conducted. This control test puts the sample under the same stress as the regular bonding tests. To eliminate the bond strength from this experiment, the sample was inverted. This way the sample will experience the same stresses and can be seen as a bond put under pressure. A picture of the setup can be seen below.

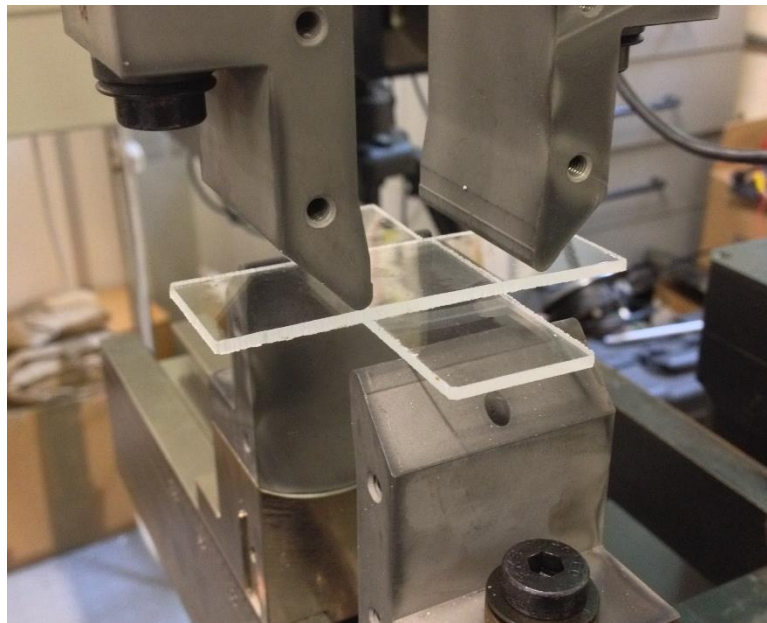


Figure 22: Control test to determine strength of the material.

This control test uses the same machine parameters as the regular strength tests. Two control tests are conducted

3.6.2 Bonding parameters

The times, which will be further tested, are 30 and 60 minutes. During the preliminary tests, shorter times were tested but these did not give a reliable bond.

The temperature parameter of 115 and 120°C are tested. A temperature higher than 120°C resulted in significant deformation. A temperature lower than 115°C was also tested during the preliminary tests but did not produce a good bond.

The same pressures as in the previous test, 0.25 MPa and 0.31 MPa, will be further used.

A summary of the test parameters can be seen in the picture 23

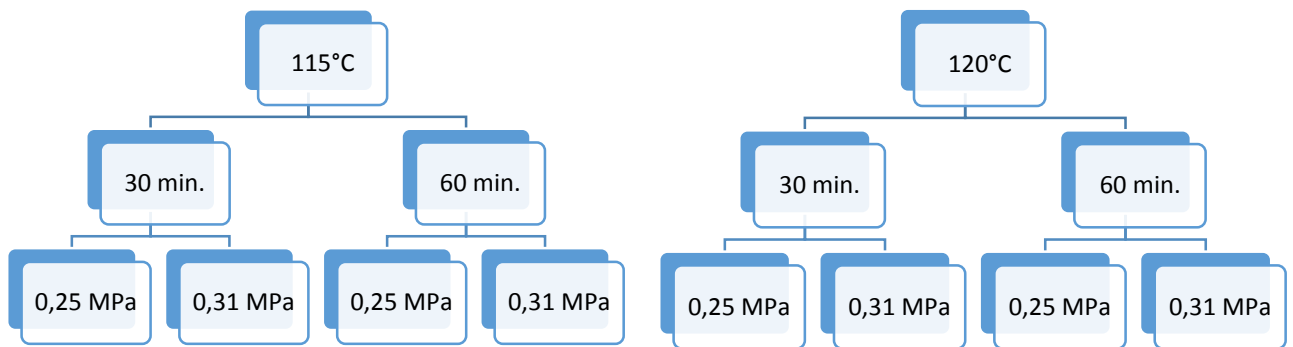


Figure 23: Parameters for the bonding tests. Each set of parameters is tested twice

Each combination is tested twice to give an indication of the repeatability. The limited amount of tests was due to time constraints.

3.6.3 Modelling the strength test

To evaluate the results from the strength tests, a finite elements modelling will be conducted. This model will essentially be a digital reproduction of the actual sample and the compression test machine. The finite elements software, which will used, is MSC Marc Mentat 2010.2.0 (32 bit)

3.6.3.1 *The model*

The model, representing the real-life setup, can be seen in the picture below. The dimensions of this model are identical to ones in the real life tests. The purple and pink sections correspond with the two sheets and are deformable bodies. The green and yellow sections represent the tools of the compression test machine and are rigid bodies. The yellow “tools” stay on the same place while the green “tools” move down.

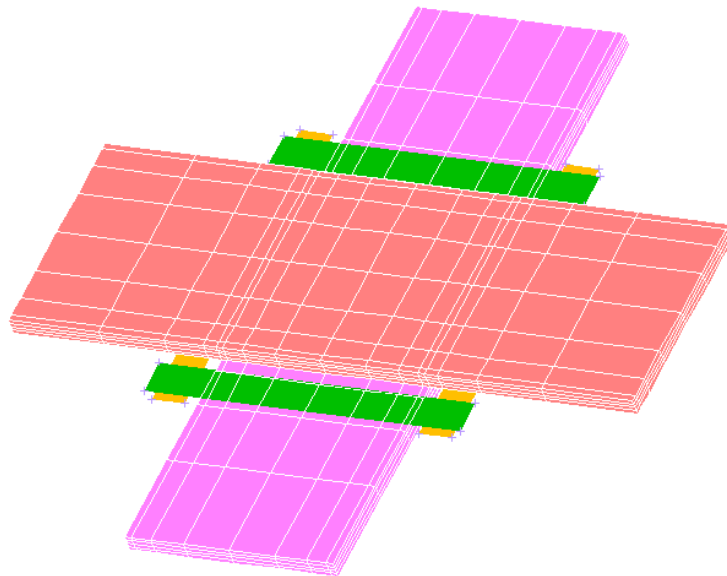


Figure 24: The 3D representation of the model. The pink and purple objects represent the upper and lower PMMA sheets. The yellow and green objects display the lower and upper tool respectively

The mesh is not uniform across the entire surface. The next picture shows more details of the mesh. It can be observed that the mesh is finer near the edges of the bond. The reason for this is that the surfaces will start to come apart at those specific places. The mesh of the deformable bodies consists of 3D solid elements.

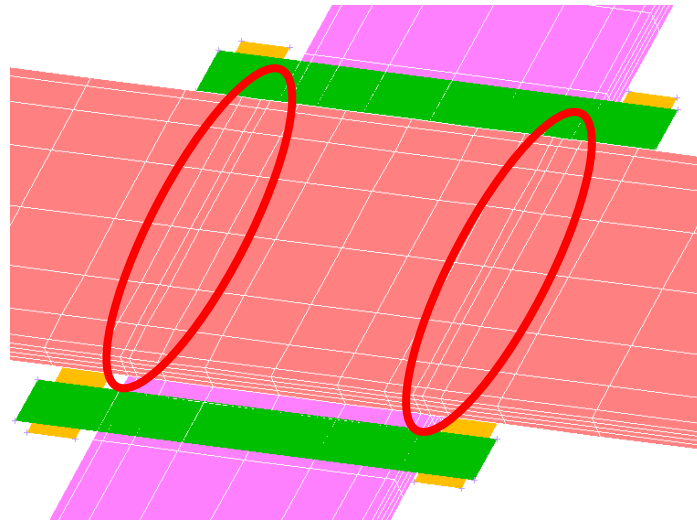


Figure 25: annotating the difference in the mesh size.

The material properties were chosen so they would match these of the real material PMMA. When looking purely at the elastic-plastic isotropic behaviour, only the young's modulus and poison's ratio are important. The Young's modulus can be determined from the stress-strain curve. The result from the tensile test can be found in appendix 4. Poison's ratio could not be determined due to the lack of the right equipment. This value was looked up in the datasheet (see appendix 2. The values for these material properties are:

- Poison's ratio: 0.37
- Young's modulus: 5 GPa

The upper and lower plates represent the two deformable bodies i.e. the PMMA sheets. The upper and lower tools correspond to the crossheads on the compression test machine. The PMMA sheets are diffusion bonded in real-life. In this modelling software a bond is approximated with a glued connection with limited strength. As mentioned before, a good diffusion bond has the same material properties as the parent material. The only important value in this application is the breaking normal stress. As mentioned above, a tensile test was conducted. The value of the resulting ultimate tensile stress during this test, i.e. 65 MPa, has also been taken as the breaking normal stress.

The lower tool, which are the yellow sections in picture 24, remains on the same place. The upper tool, which are the green sections, move down with a fixed velocity. Both the low and high tool have an approach velocity, which was done to prevent errors with the geometric bodies not "seeing" each other when running the simulation.

The loadcase has a loadcase time of 0.5 seconds with a constant time step of 0.01 seconds. This equates to a total of 50 steps.

3.7 The effect of post-annealing

3.7.1 Test setup and parameters

To test the effect of a post-annealing treatment, two samples were tested with identical process parameters. The results will be compared to the regular bonding test, while using the same process parameters shown in table 2

Bonding parameter	test value
Bond area [mm ²]	25x25
Surface cleaning	Soap + methanol
Bonding temperature [°C]	120
Bonding pressure [MPa]	0,313
Bonding time [min.]	60

Table 2: Bonding parameters to post-annealing test

These parameters were chosen because of the following reasons. In the bonding test, it was noted that these parameters did not give the highest bond strength but, on the other hand, the samples did not deform significantly. The degree of deformation is important regardless of the application. The annealing treatment is, as mentioned in the literature review, a specific process recommended by the manufacturer of the material (see appendix 5).

The annealing temperature, recommended by the manufacturer, is 75°C. The minimum required time, in hours, is given by the materials thickness divided by 3 with a minimum of two hours. The samples are made up of two, three millimetre layers. This would mean a theoretical annealing time of one hour, but the minimum required time is two hours. The last step in the annealing process is the cooling. The cooling time, in hours, is given by the material thickness divided by four with a maximum cooling speed of 15°C per hour. Three millimetres divide by four would mean a cooling time of just 45 minutes. Cooling from 75°C to ambient temperature (20 °C) in 45 minutes would translate to a cooling speed of 73 °C per hour but the maximum cooling rate is 15 °C per hour. The oven, in which the annealing was performed, had no function to control the cooling. The oven was simply turned off and the samples were left overnight to slowly cool down. The big volume of the oven ensured that it cooled down reasonably slow. The oven also contained numerous bits and pieces. This also contributed to a gentle cooling process.



Figure 26: The oven which will be used to perform the annealing

The samples were each placed between two metals plates with negligible weight to provide a solid base.



Figure 27: The setup for the annealing process

3.8 The effect of polishing

The effect of polishing will be examined the same way as with the effect post-annealing. One sample was polished with Brasso metal polish (Reckitt Benckiser). The other sample was not polished. In the preliminary tests, the technique of polishing the sample was already tried but the results were unsuccessful. The polishing technique, used in the preliminary test, consisted of rubbing the samples in a circular manner. The idea behind this is that roughness of each sample will improve the other sample (see preliminary test 11 in appendix 3). This technique did not improve the bond strength because it resulted in an unbonded sample. The test will use another polishing technique. A piece of cloth, with some metal polish, is used to manually make circular movements.

The bonding parameters can be seen in the table below.

Bonding parameter	Test value
Bond area [mm ²]	25x25
Surface cleaning	Soap + methanol
Bonding temperature [°C]	120
Bonding pressure [MPa]	0,313
Bonding time [min.]	60

Table 3: Bonding parameters to test the effect of polishing

3.9 Creating a cellular structure

In order to create a cellular structure, a way has to be found to selectively bond two polymer sheets. There are multiple ways to achieve this selective bond.

The first way this can be achieved is through the use of a stop-off. A stop-off is a substance or process that will inhibit the bonding at the areas where this substance or process is applied. A first advantage is that, depending on the substance itself, it can easily be removed after the process and does not physically modify the surface.

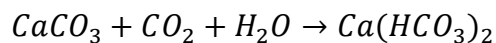
Another way is to have a moveable heat source, which can bond these sheets at certain places. However there are a couple of disadvantages with this technique. A moveable heat source will almost certain require a bespoke, and thus expensive, new device. Another disadvantage is the limited bonding speed.

3.9.1 Substances

The use of a stop-off in the bonding process of polymers has not been researched before. As a result no possible stop-off's are known. The tested stop-off are a result of observations, made during the preliminary tests.

3.9.1.1 *Stop-off 1: chalk powder*

The first substance, that will be tested, is chalk powder. The chalk powder, used in these tests, is ground up white classroom chalk. The main component of chalk is calcium carbonate (CaCO_3), a form of limestone. An added advantage of using chalk is that it can be easily removed with carbonated water. This chemical reaction will result in soluble calcium bicarbonate:



3.9.1.2 *Stop-off 2: silicone spray*

During the preliminary tests, it was observed that a greasy surface negatively affects the bonding process. This disadvantage during bonding might be used to our advantage when looking for a new stop-off. To test the effect, a silicone release agent was used. A silicone release agent S3 (MCP Tooling technologies limited) is a specific spray, used as a release agent in vacuum casting. The container notes that the spray must not be exposed

to temperatures exceeding 50°C. This might be an issue because the silicone spray might just evaporate at the temperatures, at which the bonding tests will be performed.

3.9.1.3 *Stop-off 3: surface roughening*

The third stop-off, that will be tested is a process unlike the previous stop-offs. During the preliminary tests, it was noticed that polishing improves the bonding process. This would also implicate that a rougher surface would impair the bonding process and possibly inhibit the process entirely. To roughen the surface, a medium grid sandpaper was used. The surface roughness afterwards was not determined due to the lack of specialized equipment.

3.9.2 Tests

To assert the effectiveness of these stop-offs a number of tests were conducted. In these tests, only the performance of the stop-off will be examined. The samples were bonded overnight resulting in an extremely long bonding time. If the stop-off can inhibit bonding during this time, the result will be indisputable and therefore give conclusive results regarding its effectiveness. The sample will undoubtedly deform but this is not important in these bonding tests. The setup has remained the same as previous tests.

The bonded area measures 25 mm by 12 mm. The samples were prepared in the same way as the previous tests. They were first cleaned using a mild detergent. Afterwards the samples were rinsed with methanol to remove any residue. The samples were left overnight to achieve optimal bonding conditions. The reason for the long bonding time is to have conclusive results. If the samples do not bond, even after more than 16 hours, it can be concluded that the stop-off works successfully.

3.9.2.1 *Stop-off test 1: Chalk powder and silicone spray*

The test parameters of the first test can be seen in the table below. The test consisted of three samples: one with chalk powder, one with silicone spray and one control sample without stop-off.

Bonding parameter	Test value
Bond area [mm ²]	3 x (25x12)
Surface cleaning	Soap + methanol
Bonding temperature [°C]	115
Bonding pressure [MPa]	0,256
Bonding time [min.]	1000

Table 4: Bonding parameters for stop-off test 1

The test sample can be seen in the picture below. Although it cannot be deduced from the picture, the left strip has the chalk applied to it. The middle strip is the control sample, to ensure the samples are actually bonding. Silicone spray was used as a stop-off in the right sample. This setup does not include the small supports because the purpose of this test is to see whether these substances can act as stop-off. These samples will deform heavily but this is unimportant in these tests.

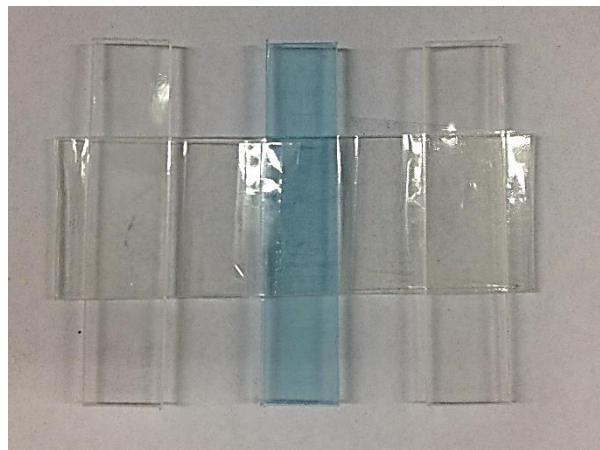


Figure 28: The geometry of the samples for the stop-off test 1

3.9.2.2 Stop-off test 2: chalk powder

The second test focuses on using chalk as a stop-off. For the test, both the temperature and pressure was increased to further test its effectiveness. The temperature was increased from 115°C to 120°C and the pressure from 0,256 MPa to 0,350 MPa. The increase in pressure is simply due to the fact that only two strips are tested, unlike the three strips in the previous test.

This was again tested overnight. The test parameters can be seen in the table below.

Bonding parameter	Test value
Bond area [mm ²]	2 x (25x12)
Surface cleaning	Soap + methanol
Bonding temperature [°C]	120
Bonding pressure [MPa]	0,3515
Bonding time [min.]	1000

Table 5: Bonding parameters for stop-off test 2

The test sample can be seen in the picture below. The left strip is the control. Chalk was applied to the right strip.

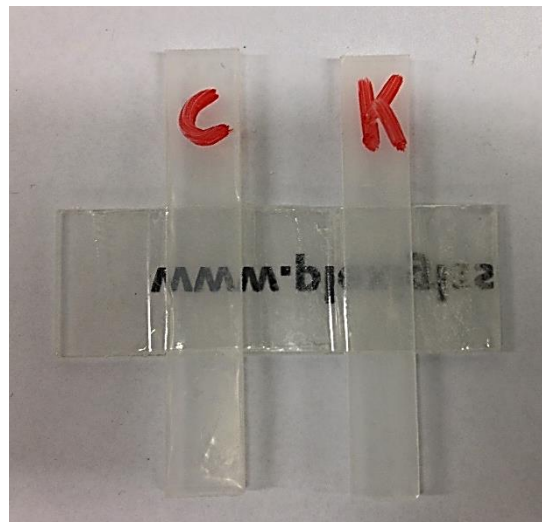


Figure 29: The geometry of the samples for the stop-off test 2

3.9.2.3 Stop-off test 3: Roughening the surface in order to inhibit bonding

In the third test, the effect of roughening the surface is examined. To increase the surface roughness a medium grid sandpaper was used. After sanding, the sample was cleaned in the same way as the other tests. The test parameters can be seen in the table 4.

Bonding parameter	Test value
Bond area [mm ²]	2 x (25x12)
Surface cleaning	Soap + methanol
Bonding temperature [°C]	115
Bonding pressure [MPa]	0,3515
Bonding time [min.]	1000

Table 6: Bonding parameters for stop-off test 3

3.10 Surface analysis of bonded area

To further investigate the bonding process, the surface of the bonded area has been looked at. A confocal laser scanning microscope was used. This type of microscope produces a high-resolution optical image. This microscope can also focus at any depth in the sample.

3.10.1 Test equipment

The confocal laser scanning microscope used in this test is the Olympus LEXT Confocal laser scanning microscope. The general specifications can be found in appendix 6.

3.10.2 Tests

The first test is a control test. This control test will be done on a blank, non-bonded sample. This will be a reference for future tests. The second test will zoom in at a good bond. The final test will look at the surface of a bad bond.

4 Presentation of findings

4.1 Determination of the rough bonding parameters

Before moving to the actual bonding tests, a couple of tests were conducted to determine the process window. As mentioned before, a flow chart was made up. The results of the tests can be seen in the figure below. The coloured balloons are the tests, which were conducted. The green balloons represent the test, which were successful. The red ones were unsuccessful. The uncoloured balloons represent the tests which were not conducted as a result of the outcome of the preceding tests. The arrows indicate the next logical step with a “yes” or a “no”.

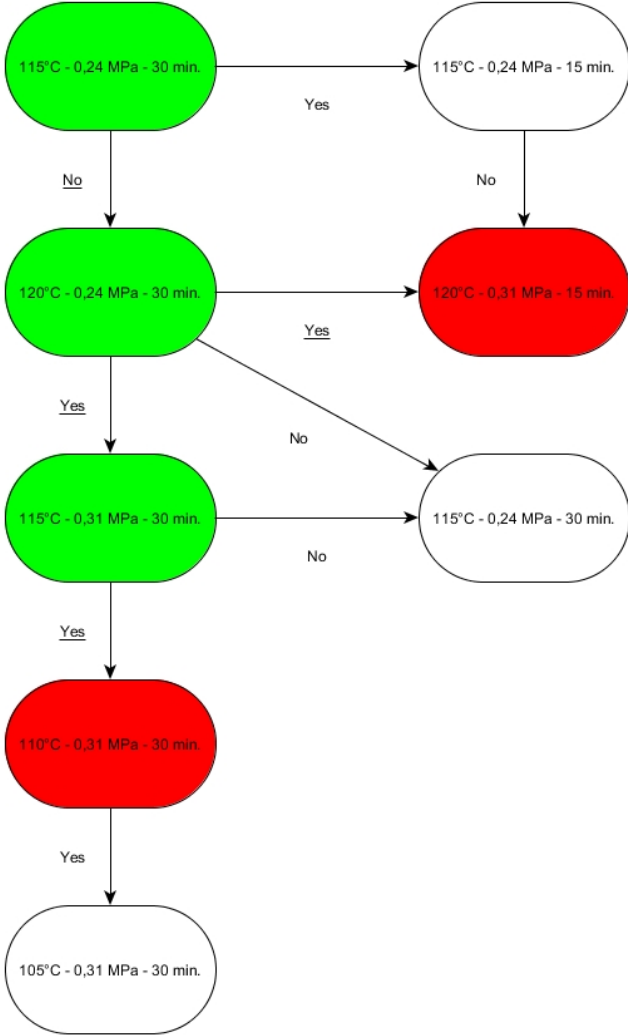


Figure 30: Resulting flowchart to determine the parameters for the following tests. The uncoloured balloons represent the tests which were not conducted. The green balloons represent the tests, which were successful. The ones were unsuccessful.

From these results, a few remarks can be made regarding the parameters. Both 115°C and 120°C are important temperatures, which will be examined further. A temperature below 115°C did not produce good bond.

This tests looks mainly for lower bond times. Only tests, with a bond time of 30 minutes or higher, were successful. The actual bond tests will certainly test bonds using a bond time of 30 minutes.

The last parameter is the pressure. This test did not really look at different pressures because of the limitation of the oven. Only 0.24 MPa and 0.31 MPa were tested, both of which can produce good bonds.

4.2 Bonding tests

4.2.1 Control test

The results from the control test can be seen in the picture 32 and table 7.

Test	Max. force [N]	Bond strength [MPa]	Elongation [mm]
1	206,24	0,33	5,69
2	221,95	0,36	4,55

Table 7: Bond strength results for the control test

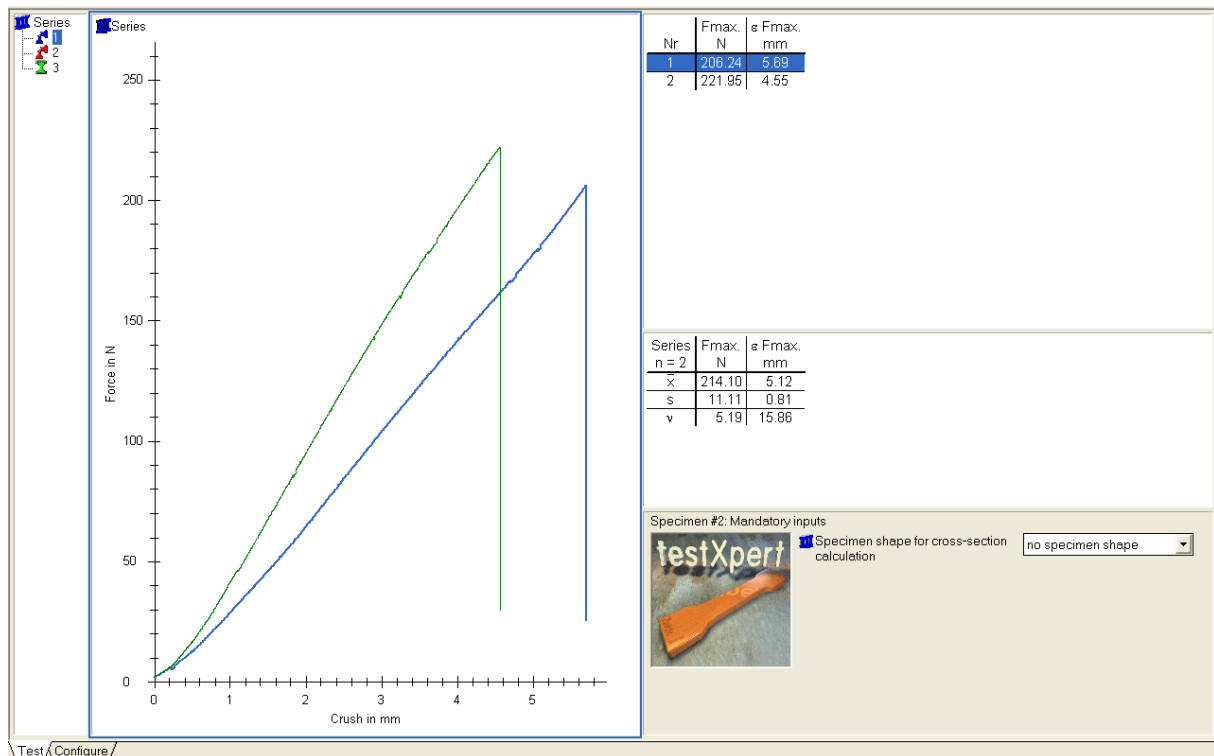


Figure 31: Compression curve for the control test

The results are somewhat surprising. The “material strength” in test 1 is 7% off in comparison with the second test. A possible reason for this difference can be the position of the sample in the tools in the tools of the tensile-compression test machine, another being the unavoidable scatter in the resulting properties.

The difference in elongation, before failure, is even more significant. The difference between test 1 and 2 is 20%.

Both the substantial difference in material strength as elongation need to be investigated further.

4.2.2 Bonding tests with a bond time of 30 minutes

The result of bonding test with a bond time of 30 minutes can be seen in the table 6. The strength curves for these tests can be found in appendix 7. This table gives the two other bonding parameters: temperature and pressure.

The results of the strength tests can also be found in the same table. The maximum force is the force which the machine exerted on the sample prior to failure. This force is measured in newton. The bond strength is the strength calculated from the maximum force and bond area. This bonded area remains the same for every test. The bonded area is 625 mm². The bond strength can thus be calculated using the following formula:

$$\text{Bond strength [MPa]} = \frac{\text{Max. force [N]}}{\text{Bonded area [mm}^2\text{]}} = \frac{\text{Max. force [N]}}{625 \text{ [mm}^2\text{]}}$$

The elongation is the distance the tools moved relative to each other measured from the beginning of the test until the sample failed. This elongation is measured in millimetres. The last column in this table is the bond state. This describes the way the sample failed. This can either be that the bond failed or that the material fails. When the materials fails, the bond stays intact. This means that the bond is stronger than its parent material.

Temperature [°C]	Pressure [MPa]	Max. force [N]	Bond strength [MPa]	Elongation [mm]	Failure
115	0,256	33,95	0,054	0,77	Bond failed
115	0,256	18,47	0,030	1,38	Bond failed
115	0,313	31,60	0,051	0,63	Bond failed
115	0,313	38,00	0,061	1,07	Bond failed
120	0,256	59,13	0,095	1,09	Bond failed
120	0,256	45,15	0,072	1,99	Bond failed
120	0,313	51,38	0,082	1,83	Material failed
120	0,313	76,64	0,123	1,85	Material failed

Table 8: Bond strength results for the bonding parameters with a fixed bonding time of 30 minutes

Table 6 is also plotted in the next figure. The x-axis is the bonding temperature in °C. The y-axis is the bonding pressure in MPa and the Z-axis is the bond strength also in MPa. Note that these are tests which were conducted with a bonding time of 30 minutes.

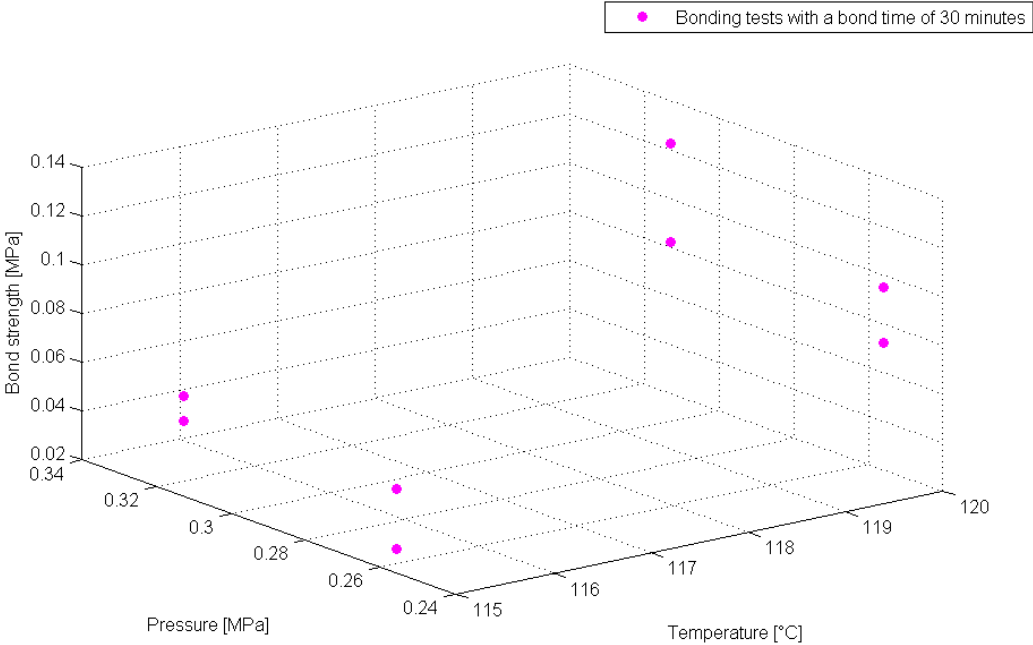


Figure 32: Graph showing the results from the bond strength tests with their bonding parameters (fixed bond time of 30 minutes)

From this graph, it can clearly be remarked that both a higher temperature and pressure will be improve the bond strength. The effect of temperature is much greater when compared with of the effect of pressure. This would indicate that the temperature has a much more profound effect on the bond quality. It must, however, be noted that the pressure range was limited by the size of the oven. The temperature on the other hand was not limited by any means, other than the deformation of the sample. The limited effect of the pressure could also be due to the fact that the surface quality of the material is good enough that it does not require a high bonding pressure.

The following figure shows the bond state during “failure”. The blue dots represent the samples of which the material failed and not the bond itself. The purple dots, on the other hand, display the samples of which the bond failed.

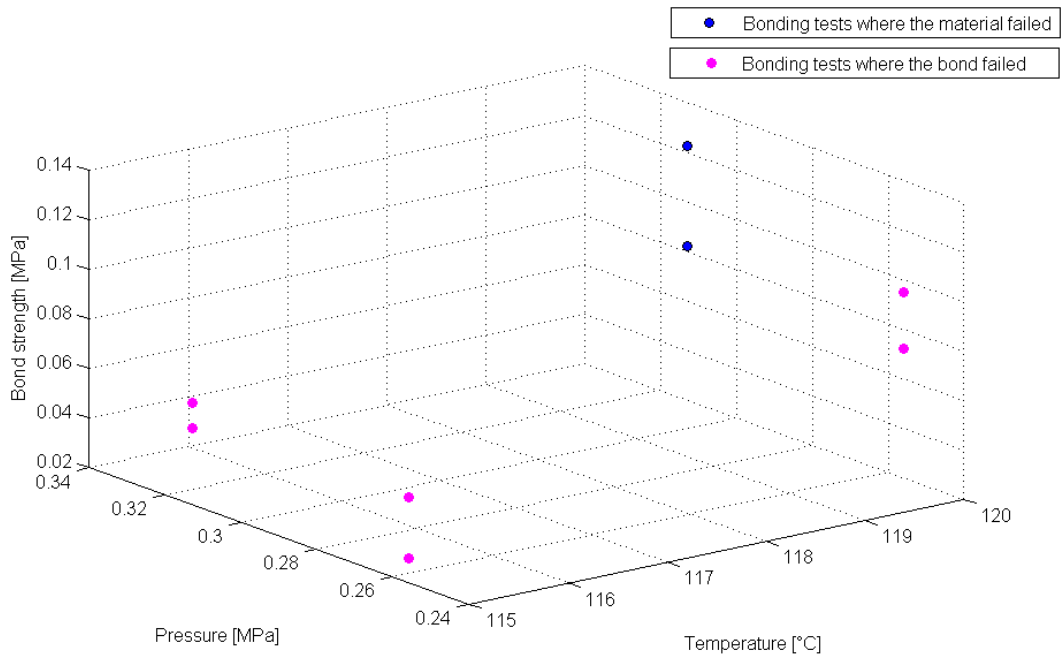


Figure 33: Graph showing the bond state after the bond strength tests with their bonding parameters (fixed bond time of 30 minutes)

For this graph, it can be observed that both an increased bonding temperature and increased bonding pressure is necessary to achieve a bond that will not fail. It, however, has to be remarked that there seem to be some irregularities with either the bond strength test or the bond itself. If for instance the following tests are compared.

Temperature [°C]	Pressure [MPa]	Max. force [N]	Bond strength [MPa]	Elongation [mm]	Failure
120	0,256	59,13	0,095	1,09	Bond failed
120	0,313	51,38	0,082	1,83	Material failed

Table 9: comparison of the results from two bonding tests with a bonding time of 30 minutes

The first test in table 9 clearly shows a higher bond strength when compared to the second sample, yet the bond of this sample failed. The second test, with a lower bond strength, did not suffer a failed bond. This might have something to do with the big difference between the elongation, before failure, of these two tests.

4.2.3 Bonding tests with a bond time of 60 minutes

The result of bonding test with a bond time of 60 minutes can be seen in the table 8. The strength curves for these tests can be found in appendix 3. This table gives the two other bonding parameters: temperature and pressure.

The bond strength is calculated the same way as in the previous tests using a bonding time of 30 minutes.

Temperature [°C]	Pressure [MPa]	Max. force [N]	Bond strength [MPa]	Elongation [mm]	Bond state
115	0,256	38,29	0,061	1,16	Bond failed
115	0,256	36,98	0,059	1,46	Bond failed
115	0,313	41,36	0,066	1,29	Bond failed
115	0,313	40,95	0,066	2,26	Bond failed
120	0,256	74,68	0,119	2,14	Material failed
120	0,256	79,13	0,127	1,9	Material failed
120	0,313	65,22	0,104	2,14	Material failed
120	0,313	83,75	0,134	2,06	Material failed

Table 10: Bond strength results for the bonding parameters with a fixed bonding time of 60 minutes

These results are plotted in the figure 34. The x-axis is the bonding temperature in °C, the y-axis the bonding pressure (MPa) and the Z-axis the bond strength (MPa).

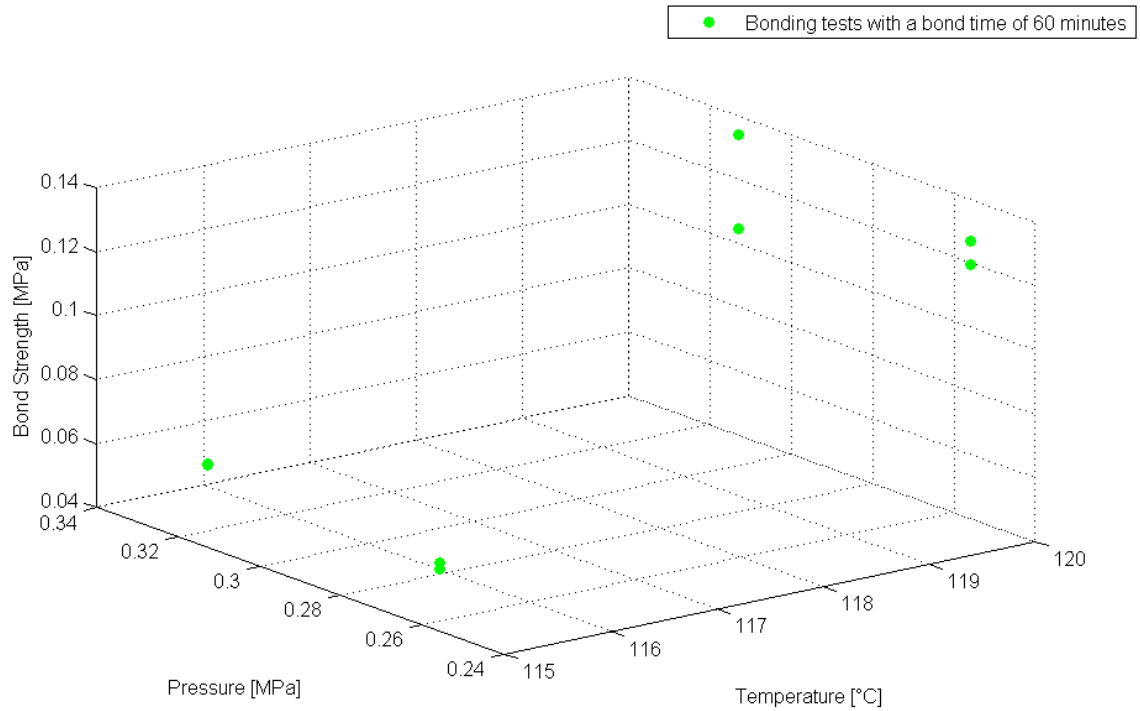


Figure 34: Graph showing the results from the bond strength tests with their bonding parameters (pressures of 0.256 and 0.313 MPa and temperatures of 115 and 120 °C, fixed bond time of 60 minutes)

Similar conclusions, as with the previous test, can be drawn for the effect of temperature. The effect of pressure however seems negligible. This could indicate, just like the previous test, that the bonding pressure might be too low. This was, however, limited by the used equipment. The other reason might again be the excellent surface quality of the material.

Figure 35 shows the bond state during “failure”. The blue dots represent the samples of which the material failed and not the bond itself. The green dots, on the other hand, display the samples of which the bond failed.

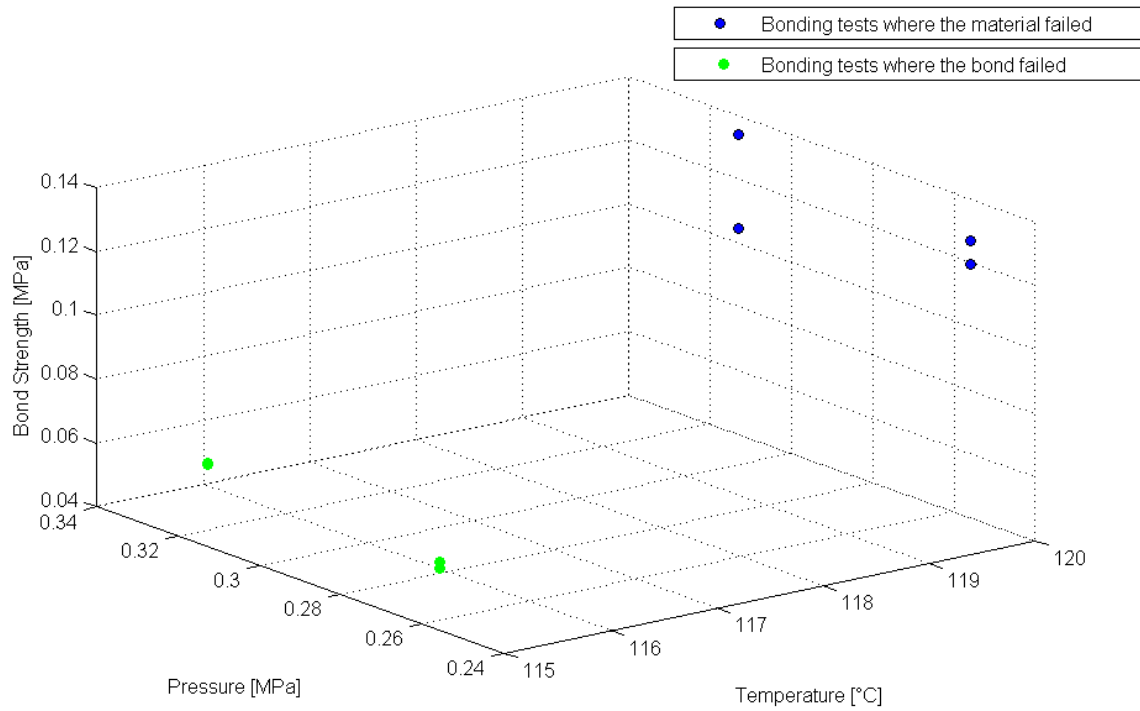


Figure 35: Graph showing the bond state after the bond strength tests with their bonding parameters (pressures of 0.256 and 0.313 MPa and temperatures of 115 and 120 °C, fixed bond time of 60 minutes)

The results from the test, using a bond time of 60 minutes, regarding the bond state is largely the same with the previous test. Bonding at 115 °C did not produce a sample, where the bond stayed intact. The difference in bonding pressure did not have a significant effect on the bond state.

4.2.4 Combined

The following picture combines the results of the tests using a bond time of 30 minutes with the results of the tests using a bond time of 60 minutes.

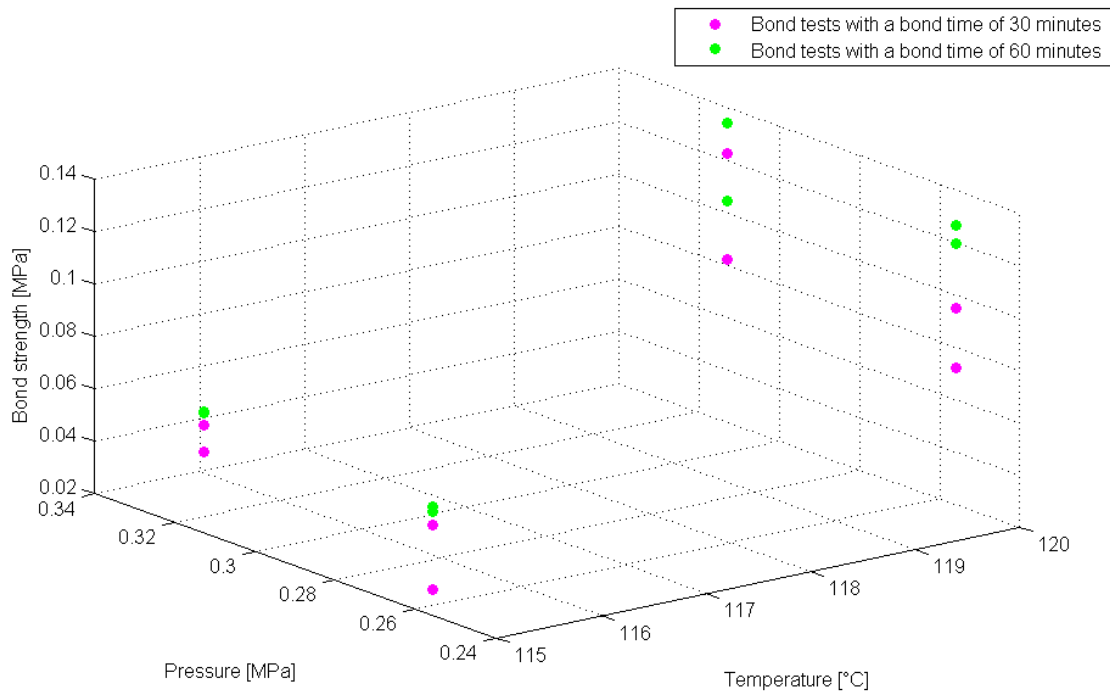


Figure 36: Comparison of the effect of different bonding times on the bond strength (pressures of 0.256 and 0.313 MPa and temperatures of 115 and 120 °C)

It can clearly be observed that the bond strength of the test using a bond time of 60 minutes are almost every time higher. The effect of the bond time on the sample which used a bond temperature of 115°C is, however, limited. The difference in this case pretty small. The effect on the samples, which used a bond temperature of 120°C, is greater but stays fairly limited. This would indicate that the bond is nearly perfect when using a bond time of 30 minutes.

Picture 37 combines the results of the bond state after the strength test with different bonding times.

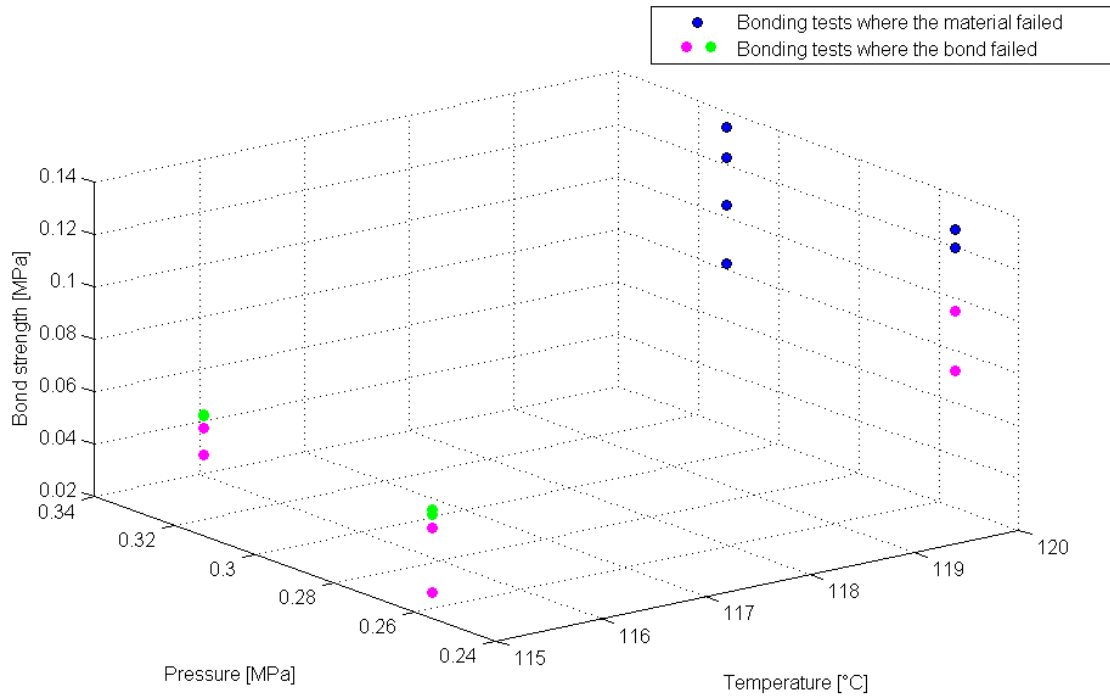


Figure 37: Comparison of the effect of different bonding times on the bond state (pressures of 0.256 and 0.313 MPa and temperatures of 115 and 120 °C)

Only at a bonding temperature of 120°C did the samples bond adequately. The bonding time did make a substantial difference to the bond state. The pressure, at which the samples were bonded, did not make a sizeable difference.

The effect of bonding pressure is limited and also the bonding time did not yield a significant difference. Increasing the bonding temperature, however, did make a substantial difference.

4.3 The effect of post-annealing

The results of the samples, which were post-annealed, are not conclusive. There are two main reasons for this. First of all, only two tests were performed. The second reason is that the results are a bit dubious. The value for the maximum strength of both tests are not really comparable.

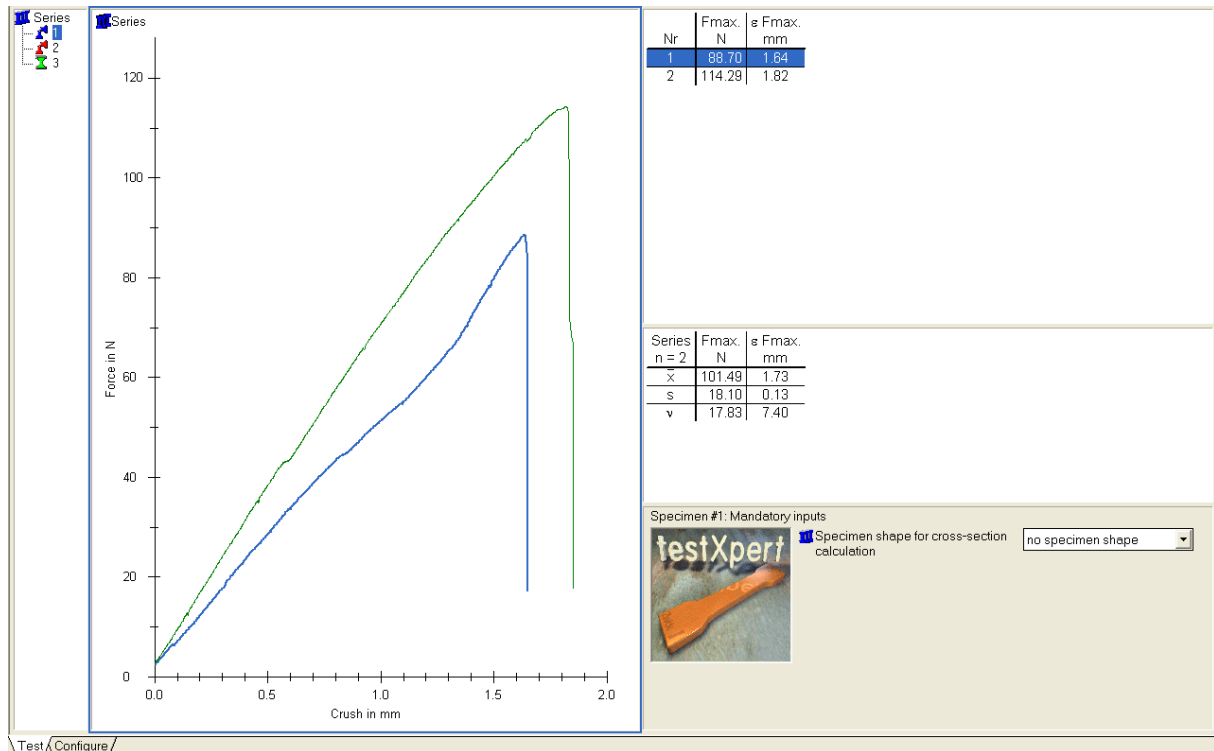


Figure 38: Graph showing the results for the experiments which look at the effect of post-annealing

When the results are compared with the samples, which not were post-annealed, a general improvement can be remarked. The results of the post-annealed samples can be found in table 11

Test	Max. force [N]	Bond strength [MPa]	Elongation [mm]
1	88,70	0,14	1,64
2	114,29	0,18	1,82

Table 11: Result from the strength test for the samples which were post-annealed

The result of the regular samples can be found in table 12. These are given for comparison.

Test	Max. force [N]	Bond strength [MPa]	Elongation [mm]
1	65,22	0,10	2,14
2	83,75	0,13	2,06

Table 12: Result from the strength test for the sample which were bonded using the same parameters

The maximum force, and therefore also the pressure, has increased in general. This can indicate a possible improvement in the bond strength but further research has to been done to confirm this. The elongation, before breaking, has dropped.

4.4 The effect of polishing

To test the effect of polishing, two tests were conducted. These results can, therefore, not be regarded as conclusive. These tests were only performed to see the possible effect of this technique. The quality of the polished surface was not inspected due to the lack of this specialist equipment.

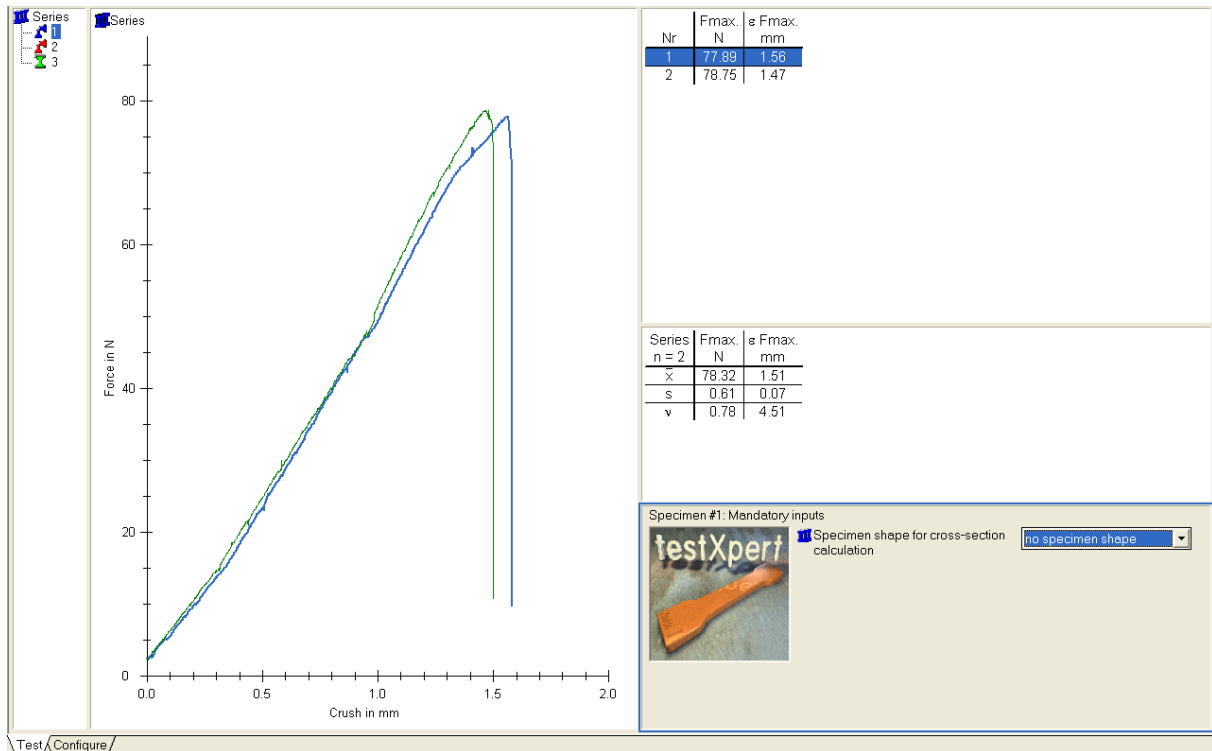


Figure 39: Graph showing the results for the experiments which look at the effect of polishing. Both curves represent the samples which were polished.

When the results are compared with the samples, which were not polished, an improvement was observed. When looking at, for example, curve “120 °C – 0.31 MPa – 60 minutes” in appendix 7 it can clearly be seen that those curves do not match in both the maximum bond strength and elongation. When looking at figure 39, it can clearly be seen that these curves are almost identical. The polishing seems to improve the repeatability of both the strength and the elongation before breaking. Although these values cannot be compared, due to the limited amount of tests conducted, it can be remarked that the bond strength did not decrease. The results of the polished samples can be found in table 13.

Test	Max. force [N]	Bond strength [MPa]	Elongation [mm]
1	77,89	0,12	1,56
2	78,75	0,13	1,47

Table 13: Result from the strength test for the sample which were polished prior to bonding

The result of the regular samples can be found in table 14. These are given for comparison.

Test	Max. force [N]	Bond strength [MPa]	Elongation [mm]
1	65,22	0,10	2,14
2	83,75	0,13	2,06

Table 14: Result from the strength test for the sample which were bonded using the same parameters

Repeatability is very important when looking at, for example, mass production. The effect of polishing can certainly be valuable but this is must be tested further in future research.

4.5 The results of the modelling

4.5.1 The contact status throughout the strength test

The contact status is a way to determine where the bond remains intact and where it will fail or already has failed. The yellow areas in figure 41 show where the sample is bonded, the blue area where no contact is made. The increments which changed noticeably were illustrated. Only the bottom plate is shown but this is identical on the top plate. Both these plates will be subjected to same stresses albeit in the opposite direction. Although the bonded area is square, the yellow area is more of a rectangular shape. This is because the contact status of the tools is also shown. These are next to the bonded area. It can clearly be observed that the bond starts to fail on the corners. On increment 32, the bond fails in such way that the remaining bond has a circular shape. Increment 40, shows that the shape of the remaining bond changes to a diamond shape. In the real-life tests similar phenomena were observed. In picture 40 the diamond shape can clearly be seen.

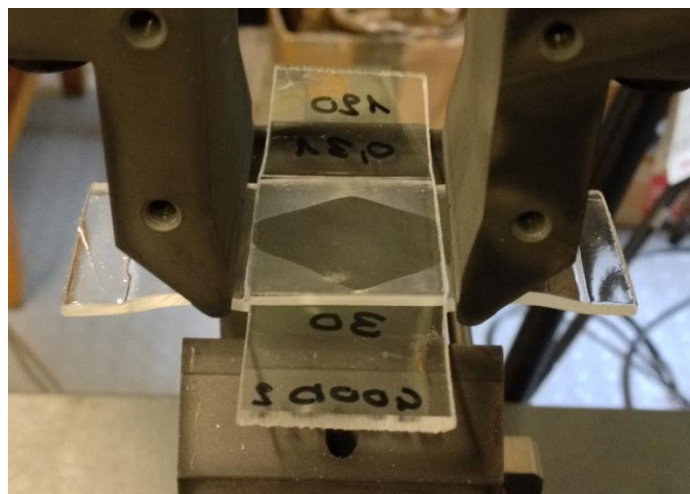


Figure 40: The bond status of sample, which is being tested

On increment 48, the bond failed entirely. The remaining yellow areas are the contact areas from the tools.

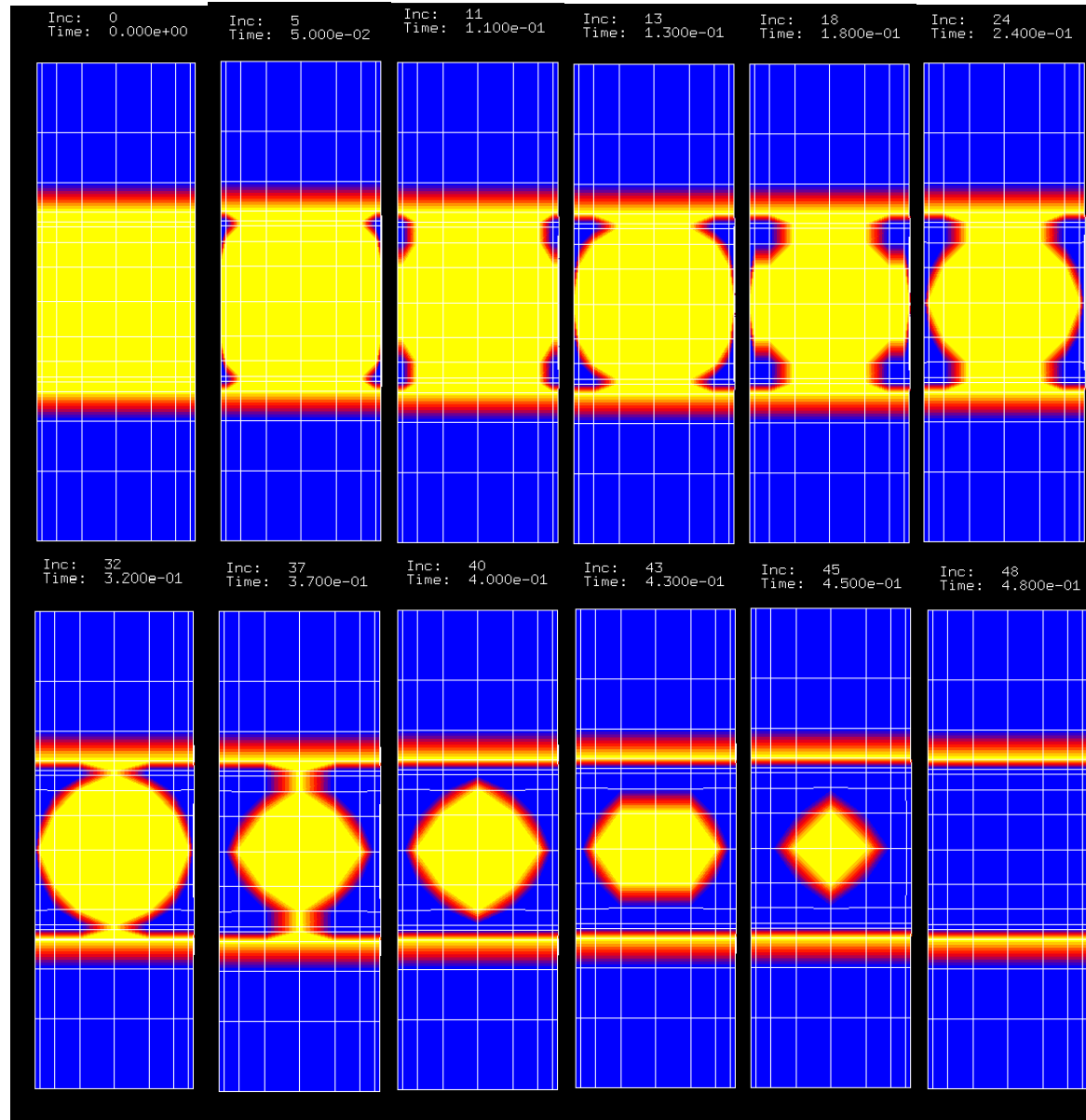


Figure 41: The bond status for different increments throughout the simulation. The yellow coloured areas represent the sections which are still bonded while the blue colour indicates the unbonded sections. The red colour shows the areas where the bond is failing.

4.5.2 Deformation of the sample

The following picture shows the maximum deformation the sample undergoes. The orange lines illustrate the sample without deformation. This model contains no parameters for the plastic behaviour.

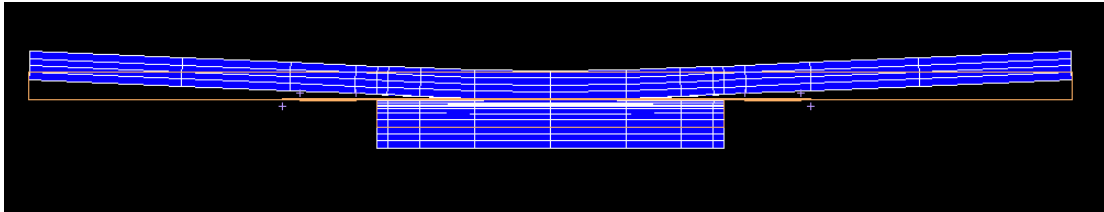


Figure 42: The maximum deformation of the sample.

The amount of deformation just before the bond fails is shown in picture 43. The top sheet ranges from the colour red to the colour yellow. The visible part of the bottom sheet has the colour blue because this a frontal view. The maximum deformation is on the edge the sheets. The red to yellow range gives the amount deformation in the positive Z-direction, the blue colour the amount of deformation in the negative Z-direction. The total deformation is therefore 2.3 millimetres.

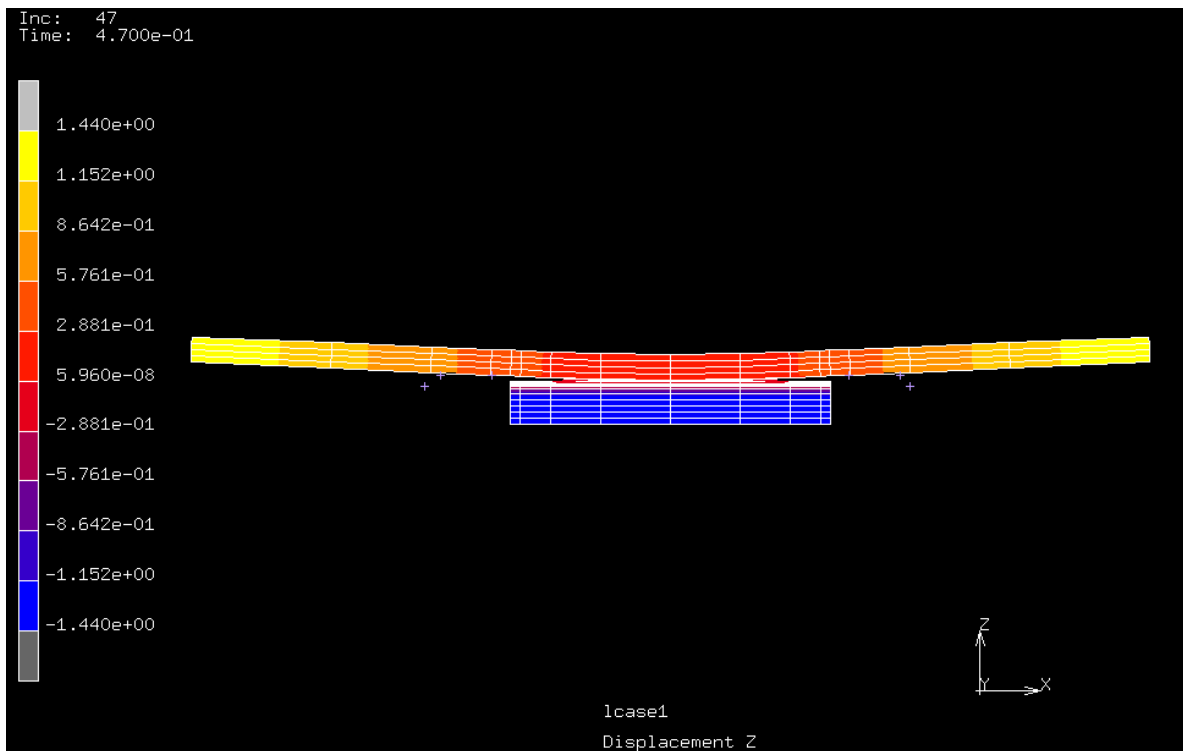


Figure 43: The amount of deformation for every section of the sample

4.5.3 The forces, which the tools exhibit on the sample

The maximum force, which the bond can resist, is the force the tools exhibit on the sample. This maximum force does not occur at the end of the strength test. This can also be seen in the curves in appendix 7. The same is true for this simulation.

The increment, where the maximum force is exhibited, occurs at 39 while the bond fails at increment 48. In the picture below, the contact normal forces in the Z-directions can be seen increment 39. The sample, depicted in this picture, are identical except for the type of plot.

The forces in the two tools range from 90 to 260 newton. The force distributions in these areas is, however, not what you would expect. The tools are straight and one would expect that the forces are distributed across this line. The average value is estimated at 180 newton. The total force the bond can withstand is, however, double this amount because there are tools at both sides. This would equate to a maximum bond strength of 360 newton.

The highest bond strengths, which was achieved during the real-life bonding tests, were between 80 to 120 newton. This is sizeable difference with the results from the simulations but are in the same order of magnitude.

There could be multiple reasons for this significant difference. The first is the fact that the samples were slightly deformed in real-life tests. This will shift the stress distribution and potentially concentrate the stress in a specific point or multiple points. The simulations assume perfect conditions which could never be achieved in real-life. Another reason behind this difference is the location of the sample on the tools. The samples can, in real-life, never be positioned exactly on the perfect place i.e. perfect in the middle.

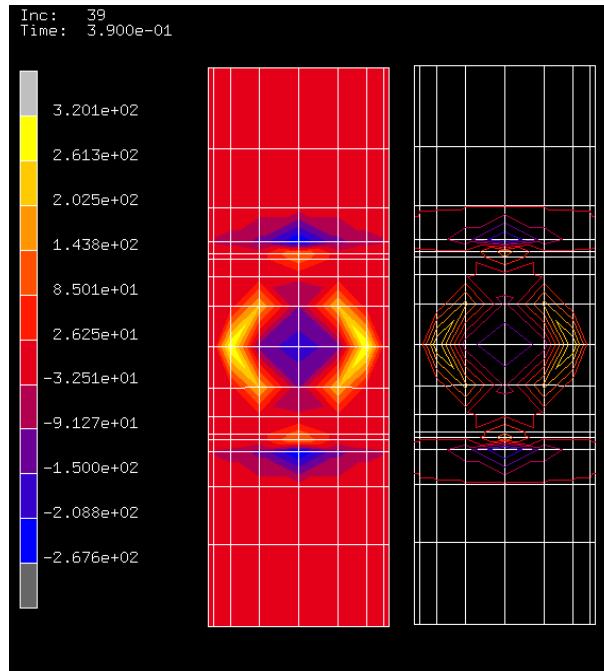


Figure 44: The contact normal forces in the Z-direction on the sample. The forces in left sample are illustrated using contour bands while the forces in the right sample are illustrated using contour lines.

4.5.4 The stress distribution throughout the strength test

In figure 48 the stresses at the interface can be seen. These are the “comp 11 of stress” or axial stresses. The same increments, as with the contact status, are depicted. In the first increments, the stress built-up around the corners can clearly be seen. When stresses reach the limit of the bond strength, the bond will start to fail at these places. When looking at the contact status in picture 41, the bond starts failing around the corners. Immediately upon failing the stresses redistribute towards the middle. The same process will repeat itself. The stresses will again built-up and the bond will when the limit is reached. At every increment the stresses built-up will correspond with the edge of the remaining contact. At increment 40, for example, the same diamond shape can be recognized.

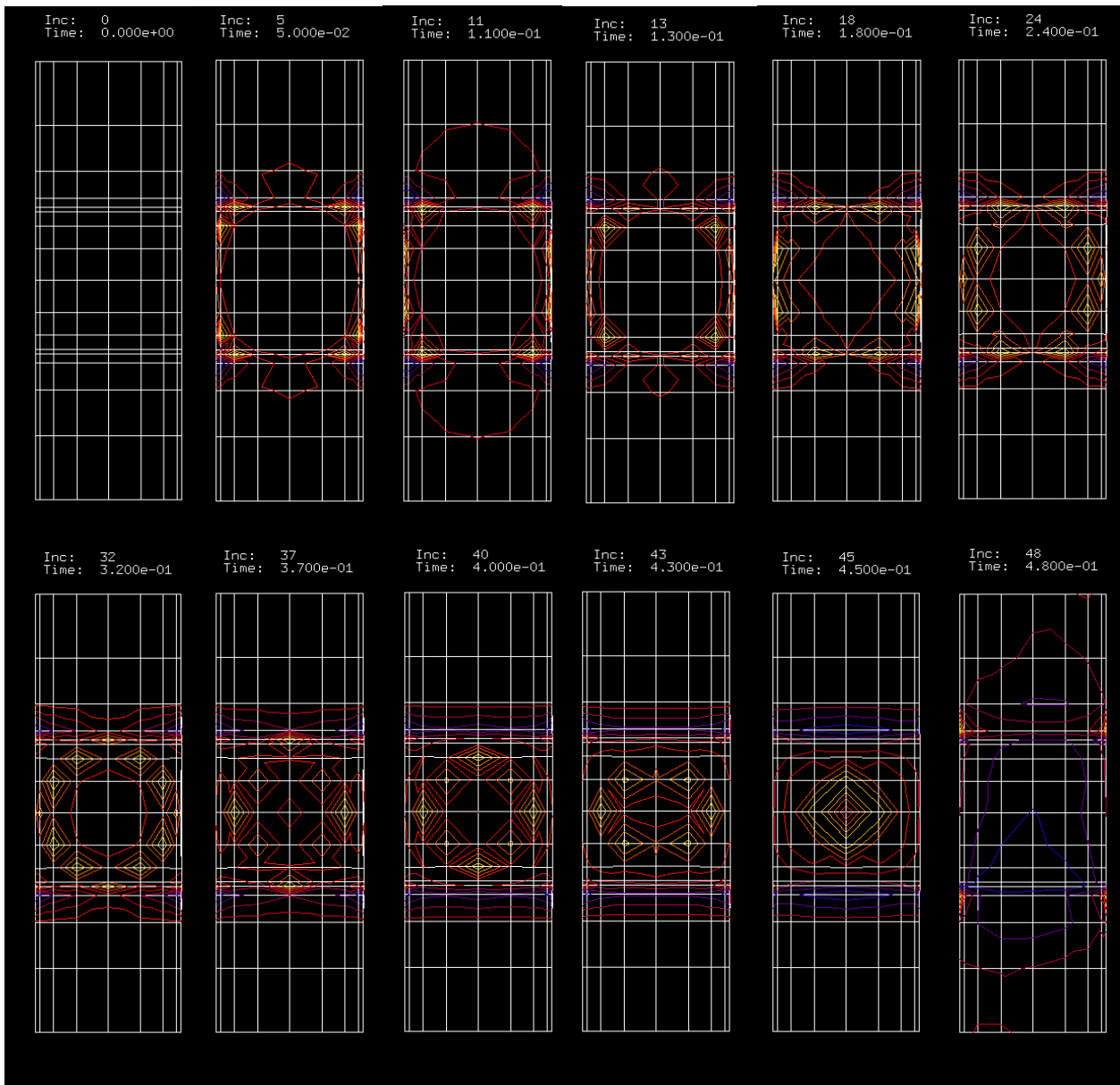


Figure 45: The comp 11 stresses for certain increments.

4.5.5 History plot of the load

The history plot shows a very similar outline as the real-life results. The peak does not occur in de end but rather towards the end. It however has to be noted that this load curve is measured in just one node. As mentioned before, the load distribution of the tools on the sample is not distributed equally along its contact line. The node in the centre was chosen. In figure 46, the load curve of the bonding test “120 °C – 0.31 MPa – 30 min.” is presented. Figure 47 shows the history plot of the simulations. It can clearly be seen that this history plot is not smooth. This is a result of the limited fineness of the mesh. The general outline of the plot can however be observed. The history plot first shows a positive increase followed by a negative part. The load in this node is in the negative Z-direction. The first positive part is therefore somewhat surprising because this first positive increase was not expected. This is probably an anomaly in the model.

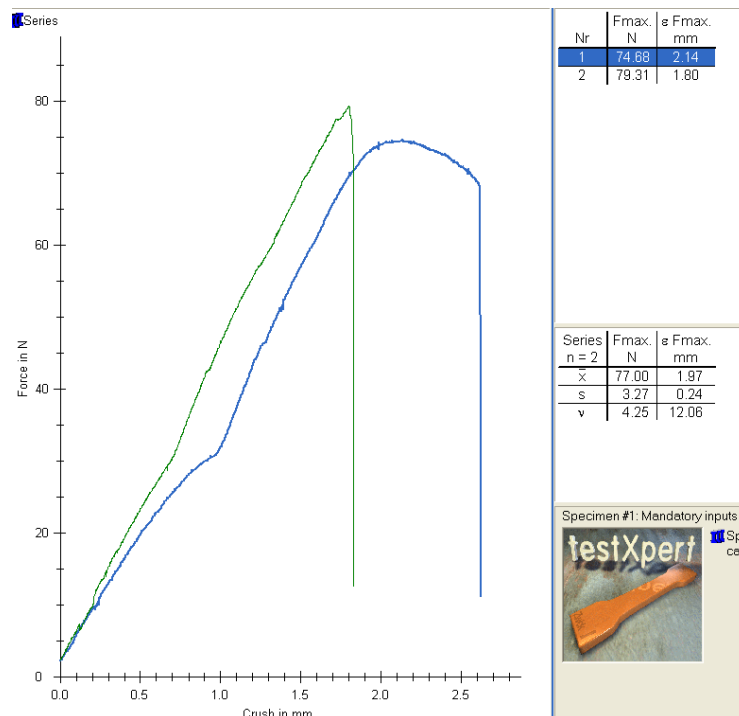


Figure 46: Load curve for the bonding test (120 °C - 0.31 MPA - 30 min.)

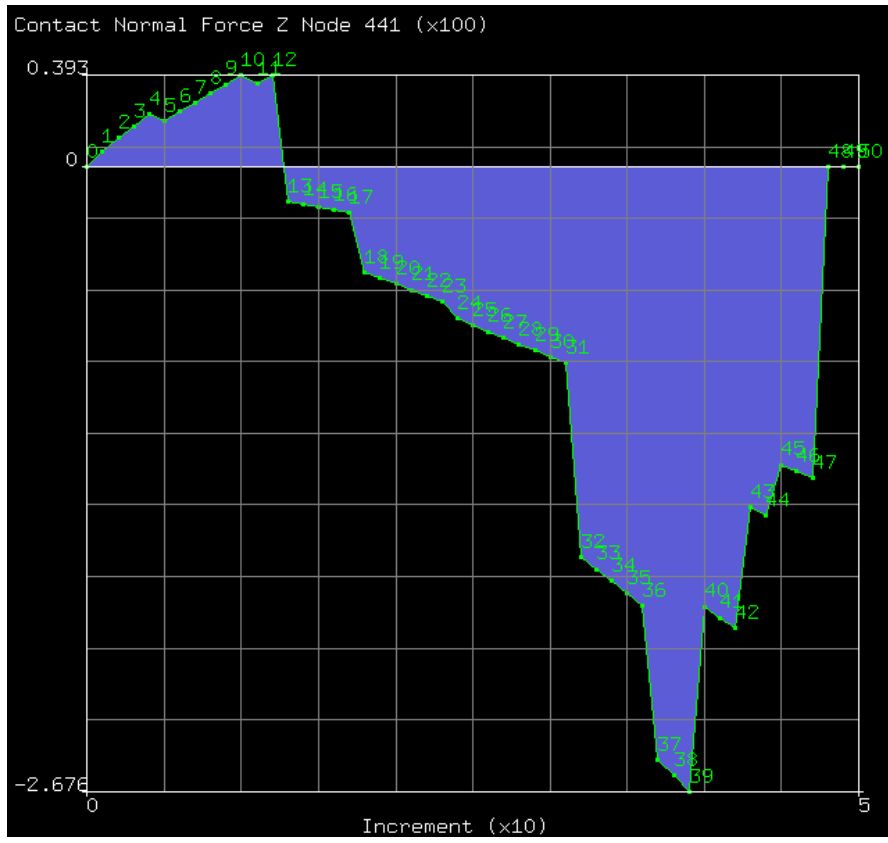


Figure 47: The simulated load curve

4.6 Creating a cellular structure

4.6.1 Stop-off Test 1: Chalk powder and Silicone spray

The results showed that both control sample and the one sprayed with silicone are both bonded. This implies that the silicone spray does not work as a stop-off. The sample with chalk powder however did not produce an adequate bond. This bond could be broken very easily. This shows that the chalk powder is promising as stop-off. In figure 48 it can clearly be remarked that the sample deformed heavily during bonding.

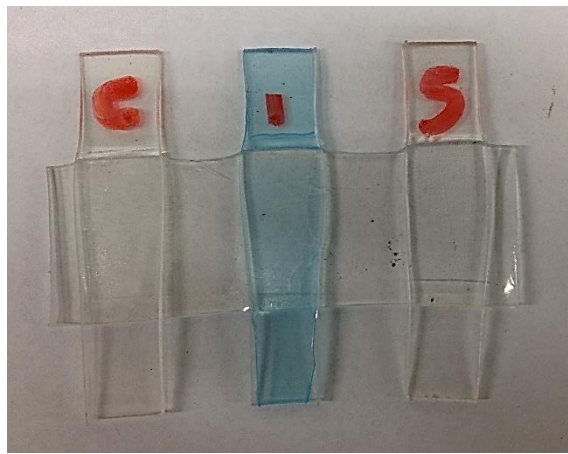


Figure 48: The result of stop-offtest 1. The samples deformed heavily during bonding

4.6.2 Stop-off test 2: Chalk powder

The second stop-off test focused on chalk powder as a stop-off. The sample with a “C” is the chalk powder while the sample with the “K” is the control sample. The chalk again proved to be a very good stop-off. The sample did not even stay connected when removing it from the oven. Also the high pressure and temperature combined with an extremely long bonding time, proved the effectiveness of chalk, as a stop-off.

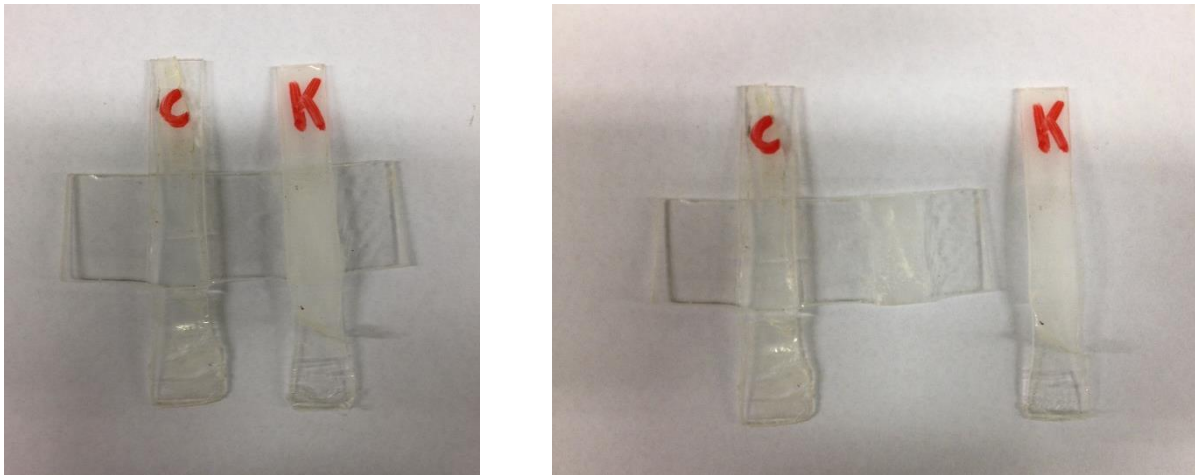


Figure 49: The result from stop-off test 2. The right picture shows that the K-sample was not bonded.

4.6.3 Stop-off test 3: Surface roughening

Roughening the surface did not inhibit the bonding process. Both the test sample and the control sample were bonded. Only one test was performed testing this technique but it does not show much promise.

4.7 Surface analysis of bonded area

The transparent nature of PMMA resulted in some difficulties when taking the microscopic images especially when focusing.

4.7.1 Sample with a good bond

Picture 50 shows a microscopic image of a sample which was bonded on the left side of the sample. The right side shows a portion of the samples which was not bonded. A clear difference can be seen. The left side of the images shows a rough, irregular surface. The right side essentially shows a microscopic image of the surface in delivery conditions. The banding runs alternately but in a structured way but the reason behind this banding is unknown.

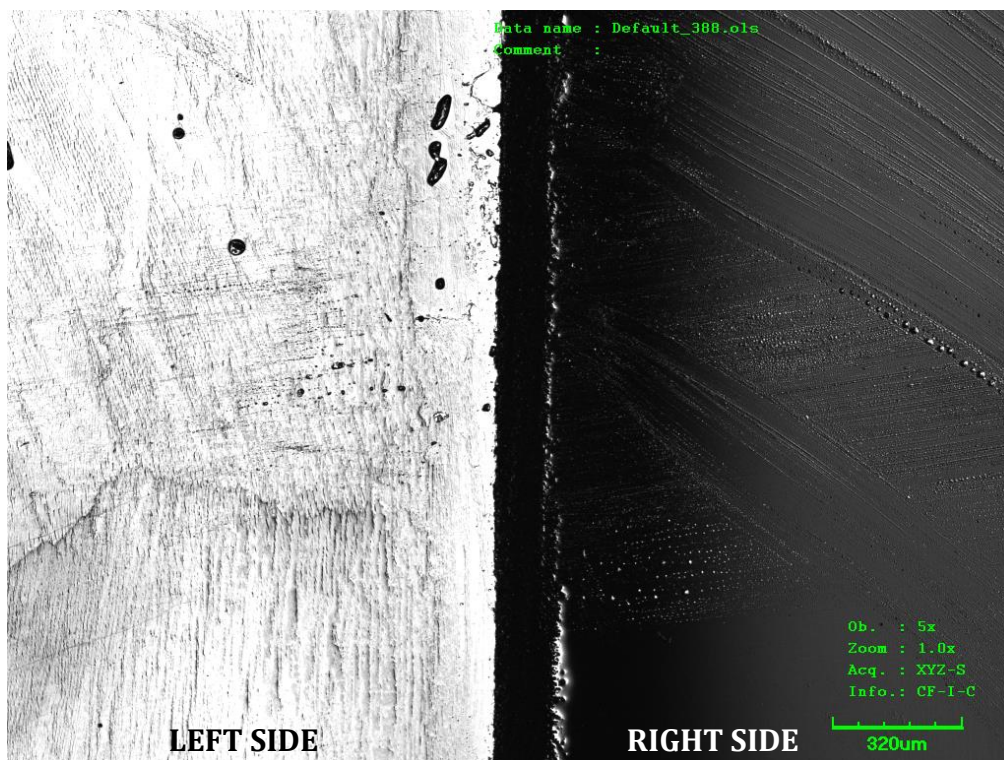


Figure 50: A microscopic image of the surface of a sheet. The left side of the image shows the bond area. The right side shows an unbonded area. (magnification: 5x)

Picture 51 shows the surface of a sheet which was bonded with significant strength. The image again shows an irregular surface but magnified when compared with the previous image.

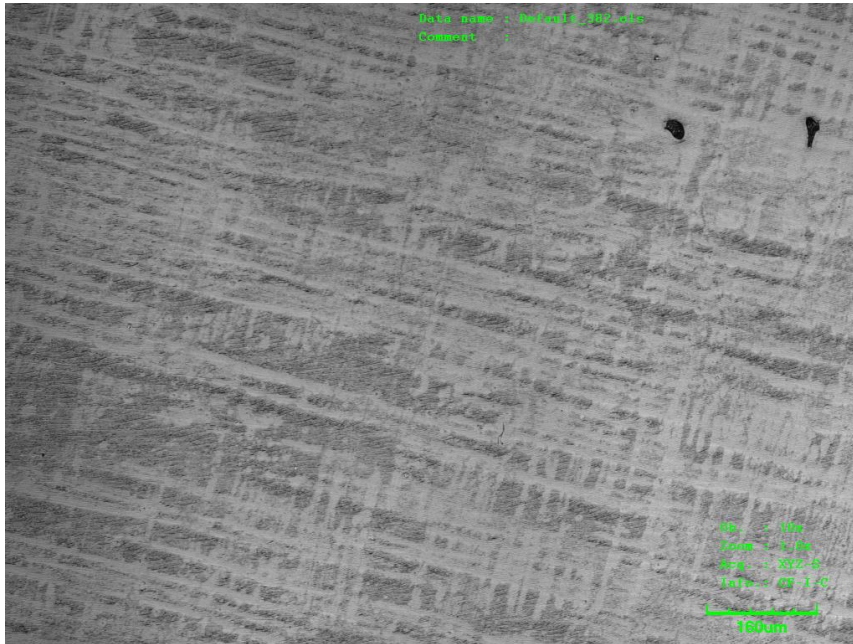


Figure 51: A microscopic image of the surface of a sheet which was bonded with significant strength (magnification: 10x)

4.7.2 Sample with an incomplete bond

The picture below shows the surface of incomplete bond. The grey area is the part which was bonded and show the same irregular pattern as in picture 52. The white surface shows the areas which did not bond.

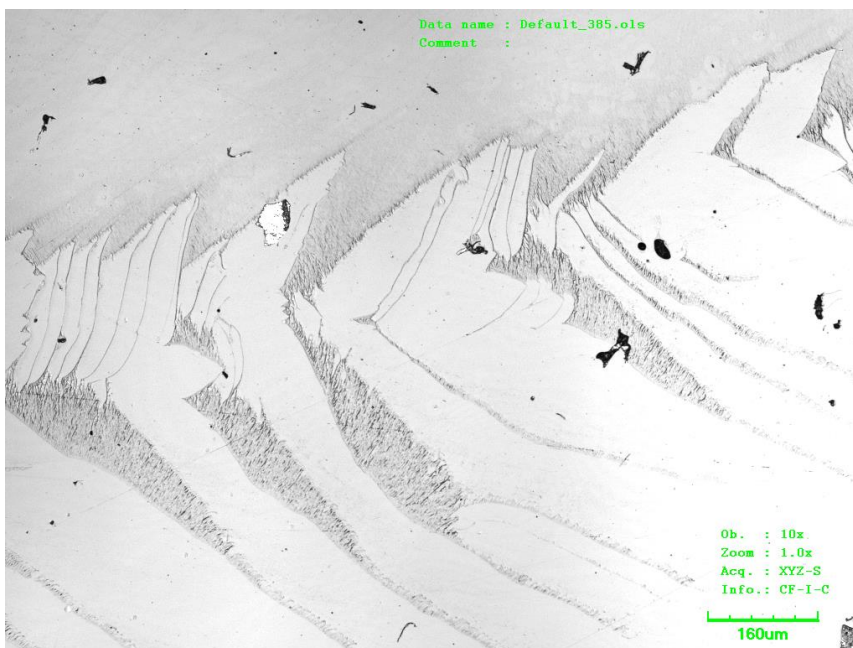


Figure 52: A microscopic image of the surface of incomplete bond (magnification: 5x)

5 Discussion and implications of the findings

The literature review has revealed the issues for the various bonding techniques and the possible solutions. The different bonding techniques were explained, using the same process with metals, with the emphasis on diffusion bonding. It has also showed the possible polymers which could be used for diffusion bonding, each with their difficulties. PMMA was eventually chosen due the relatively low bonding parameters and the abundance of other research papers conducted in the past. Finally the literature review revealed the bonding parameters, other people have used to successfully diffusion bond PMMA. These parameters were used as a starting point for the bonding tests, which were performed

The bonding tests have yielded good results. Multiple samples were bonded where the strength of the bond match or exceeded the strength of the material. In some cases the material failed instead of the bond. The results have also shown that the temperature is the most critical temperature when looking at the resulting bond strength. Variations in bonding pressure and bonding time did not make a sizeable difference. The bonding test, which yielded the best results in term of bond strength and deformation, was done with the following parameters: a bonding temperature of 120 °C, a bonding pressure of 0.31 MPa and bonding time of 60 minutes. It, however, has to be noted that these parameters far exceeded the bonding parameters which other people used. This is probably due the type of equipment which was used, especially the way the pressure had to be applied.

The effect of post-annealing showed a slight increase in bond strength but the significance of this effect should be investigated in more detail. The effect of polishing did show a positive effect on the bond strength. However, the two tests, which were performed, did have nearly identical loading curves up to failure. This could indicate that polishing could improve the repeatability, which could be useful when looking at for example mass-production. Both the effect of post-annealing and the effect polishing could interesting for future work.

Another part of this thesis was to look for a way to achieve selective bonding through the use of a stop-off. There were no known examples where researchers achieved selective bonding in the literature. Multiple substances were tested such as chalk powder and silicone spray. One surface modification was tested in the form of surface roughening in order to inhibit bonding. Only the chalk powder proved to be an effective stop-off. Even when bonding with extreme bonding parameters did this stop-off perform excellent. An added benefit is that chalk powder would be extremely easy to remove afterwards with just carbonated water.

In order to test the quality of bonding process a novel strength test was used. To verify this test, finite element modelling was used to give an indication of the reliability of the test results. The results from this FE modelling were very similar with the real-life results. The maximum load, predicted by the modelling, was in the same magnitude as the real-life tests and the load curve showed a similar outline as in the real-life experiments. The bond status

throughout the simulation displayed the same behaviour in bond failure. The remaining bond just before failure, for example, showed the same diamond-shape as in the real-life experiments.

Reference list

- Ahn, C.H., Choi, J.-W., Beaucage, G., Nevin, J.H., Lee, J.-B., Puntambekar, A., Lee, J.Y., 2004. Disposable Smart lab on a chip for point-of-care clinical diagnostics. *Proc. IEEE* 92, 153–173.
- Campbell, F.C., 2011. Chapter 6: Solid-state Welding and Bonding, in: *Joining: Understanding the Basics*. ASM International, p. 260.
- CES EduPack 2013, n.d. Granta Design, United Kingdom.
- Dang, F., Shinohara, S., Yamaoka, Y., Kurokawa, M., Shinohara, Y., Ishikawa, M., Baba, Y., 2005. Replica multilayer polymer chips with a network of sacrificial channels sealed by adhesive printing method. *Lab Chip* 5, 472–478.
- Du, L., Chang, H., Song, M., Liu, C., 2012. A method of water pretreatment to improve the thermal bonding rate of PMMA microfluidic chip. *Microsyst. Technol.* 18, 423–428.
- Ebnesajjad, S., 2008. 3.4.6 Plasma Treatment, in: *Adhesives Technology Handbook*. William Andrew Inc., Norwich NY, p. 378.
- Fitzpatrick, G.A., Lloyd, A.D., 1998. Establishing Best Practice in the Design and Manufacture of Hollow Titanium Fan Blades, in: *Intelligent Processing of High Performance Materials*. Presented at the RTO AVT Workshop, Brussels, Belgium.
- Hansen, R.H., Schonhorn, M., 1966. A new technique for preparing low surface energy polymers for adhesive bonding. *J. Polym. Sci. [B]* 4, 203–209.
- Kazakov, N.F., 1985. *Diffusion Bonding of Materials*, 1st ed. Pergamon Press Ltd.
- Lee, H.S., Kim, D.S., Kwon, T.H., 2003. A novel low temperature bonding technique for plastic substrates using X-ray irradiation. Presented at the 12th International Conference on Transducers, Solid-state Sensors, Actuators and Microsystems, IEEE, Boston USA, pp. 1331–1334.
- Li, H., Fan, Y., Kodzius, R., Foulds, I.G., 2012. Fabrication of polystyrene microfluidic devices using a pulsed CO₂ laser system. *Microsyst. Technol.* 18, 373–379.
- Liu, Y., Ganser, D., Schneider, A., Liu, R., Grodzinski, P., Kroutchinina, N., 2001. Microfabricated Polycarbonate CE Devices for DNA Analysis. *Anal. Chem.* 73, 4196–4201.
- Lu, C., Lee, L.J., Juang, Y.-J., 2008. Packaging of Microfluidic Chips via Interstitial Bonding Technique. *ELECTROPHORESIS* 29, 1407–1414.
- MacDonald, W.D., Eagar, T.W., 1992. Transient liquid phase bonding processes. *Annu. Rev. Mater. Sci.* 22.
- Midland Simulation Group | Industry Expertise [WWW Document], n.d. URL <http://www.midsim.org.uk/about-us/industry-expertise/> (accessed 3.19.14).
- NG, S.H., Tjeung, R.T., WANG, Z.F., Lu, A.C.W., Rodriguez, I., Rooij, N.F., 2008. Thermally activated solvent bonding of polymers. *Microsyst. Technol.* 14, 753–759.
- Partridge, P.G., 1987. Diffusion Bonding of metals. *AGARD* 154, 5.1.–5.23.
- Riegger, L., Strohmeier, O., Faltin, B., Zengerle, R., Koltay, P., 2010. Adhesive bonding of microfluidic chips: influence of process parameters. *J. Micromechanics Microengineering* 20.
- Satas, D., Tracton, A.A., 2001. *Coatings Technology Handbook*, 2nd ed. Marcel Dekker, Inc., New York.
- Shah, J.J., Geist, J., Locascio, L.E., Gaitan, M., Rao, M.V., Vreeland, W.N., 2006. capillarity induced solvent-actuated bonding of polymeric microfluidic devices. *Anal. Chem.* 78, 3348–3358.
- Sharp, K.V., Adrian, R.J., Santiago, J.G., Molho, J.I., n.d. *Liquid Flows in Microchannels*. MEMS Backgr. Fundam.
- Shirzadi, A.A., 1997. *Diffusion Bonding Aluminium Alloys and Composites: New Approaches and Modelling*. King's College; University of Cambridge.
- Sood, V., 2007. *An Experimental Study on Thermal Bonding Effects of PMMA Based Micro-devices*. University of Texas.
- Stankiewicz, A.I., Moulijn, J.A., 2000. *Process Intensification: Transforming Chemical Engineering*. Chem. Eng. Prog.
- Sun, Y., Kwok, Y.C., Nguyen, N.-T., 2006. Low-pressure, high-temperature thermal bonding of polymeric microfluidic devices and their applications for electrophoretic separation. *J. Micromechanics Microengineering* 16.

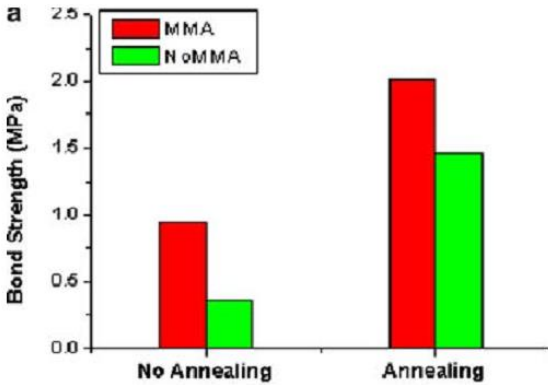
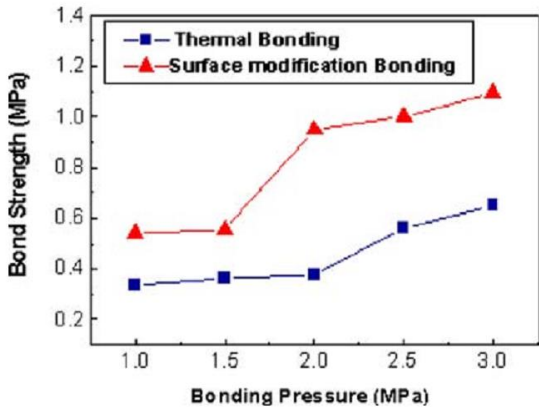
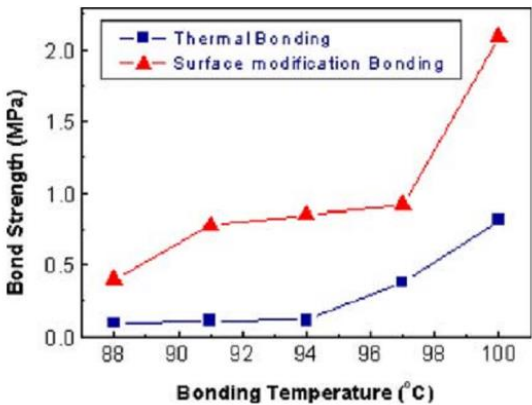
- T'joen, C., Park, Y., Wang, Q., Sommers, A., Han, X., Jacobi, A., 2009. A review on polymer heat exchangers for HVAC&R application. *Int. J. Refrig.* 763–779.
- Tsao, C.-W., DeVoe, D.L., 2009. Bonding of thermoplastic polymer microfluidics. *Microfluid. Nanofluidics* 6, 1–16.
- Tsao, C.W., Hromada, L., Liu, J., Kumar, P., DeVoe, D.L., 2007. Low Temperature bonding of PMMA and COC microfluidic substrates using UV/ozone surface treatment. *Lab. Chip* 7, 499–505.
- Wang, Y., Chen, H., He, Q., Soper, S.A., 2008. A high performance polycarbonate electrophoretic microchip with integrated three-electrode system for end channel amperometric detection. *ELECTROPHORESIS* 29, 1881–1888.
- Weisert, E.D., Fischer, J.R., McCauley, W.L., 1988. Superplastic forming diffusion bonding process. US4882823 A.
- Wolf, R.A., 2014. Corona Treatment: A Process Overview [WWW Document]. idspackaging. URL http://www.idspackaging.com/common/paper/Paper_177/Corona%20Treatment-%20A%20Process%20Overview.htm (accessed 4.16.14).
- Yi, W., Qiaohong, H., Yuanyuan, D., Hengwu, C., 2010. In-channel modification of biosensor electrodes integrated on a polycarbonate microfluidic chip for micro flow-injection amperometric determination of glucose. *Sens. Actuators B* 145, 553–560.
- Young, E.W.K., Berthier, E., Guckenberger, D.J., Sackmann, E., Lamers, C., Meyvantsson, I., Huttenlocher, A., Beebe, D.J., 2011. Rapid prototyping of arrayed microfluidic systems in polystyrene for cell based assays. *Anal. Chem.* 3, 9.32.
- Zhu, X., Liu, G., Guo, Y., Tian, Y., 2007. Study of PMMA thermal bonding. *Microsyst. Technol.* 13, 403–407.

Appendices

Appendices	93
Appendix 1: Figures of the journal article “Study of PMMA thermal bonding”	95
Appendix 2: Material properties according to the manufacturer (Plexiglas®)	97
Appendix 3: The preliminary tests	101
Preliminary test 1: unsuccessful	101
Preliminary test 2: unsuccessful	101
Preliminary test 3: unsuccessful	102
Preliminary test 4: unsuccessful	102
Preliminary test 5: semi-successful (I).....	103
Preliminary test 6: semi-successful (II)	103
Preliminary test 7: unsuccessful	104
Preliminary test 8: semi-successful (III).....	105
Preliminary test 9: semi-successful (IV)	105
Preliminary test 10: semi-successful (V)	106
Preliminary test 11: unsuccessful	106
Preliminary test 12: semi-successful	107
Preliminary test 13: successful VI	107
Preliminary test 14: successful VII.....	108
Preliminary test 15: unsuccessful	109
Appendix 4: Tensile test of PMMA	111
Test setup.....	111
Results	112
Appendix 5: post-annealing conditions according to the manufacturer (Plexiglas®)	115
Appendix 6: Olympus LEXT Confocal laser scanning microscope	117
Appendix 7: Resulting curves for the bonding tests	119
115 °C – 0.25 MPa – 30 minutes.....	119
115 °C – 0.31 MPa – 30 minutes.....	119
120 °C – 0.25 MPa – 30 minutes.....	120
120 °C – 0.31 MPa – 30 minutes.....	120
115 °C – 0.25 MPa – 60 minutes.....	121
115 °C – 0.31 MPa – 60 minutes.....	121

120 °C – 0.25 MPa – 60 minutes.....	122
120 °C – 0.31 MPa – 60 minutes.....	122

Appendix 1: Figures of the journal article "Study of PMMA thermal bonding"



Appendix 2: Material properties according to the manufacturer (Plexiglas®)

Typical Property Values (at 23 °C and 50% relative humidity)

Mechanical properties

	PLEXIGLAS® GS 0F00; 0F00; 0Z09 (233; 222; 209)	PLEXIGLAS® XT 0A000; 0A070 (20070; 29070)	PLEXIGLAS® Resist 45; 65; 75; 100	Unit	Teststandard
Density ρ	1.19	1.19	1.19	g/cm ³	ISO 1183
Impact strength a_{cu} (Charpy)	15	15	45; 65; 75; no break	kJ/m ²	ISO 179/1fu
Notched impact strength a_N (Izod)	1.6	1.6	2.5; 4.5; 6.0; 6.5	kJ/m ²	ISO 180/1 A
Notched impact strength a_{en} (Charpy)	–	–	3.5; 6.5; 7.5; 8.0	kJ/m ²	ISO 179/1eA
Tensile strength σ_M				MPa	ISO 527-2/1B/5
–40 °C	110	100	–		
23 °C	80	72	60; 50; 45; 40		
70 °C	40	35	–		
Elongation at break ϵ_B	5.5	4.5	–	%	ISO 527-2/1B/5
Nominal elongation at break ϵ_{tB}	–	–	10; 15; 20; 25	%	ISO 527-2/1B/50
Flexural strength σ_{f0} Standard test specimen (80 x 10 x 4 mm²)	115	105	95; 85; 77; 69	MPa	ISO 178
Compressive yield stress σ_{cF}	110	103	–	MPa	ISO 604
Max. safety stress σ_{zul} (up to 40 °C)	5–10	5–10	5–10	MPa	–
Modulus of elasticity E_1 (short-term value)	3300	3300	2700; 2200; 2000; 1800	MPa	ISO 527-2/1B/1
Min. cold bending radius	330 x thickness	330 x thickness	270 x thickness; 210 x thickness; 180 x thickness; 150 x thickness	–	–
Dynamic shear modulus G at approx. 10 Hz	1700	1700	–	MPa	ISO 537
Indentation hardness $H_{965/30}$	175	175	145; 130; 120; 100	MPa	ISO 2039-1
Abrasion resistance in Taber abrader test (100 rev.; 5,4 N; CS-10F)	20–30	20–30	20–30; 30–40; 30–40; 30–40;	% Haze	ISO 9352
Coefficient of friction μ				–	–
plastic / plastic	0.8	0.8	–		
plastic / steel	0.5	0.5	–		
steel / plastic	0.45	0.45	–		
Poisson's ratio μ_b (dilatation speed of 5% per min; up to 2% dilatation; at 23 °C)	0.37	0.37	0.41; 0.42, 0.41; 0.43	–	ISO 527-1
Resistance to puck impact from thickness (Test Certificate No. from FMPA Stuttgart)	–	12 mm (46/900 549)	–; 6 ¹⁾ ; (6); 6 ²⁾ mm (¹⁾ 46/901 869/ Sm/C; ²⁾ 46/901 870/Sm/C)	–	similar to DIN 18 032, Part 3

Thermal properties

	PLEXIGLAS® GS 0F00; 0F00; 0Z09 (233; 222; 209)	PLEXIGLAS® XT 0A000; 0A070 (20070; 29070)	PLEXIGLAS® Resist 45; 65; 75; 100	Unit	Teststandard
Coefficient of linear thermal expansion α for 0–50°C	$7 \cdot 10^{-5}$ (=0.07)	$7 \cdot 10^{-5}$ (=0.07)	$7 \cdot 10^{-5}$; $8 \cdot 10^{-5}$; $9 \cdot 10^{-5}$; $11 \cdot 10^{-5}$ (0,07; 0,08; 0,09; 0,11)	1/K (mm/m°C)	DIN 53752-A
Possible expansion due to heat and moisture	5	5	5; 6; 6; 8	mm/m	–
Thermal conductivity λ	0.19	0.19	–	W/mK	DIN 52612
U-value, for thickness				W/m²K	DIN 4701
1 mm	5.8	5.8	5.8	MPa	ISO 527-2/1B/5
3 mm	5.6	5.6	5.6		
5 mm	5.3	5.3	5.3		
10 mm	4.4	4.4	4.4		
Specific heat c	1.47	1.47	1.47	J/gK	–
Forming temperature	160–175	150–160	150–160; 140–150; 140–150; 140–150	°C	–
Max. surface temperature (IR radiator)	200	180	–	°C	–
Max. permanent service temperature	80	70	70; 70; 70; 65	°C	–
Reverse forming temperature	> 80; > 80; > 90	> 80; > 80	> 80; > 80; > 75; > 70	°C	–
Ignition temperature	425	430	–	°C	DIN 51794
Smoke gas volume	very little	very little	very little	–	DIN 4102
Smoke gas toxicity	none	none	none	–	DIN 53436
Smoke gas corrosiveness	none	none	none	–	–
Class					DIN 4102
	B2	B2	B2	–	BS 476, Part 7+6
	Class 3	Class 3	–	–	BS 2782
	TP (b)	TP (b)	–	–	Method 508 A
	E	E	E	–	DIN EN 13501
German building inspectorate test report	P-K017 / 11.06	P-K018 / 02.07	P-K019 / 05.07	–	–
Vicat softening temperature	115	103	102; 100; 100; 97	°C	ISO 306, Method B 50
Heat deflection temperature under load (HDT)				°C	ISO 75
deflection 1.8 MPa	105; 105; 107	95	94; 93; 92; 90		
deflection 0.45 MPa	113; 113; 115	100	99; 98; 96; 93		

Acoustical properties

	PLEXIGLAS® GS 0F00; 0F00; 0Z09 (233; 222; 209)	PLEXIGLAS® XT 0A000; 0A070 (20070; 29070)	PLEXIGLAS® Resist 45; 65; 75; 100	Unit	Teststandard
Sound velocity (at room temperature)	2700–2800	2700–2800	–	m/s	–
Weight sounded reduction index R_w at thickness				dB	–
4 mm	26	26	–		
6 mm	30	30	–		
10 mm	32	32	–		

Optical properties (of clear grades, at 3 mm thickness)

	PLEXIGLAS® GS 0F00; 0F00; 0Z09 (233; 222; 209)	PLEXIGLAS® XT 0A000; 0A070 (20070; 29070)	PLEXIGLAS® Resist 45; 65; 75; 100	Unit	Teststandard
Transmittance τ_{pass}	~ 92	~ 92	~ 91	%	DIN 5036, Part 3
UV transmission	no; no; no	no; yes	no; no; no; no	–	–
Reflection loss the visible range (for each surface)	4	4	4	%	–
Total energy transmittance g	85	85	85	%	DIN EN 410
Adsorption in the visible range	< 0.05	< 0.05	< 0.05	%	–
Refractive index n_D^{20}	1.491	1.491	1.491	–	ISO 489

Electrical properties

	PLEXIGLAS® GS 0F00; 0F00; 0Z09 (233; 222; 209)	PLEXIGLAS® XT 0A000; 0A070 (20070; 29070)	PLEXIGLAS® Resist 45; 65; 75; 100	Unit	Teststandard
Volume resistivity ρ_D	> 10^{15}	> 10^{15}	> 10^{14}	Ohm · cm	DIN VDE 0303, Part 3
Surface resistivity σ R_{DA}	$5 \cdot 10^{13}$	$5 \cdot 10^{13}$	> 10^{14}	Ohm	DIN VDE 0303, Part 3
Dielectric strength E_z (1 mm thickness)	~ 30	~ 30	–	kV/mm	DIN VDE 0303, Part 2
Dielectric constant ϵ					DIN VDE 0303, Part 4
at 50 Hz	3.6	3.7	–	–	
at 0.1 MHz	2.7	2.8	–	–	
Dissipation factor $\tan \delta$					DIN VDE 0303, Part 4
at 50 H	0.06	0.06	–	–	
at 0.1 MHz	0.02	0.02	–	–	
Tracking, CTI-Value	600	600	–	–	DIN VDE 0303, Part 1

Appendix 3: The preliminary tests

Preliminary test 1: unsuccessful

Bonding parameter	test values
Bond area [mm ²]	25x25
Surface cleaning	none
Bonding temperature [°C]	100
Bonding pressure [MPa]	0,10
Bonding time [min.]	30

0.1 MPa was achieved by using a weight of 6 kg. The weight was loaded directly on to the samples. A steel plate was used as a base. This temperature was specifically chosen so it would be below the glass transition temperature of PMMA. The protective film was removed. The surface was not cleaned prior to bonding. These bonding parameters did not produce a bond with adequate bond strength. The two pieces did, however, stay together under their own weight.

Preliminary test 2: unsuccessful

Bonding parameter	test values
Bond area [mm ²]	25x25
Surface cleaning	none
Bonding temperature [°C]	100
Bonding pressure [MPa]	0,18
Bonding time [min.]	30

In this test a weight of 11.44 kg was used to achieve a pressure of 0.18 MPa. Unlike test 1, the weight was not directly loaded on to the samples. To produce a uniform load, a steel plate was used. The plate also acted as extra weight. The protective film was removed. The surface was not cleaned prior to bonding. These bonding parameters resulted in bond with negligible bond strength. Although the bond strength could not be measured, the strength had increased ever so slightly over the previous test.

Preliminary test 3: unsuccessful

Bonding parameter	test values
Bond area [mm ²]	25x25
Surface cleaning	none
Bonding temperature [°C]	107
Bonding pressure [MPa]	0,18
Bonding time [min.]	30

In the third test, the bonding temperature was changed. Unlike previous tests, where the temperatures were kept below T_G , the temperature was increased to 107°C. The other parameters were kept the same. These parameters unfortunately did not produce a bond with adequate strength.

Preliminary test 4: unsuccessful

Bonding parameter	test values
Bond area [mm ²]	25x25
Surface cleaning	methanol
Bonding temperature [°C]	107
Bonding pressure [MPa]	0,18
Bonding time [min.]	30

The basic outline of the previous test was kept the same. The surface were, however, cleaned before bonding the samples. Ethyl ethanol (methanol) was used to clean the surfaces. The bond created with this process was better but was still inadequate. The interface, however, showed signs of bonding. This proofed, to some extent, the reason for the weak bonds. The glue, for holding the protective film, inhibits the bonding process.

Preliminary test 5: semi-successful (I)

Bonding parameter	test values
Bond area [mm ²]	25x25
Surface cleaning	methanol
Bonding temperature [°C]	104
Bonding pressure [MPa]	0,18
Bonding time [min.]	1000

In an attempt to increase the bond strength, the bond time was increased significantly. The samples were kept overnight (17.15-10.00) in the furnace at 104°C. The bond pressure and area were kept the same. The bond was fairly strong but the bond area was not uniform. This might be a result of uneven loading despite using a thick top layer, between the weights and samples.

Preliminary test 6: semi-successful (II)

Bonding parameter	test value
Bond area [mm ²]	25x25
Surface cleaning	Soap + methanol
Bonding temperature [°C]	120
Bonding pressure [MPa]	0,18
Bonding time [min.]	60

To shorten the bonding time, the temperature was increased to 120°C. In an attempt to completely remove the glue, the sample was first cleaned with detergent and water. To remove the residue of the water, the sample was subsequently cleaned with methanol. The time was increased, in relation to the first tests and was set to one hour. The pressure and area was kept the same. The bond strength of this sample was relatively good. The high temperature did cause some deformation of the geometry of the sample. The thick steel plates, that were used to spread the weight, also cause some deformation the outer surfaces of the samples. This deformation was in the form of a sort of surface roughness. On later inspection, it was concluded that this was the same surface roughness, albeit in its negative form, of the thick steel plates. Due to the deformation, caused by primarily by the high temperature, these parameters are not really useful, especially if the aim is to incorporate microchannels in these layers. It was also observed that the load had shifted

(tilted) as a result of the deformation. This would also question the flatness of the thick steel plates.

Preliminary test 7: unsuccessful

Bonding parameter	test value
Bond area [mm ²]	25x25
Surface cleaning	Soap + methanol
Bonding temperature [°C]	105
Bonding pressure [MPa]	0,18
Bonding time [min.]	60

To improve the distribution of the load, thin aluminium sheets were placed between the thick steel plates and the samples itself. This improved the “surface roughness” and hopefully also the distribution. The temperature was also lowered to prevent deformation of the layers. The rest of parameters were kept the same as the previous test. These parameters did not produce a bond with adequate strength. It was, however, observed that the two pieces did start to bond but only in certain areas. One possible hypothesis for this problem can be that there was a small particle of some kind. This particle could have concentrated the pressure to a certain area. When using a temperature of 105°C, no deformation was observed. The lack of bond might also be due to the fact that thick steel plates (~1 cm) were used. These plates have a relatively low thermal conductivity which means that they heat up very slowly in comparison to, for example, aluminium. This might prevent the aluminium plates, which are used to achieve a flat surface, from heating up to the desired temperature.

Preliminary test 8: semi-successful (III)

Bonding parameter	test value
Bond area [mm ²]	25x25
Surface cleaning	Soap + methanol
Bonding temperature [°C]	110
Bonding pressure [MPa]	0,24
Bonding time [min.]	90

To isolate the thick steel plates from the aluminium, a thick fabric was used. This should prevent the high thermal conductivity from the steel to have adverse effects on the entire system. It was also noted, during the previous test, that only a part of the bond area was actually being bonded. In an attempt to improve this, a higher load was applied. The temperature was also increased but the time has remained the same i.e. one hour. The general quality of the bond has improved. The bond area, however, has still not covered the entire intended bond area. This points to unequal distribution of the load.

Preliminary test 9: semi-successful (IV)

Bonding parameter	test value
Bond area [mm ²]	25x25
Surface cleaning	Soap + methanol
Bonding temperature [°C]	115
Bonding pressure [MPa]	0,24
Bonding time [min.]	60

To achieve a good bond in a reasonable time, the temperature was increased. The bond strength was pretty good although it didn't bond the entire area. This was due to a slight misplacement of the weights. This resulted in a deformation on one side. As expected the other side didn't bond so well. Placing the weights on exactly the right place is very hard. The deformation made the stack of weights tilt even more.

Preliminary test 10: semi-successful (V)

Bonding parameter	test value
Bond area [mm ²]	25x25+ small supports
Surface cleaning	Soap + methanol
Bonding temperature [°C]	115
Bonding pressure [MPa]	0,24
Bonding time [min.]	60

The small supports did improve the circumstances. As mentioned in test 9, where the stack of weights tilted when one side of the samples deformed little bit quicker than the other side, due to a slight imbalance of the weights. In this test, small supports were introduced to counter this effect. The support are the same material as the samples so they should behave similarly at the same temperatures. A minor disadvantage is the lower pressure because the surface area was increased. Instead of the whole stack of weights tilting to one side with any slight misplacement of the weights, the weights remained upright.

Preliminary test 11: unsuccessful

Bonding parameter	test value
Bond area [mm ²]	25x25
Surface cleaning	Polishing + soap + methanol
Bonding temperature [°C]	115
Bonding pressure [MPa]	0,24
Bonding time [min.]	60

In an attempt to improve bonding quality, the sample was polished with Brasso (metal polish). Despite numerous sources, which claim that polishing, with Brasso, will improve the bond, the bond quality of this samples was not adequate. It was worse than without polishing. This might be a result of a bad polishing technique. This test will done again in a later stage.

Preliminary test 12: semi-successful

Bonding parameter	test value
Bond area [mm ²]	25x25
Surface cleaning	soap + methanol
Bonding temperature [°C]	115
Bonding pressure [MPa]	Unknown (clamped)
Bonding time [min.]	60

In this test an alternative method was used to apply pressure. Instead of weights, a U clamp was used. This was just a proof of concept because you can't measure the applied force. This technique is basically the same as a displacement method to apply pressure, instead of a force to apply pressure. This clamp method produced a very strong bond but the samples deformed heavily. The thickness of both sheets reduced from 2 mm to 1.34 mm.

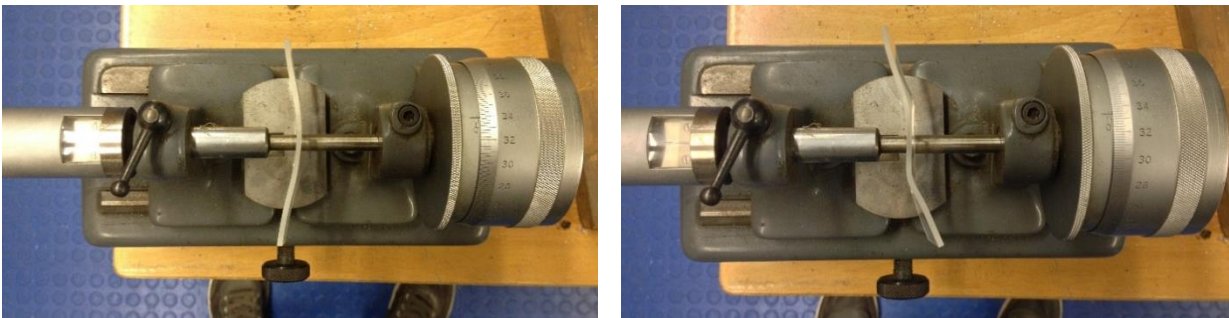


Figure 53: The two sheets which deformed heavily after a bonding test using a U-clamp to provide the bonding pressure

Preliminary test 13: successful VI

Bonding parameter	test value
Bond area [mm ²]	25x25 + small supports
Surface cleaning	Soap + methanol
Bonding temperature [°C]	115
Bonding pressure [MPa]	0,24
Bonding time [min.]	60

At previous test were conducted on a steel grill. This grill bends on the weight, making it a not so stable base. To provide a better base, this test was conducted on the bottom of the oven. Again small supports are used to counter the effect of a misplacements of the weights. This setup resulted in a near perfect bond. The sample was a little bit deformed but significantly.

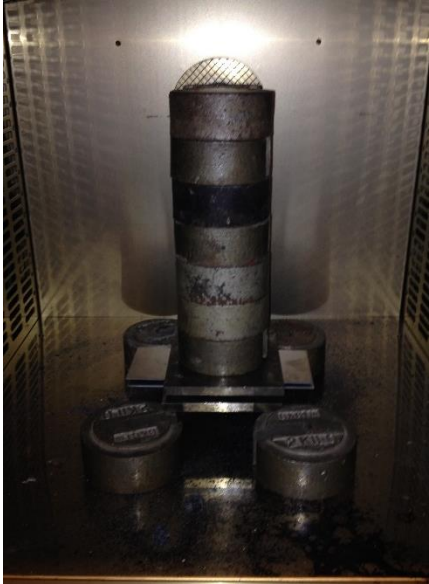


Figure 54: The new setup showing the new ground surface

Preliminary test 14: successful VII

Bonding parameter	test value
Bond area [mm ²]	25x25 + small supports
Surface cleaning	Soap + methanol
Bonding temperature [°C]	115
Bonding pressure [MPa]	0,24
Bonding time [min.]	60

The test parameters were kept the same as the previous test but improve the quality all the features, like supports, are taped with clear tape to stop them from moving when loading them in the oven. Like previous test, the bond was pretty good but yet again not a perfect bond over the entire bond area.

Preliminary test 15: unsuccessful

Bonding parameter	test value
Bond area [mm ²]	25x25 + small supports + small plate
Surface cleaning	Soap + methanol
Bonding temperature [°C]	125
Bonding pressure [MPa]	0,24
Bonding time [min.]	30

To lower the required time, the temperature was increased to 125°C. The other parameters were kept the same as before. To improve the pressure distribution a small plate, which is slightly bigger than the bond area, was placed on top of the samples. This temperature is just too high to get reliable results. To samples deformed after just 5 minutes. This establishes the fact that a temperature of 125°C is too high.

Appendix 4: Tensile test of PMMA

To determine the strength of the material, two tensile tests were performed. These tests were performed on the *Zwick-Roell 1474 100kN Mechanical Test Machine*.

Test setup

The test sample has a standardized sample cross-section. The dimension for these samples can be found on the picture below.

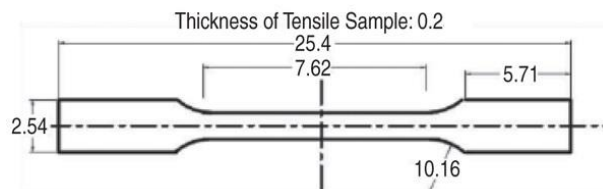


Figure 55: The dimensions of the test samples in centimetres according to ASTM D638-03

The test parameters for the apparatus are:

- Pre-load: 50 N
- Pre-load speed: 10 mm/min
- Test speed: 1 mm/min (position controlled)

Results

The graph below shows the resulting stress-strain curve. The ultimate tensile strength is on average 65 MPa.

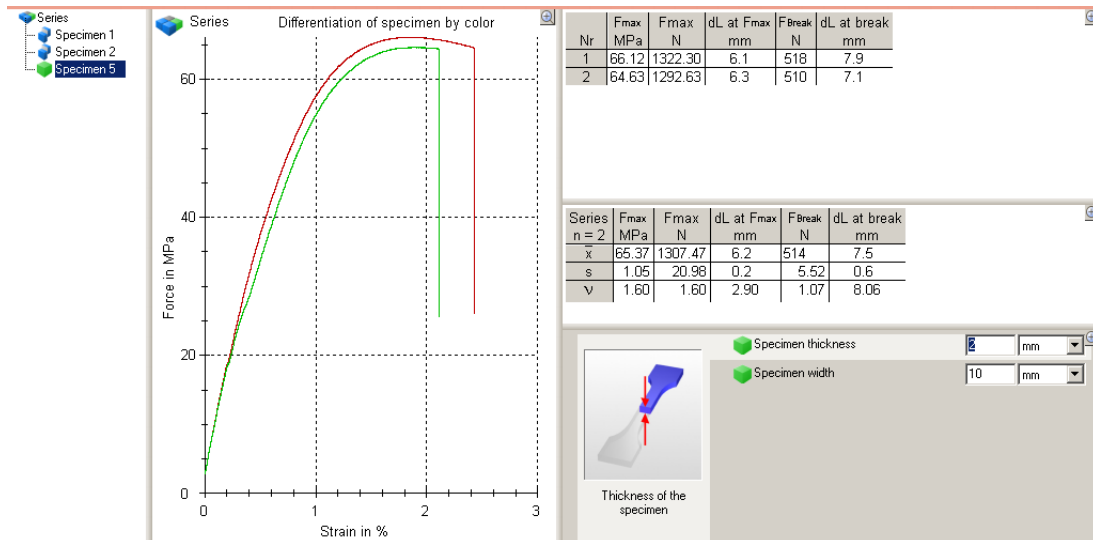


Figure 56: The resulting stress-strain curve for the material PMMA in delivery conditions

The young's modulus can also be derived from this stress-strain curve. The young's modulus is the ratio of the applied normal stress σ to the resulting normal strain ε in the direction of the loading.

$$E = \frac{\sigma}{\varepsilon}$$

It has to be noted that relation only applies until the elastic limit is reached. The young's modulus is, when we look at the stress-strain curve, the slope of the elastic part of this curve. To determine the slope the following equation was used:

$$E = \frac{\sigma}{\varepsilon} = \frac{52.5 - 10 [MPa]}{0,0085 - 0 [1]} = 5 \text{ GPa}$$

The database *CES EduPack (2013)* gives the following range of values for the young's modulus of PMMA: 2.24 – 3.24 GPa. This is sizeable difference with the value, which was determined with the stress-strain curve.

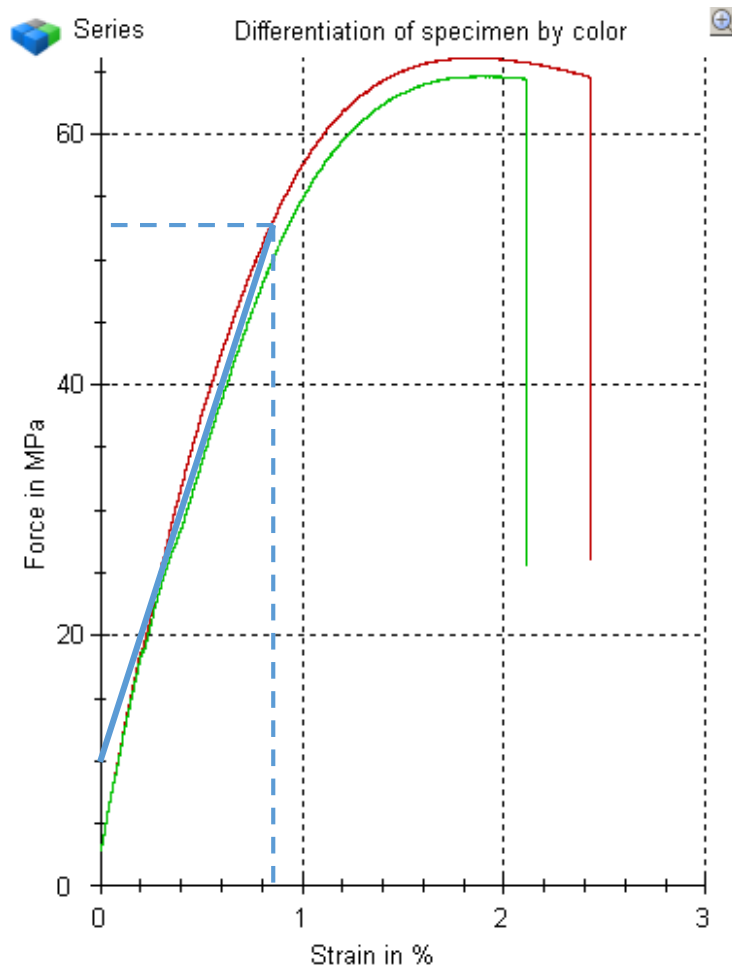


Figure 57: The resulting stress-strain curve with the elastic part highlighted in order to determine the young's modulus

2 Bonding

2.4 Health and Safety Measures

All containers for adhesives and auxiliary bonding agents are labeled in accordance with Directive 1999/45/EC.

When handling adhesives and additives together with PLEXIGLAS® GS and XT or other materials, it is necessary to take the measures provided for by Directive 1999/45/EC, the German Toxic Chemicals Ordinance (GEFStoffV), to observe the regulations for workplace safety and the prevention of accidents as well as all other generally acknowledged standards of safety engineering, industrial medicine and hygiene as well as proven ergonomic findings.

Most adhesives constitute a fire hazard.

The vapors they give off may form explosive mixtures with air. Open sources of heat (flames, electric radiators) and sparking (ignition sparks, static discharges) are to be avoided. Moreover, smoking, eating or drinking at the workplaces should be prohibited.

For workplaces and storerooms, the (German) statutory order on flammable liquids (VbF) is to be observed and for electrical installations in these areas, the (German) regulations VDE 0165 and VDE 0171.

Continuous inhalation of solvent vapors and frequent skin contact may have a mutually intensifying effect, thereby being detrimental to health and provoking allergies. Therefore, bonding work is to be performed in well-ventilated rooms without drafts.

Since the solvent vapors are heavier than air, extractors have to be installed at floor level. Where substantial quantities of adhesive are handled, an additional extractor at the workplace itself is recommended (see Fig. 18).

The ventilation system must be designed in such a way that the threshold limit value (TLV) is not exceeded. Gas detectors with special test tubes for different solvents are available for determining the TLV.

Solvents destroy the skin's protective sebaceous layer. Therefore, **skin contact with adhesives should be avoided.** Wipe

affected skin immediately with a cloth, then clean with soap and water (cleansing cream) and apply a skin barrier cream. It is also advisable to apply such a cream before starting to work.

Do not discard adhesive waste in an uncontrolled manner, but dispose of it by incineration according to the official regulations for waste or special waste (adhesives containing dichloromethane) or else by controlled landfill. Take up liquid spillage or leakage with absorbent material (sand, fuller's earth, expanded mica), store in special containers and dispose of in compliance with the regulations.

For more information on safety measures, the exclusion of health risks and disposal, see **our material safety data sheets (MSDS)**, which are automatically provided to our customers by authorized distributors of PLEXIGLAS® and ACRIFIX®.

2.5 Pre- and Post-Bonding Work

The quality of bonds between parts of PLEXIGLAS® depends to a large extent on the careful preparation of these parts, on the adhesive used, the auxiliary agents and the bonding technique.

Preparing the Workpieces

If possible, the preparation work should be conducted in this order:

- machining,
- cleaning,
- annealing, where required,
- covering the surrounding area with adhesive tape or coating it to protect against solvent attack or scratching
- wiping or degreasing the adherends.

Subsequent Measures

- Post-annealing, if necessary.

The "pre- and post-bonding" work in detail:

When **machining** PLEXIGLAS®, please consult our Guidelines for Workshop Practice, 'Machining PLEXIGLAS®', and observe our instructions to the letter. For roughing the sheet surface – advisable with PLEXIGLAS® GS in general and a must with crosslinked PMMA, e.g. PLEXIGLAS® GS 209/0Z09 and

sanitaryware material such as PLEXIGLAS® GS SW – use wet abrasive paper (grit 320 to 400).

For cleaning, use ionized air or preferably warm water containing some dishwashing liquid. Absorbent, non-linting cloth, e.g. glove-lining fabric is best suited for wiping the material dry. When using polymerization adhesives on PLEXIGLAS®, the adherends should be precleaned, or rather degreased, with ACRIFIX® CA 0030 just before applying the adhesive (to stress-free or annealed material!). This is best done by wiping the surfaces with soaked, undyed absorbent paper or a cloth (washed glove-lining fabric) soaked with ACRIFIX® CA 0030. This easily removes accidentally applied traces of adhesive from the PLEXIGLAS® surface ('stringiness') as long as they have not hardened. If solvent adhesives are used, the adherends must first be cleaned with petroleum ether or isopropyl alcohol.

Stress Test

Simple test methods with solvents are available for crystal-clear or not opaquely colored material. Although these methods do not indicate the exact internal stress level, they provide valuable information on the practical behavior of the items when brought into contact with certain solvents:

Another and absolutely non-destructive test for crystal-clear workpieces of PLEXIGLAS® is visual inspection between two **polarizing sheets**.

Although this does not provide the exact stress level either, you can pinpoint the stress areas via the location and shape of the emerging rainbow colors.

Annealing prior to bonding

serves to relieve stress and avoids cracking as a possible result of tensile stress in the presence of solvents contained in polymerization and solvent borne adhesives.

Crazing in the bond area reduces the adhesion and affects the appearance. Therefore, it has to be avoided at all costs. Stress is generated in all materials, including acrylics, during machining operations like sawing, routing, turning, sanding and polishing, as well as during thermoforming and cold curving. It may, however, also be the result of deformations in the parts

to be bonded, e.g. caused by weights, clips or G-clamps. Extruded profiles, and especially tubes, as well as injection-molded items are almost always internally stressed as a result of the cooling conditions. Heat treatment eliminates this stress. The annealing conditions described below depend on the heat deflection temperature under load and the stress level of the parts to be bonded.

Annealing after bonding

provides better curing of the joint with polymerization adhesives and thus leads

Annealing Conditions

Temperature (in the airflow oven):

- PLEXIGLAS® GS: 80 °C (unformed parts up to a maximum of 100 °C)
- PLEXIGLAS® XT: 70 to 80 °C (unformed parts up to a maximum of 85 °C)

Annealing Time

- PLEXIGLAS® GS and PLEXIGLAS® XT: The material thickness in mm divided by 3 is the annealing time in hours, but the minimum is 2 hours.

(3) COLORANT

(4) REACTION MODERATOR

(5) CATALYST

For good bonding results it is essential to **mix the adhesive composition very thoroughly**. Therefore the following hints must be observed:

- Make sure to skim the wall of the container and also to lift and plunge the stirring rod.
- For larger compositions use an electrically or pneumatically operated agitator. The diameter of the propeller or stirrer blade should be only slightly

Method	Workpieces made of	Test Medium	Procedure	Testing Time	Result	Remarks
Acetic ester test	PLEXIGLAS® GS PLEXIGLAS® XT PLEXIGLAS® FM	Acetic ester (ethyl acetate)	Immersion or wetting	6 min	<ul style="list-style-type: none"> • Crazes within testing time: too much stress • No crazes: part is ready for use. 	solvent acts destroying
Ethyl alcohol test	PLEXIGLAS® XT PLEXIGLAS® FM	Ethyl alcohol	Immersion or wetting	15 min		no solvent action

to greater adhesive strength and a good long-term appearance with crazes.

The precondition is that annealing is performed within 24 hours of bonding.

This also relieves stresses that may have been generated in the adhesive or the part to be joined during the bonding process and may cause subsequent damage in the material. The conditions described above for annealing prior to bonding with polymerization adhesives also apply to annealing after bonding.

Bonds between parts of more than 20 mm wall thickness should be gradually heated to the required annealing temperature, i.e. by no more than 10 °C per hour. With bonds whose formulation contains ACRIFIX® MO 0070, this stepwise heating should be performed even more slowly to prevent air entrapment in the joint and to enhance the chemical reaction.

When using solvent adhesives, there is an increased **risk of foaming** of solvent residues if heating is performed too quickly during post-annealing.

Cooling

- The cooling time in the oven in hours is the material thickness of PLEXIGLAS® in mm divided by 4. The cooling rate must not exceed 15 °C per hour.
- Upon removal from the oven, the temperature of the bonded PLEXIGLAS® part must not exceed 60 °C on any account.

Surface Protection

Sometimes it may be necessary to protect the area around the joint against solvent attack or scratching. This can be done with self-adhesive films of polyethylene or compatible adhesive tapes, or by applying liquid coating systems which can later be stripped off as films (e.g. 30% aqueous solutions of PVAL).

Preparing the Adhesive

No preparatory work is required when using solvent adhesives, adhesive solutions or one-component polymerization adhesives. In the case of two- and multi-component polymerization adhesives it is **very important to observe certain basic rules**:

The individual products should be mixed in the following order:

- (1) adhesive
- (2) THINNER or thickener

smaller than the diameter of the vessel.

- After mixing, the adhesive must be free from striation.
- Before applying the adhesive, remove the air pockets formed by stirring. To this end, leave the composition to stand for some time (observe the pot life); the air pockets will rise to the surface and disappear. Keep the vessel covered during this time to avoid skin formation on polymerization adhesives and contamination in general.

To speed up the process, put the covered container in a vacuum desiccator. Polymerization adhesives require a negative pressure of about 0.8 bar, in which case the absolute pressure is approx. 0.2 bar. The absolute pressure must never fall below this value, because otherwise the adhesive will foam due to evaporating monomer. Repeated ventilation of the vacuum vessel eventually causes the air pockets at the surface to burst.

Under no circumstances may the adhesive composition be prepared in the applicators (e.g. syringes), because they do not permit thorough mixing.

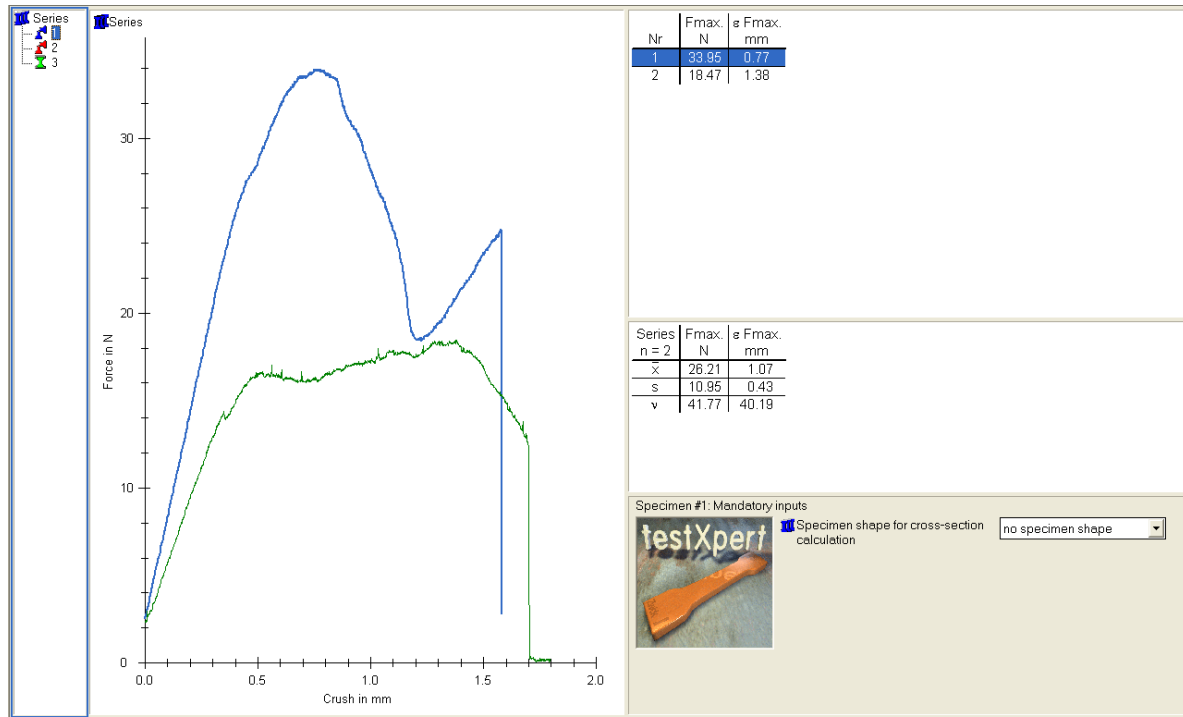
Appendix 6: Olympus LEXT Confocal laser scanning microscope

			Laser Scan	Universal	
Observation method			Laser	Laser, Laser confocal DIC, Brightfield, DIC	
Microscope stand	Illumination	Laser	408nm LD laser Class 2		
		White light	-	White LED illumination	
	Z stage	Vertical movement	70mm		
		Maximum height of specimen	100mm		
	Z revolving nosepiece	Stroke	10mm		
		Resolution	0.01 μ m		
Repeatability		3 σ =0.04+0.002L μ m			
Objective lens			5x, 10x, 20x, 50x, 100x		
Total magnification			120x~14400x		
Field of view			2560x2560~21x21 μ m		
Optical zoom			1x~6x		
Stage	Manual stage		100x100mm		
	Motorized stage		150x100mm		
Frame memory	Intensity		1024x1024x12bit		
	Height		1024x1024x16bit		
AF			Laser reflection type		
Dimensions			464(W)x559(D)x620(H)mm		
Weight			56.9kg	57.5kg	

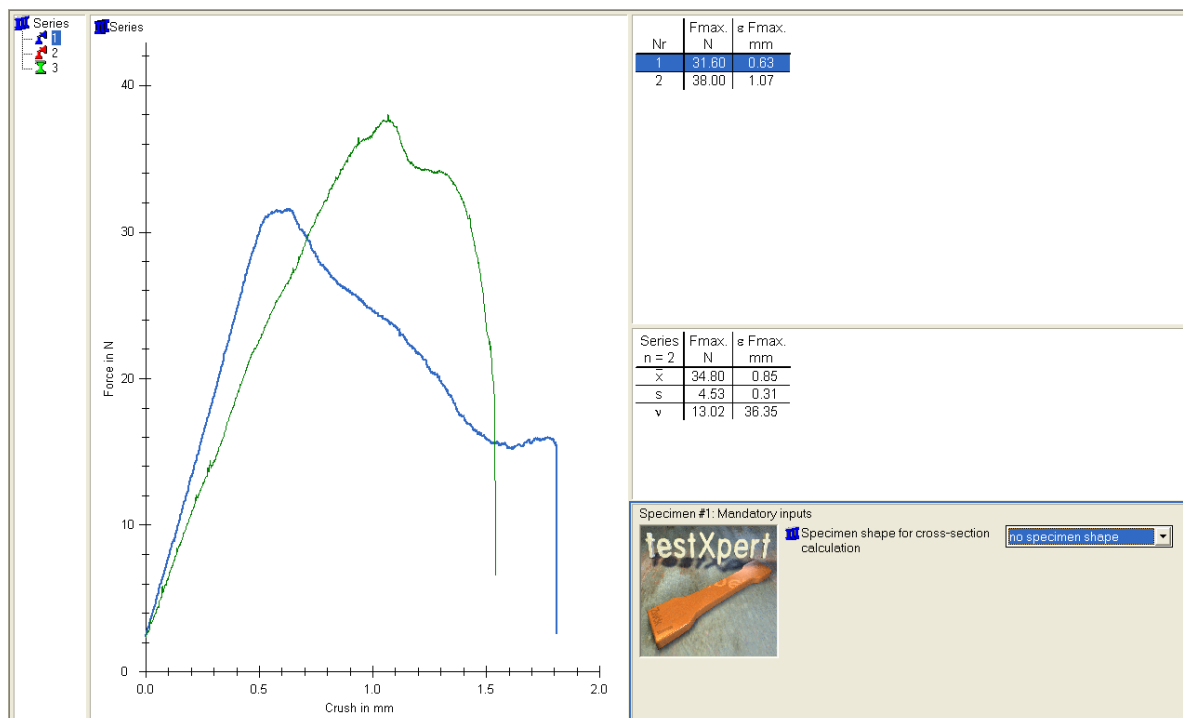
Figure 58: The technical specifications of the Olympus LEXT confocal Laser Scanning Microscope (source: <http://www.olympus-global.com/en/news/2007a/nr070125lect31e.jsp>)

Appendix 7: Resulting curves for the bonding tests

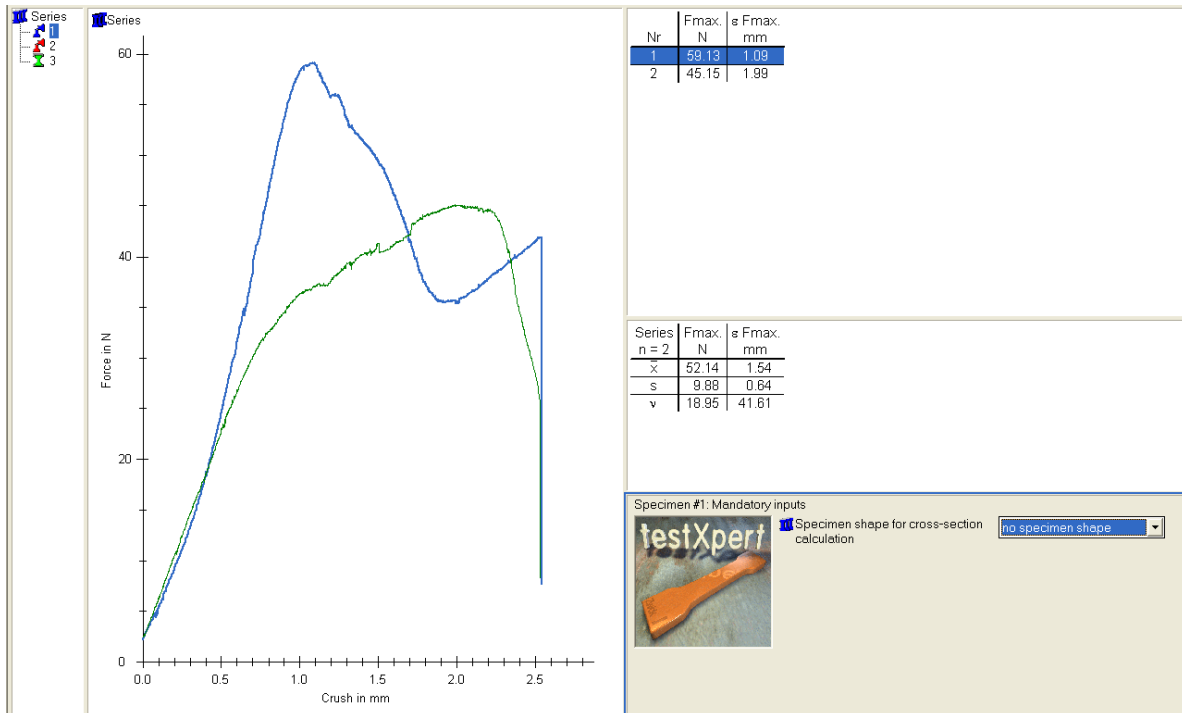
115 °C – 0.25 MPa – 30 minutes



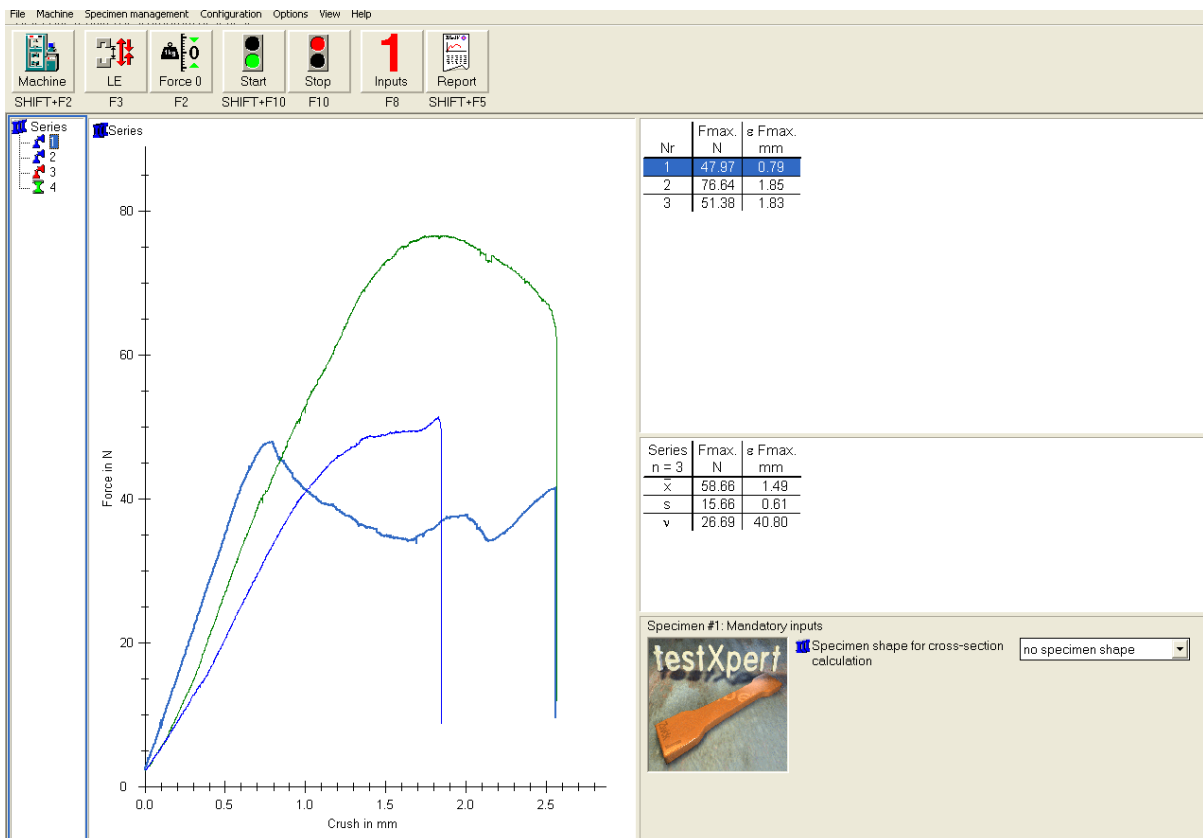
115 °C – 0.31 MPa – 30 minutes



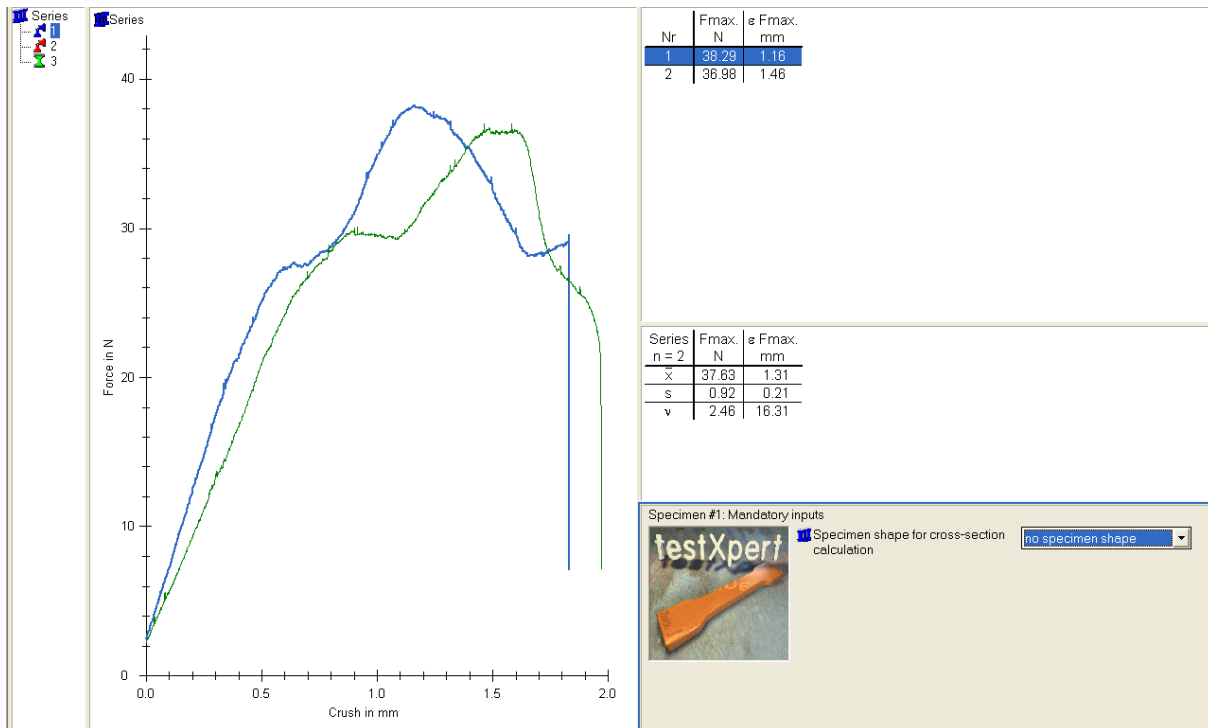
120 °C – 0.25 MPa – 30 minutes



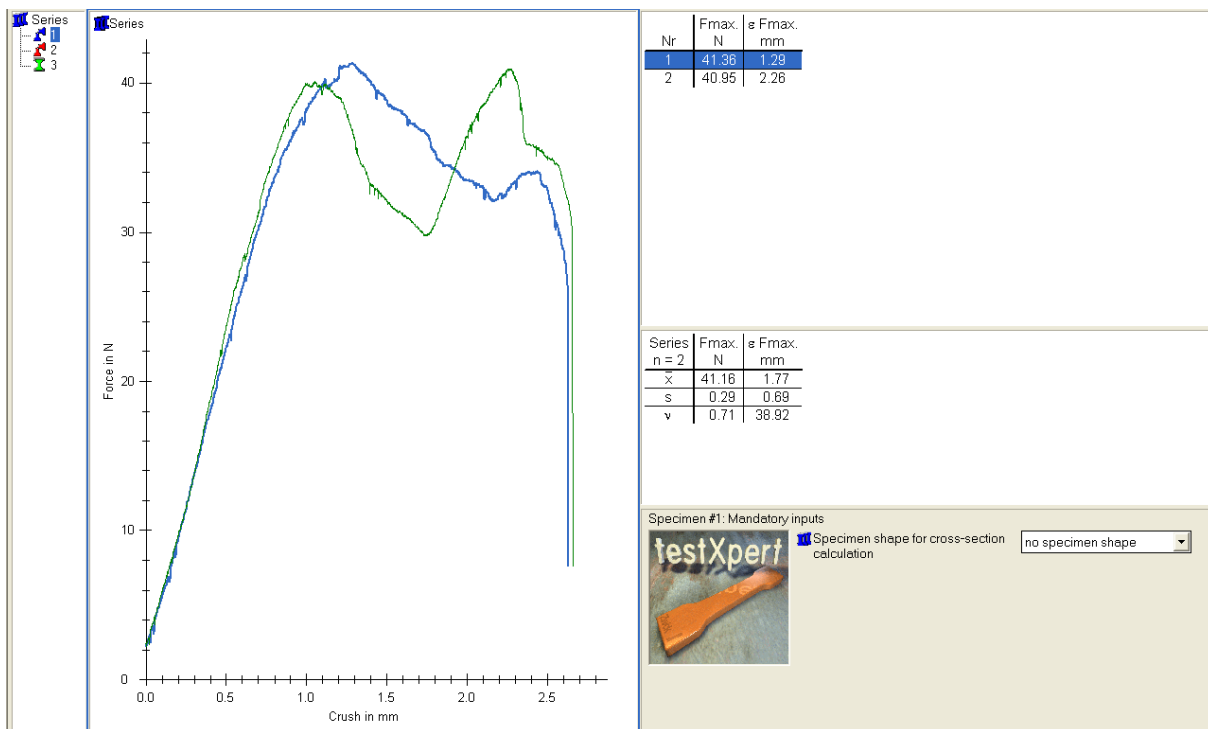
120 °C – 0.31 MPa – 30 minutes



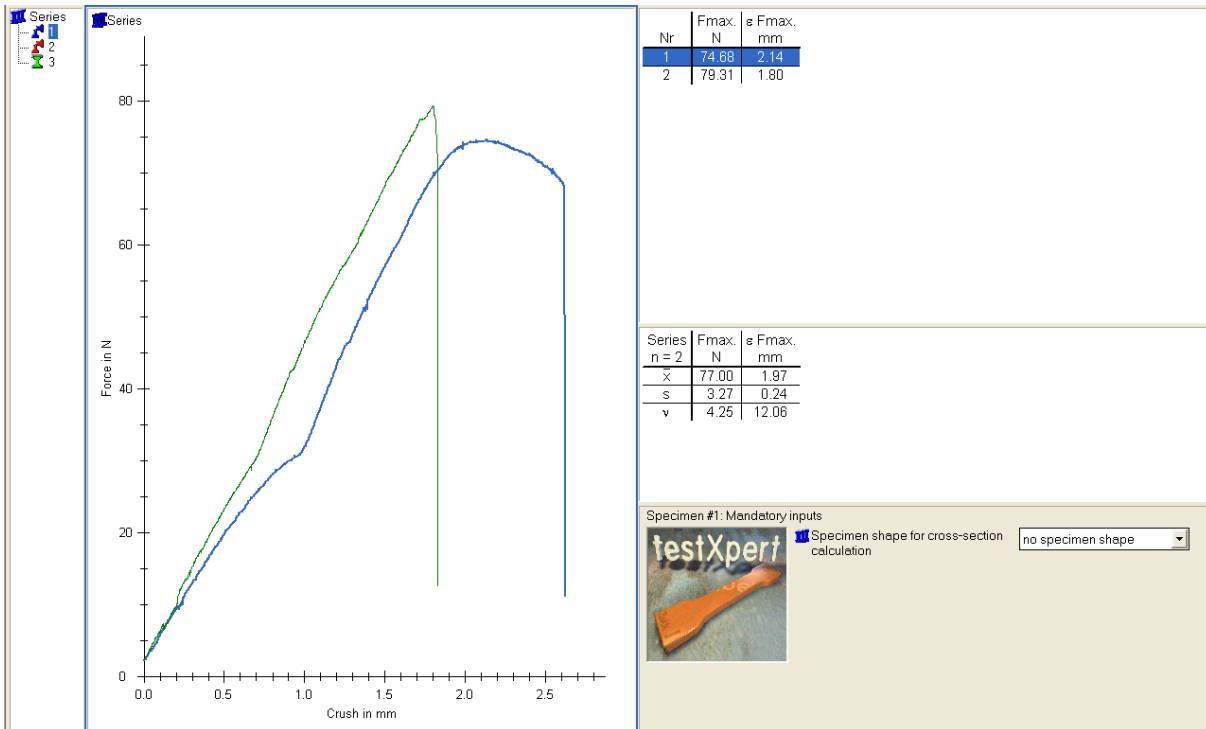
115 °C – 0.25 MPa – 60 minutes



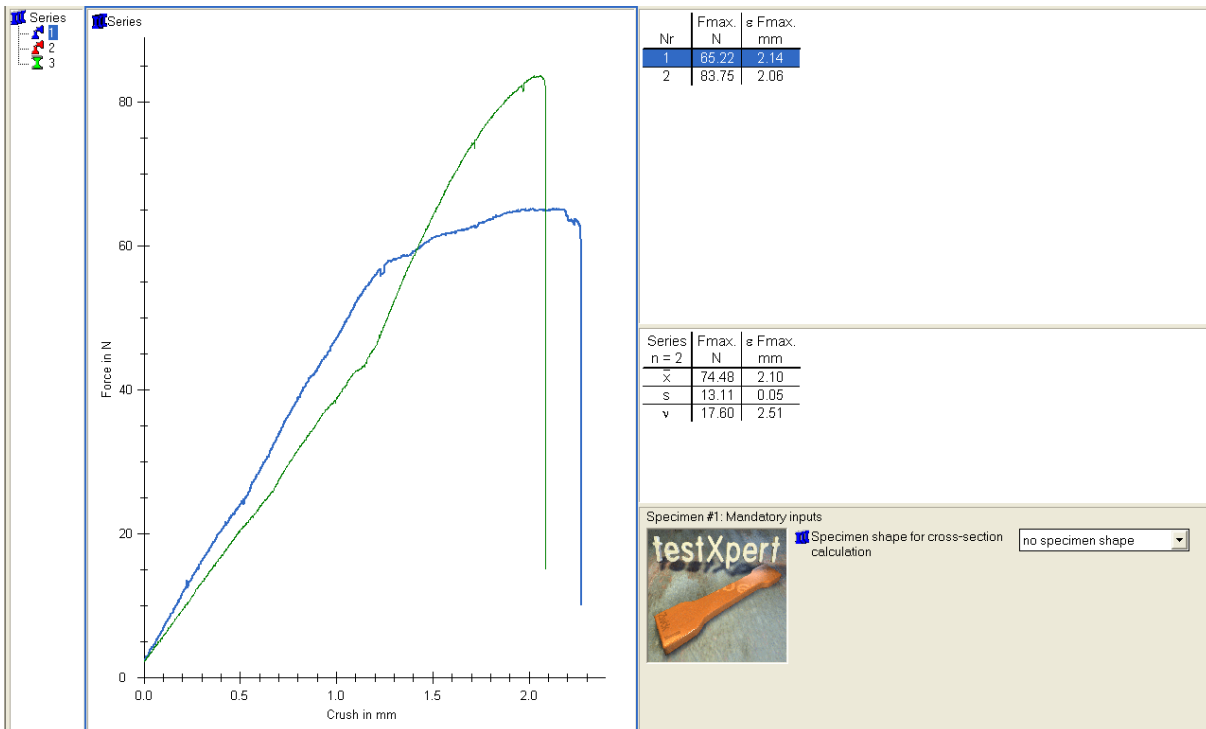
115 °C – 0.31 MPa – 60 minutes



120 °C – 0.25 MPa – 60 minutes



120 °C – 0.31 MPa – 60 minutes



Auteursrechtelijke overeenkomst

Ik/wij verlenen het wereldwijde auteursrecht voor de ingediende eindverhandeling:

Manufacture of lightweight (structured cellular) polymeric parts

Richting: **master in de industriële wetenschappen: elektromechanica**

Jaar: **2014**

in alle mogelijke mediaformaten, - bestaande en in de toekomst te ontwikkelen - , aan de Universiteit Hasselt.

Niet tegenstaand deze toekenning van het auteursrecht aan de Universiteit Hasselt behoud ik als auteur het recht om de eindverhandeling, - in zijn geheel of gedeeltelijk -, vrij te reproduceren, (her)publiceren of distribueren zonder de toelating te moeten verkrijgen van de Universiteit Hasselt.

Ik bevestig dat de eindverhandeling mijn origineel werk is, en dat ik het recht heb om de rechten te verlenen die in deze overeenkomst worden beschreven. Ik verklaar tevens dat de eindverhandeling, naar mijn weten, het auteursrecht van anderen niet overtreedt.

Ik verklaar tevens dat ik voor het materiaal in de eindverhandeling dat beschermd wordt door het auteursrecht, de nodige toelatingen heb verkregen zodat ik deze ook aan de Universiteit Hasselt kan overdragen en dat dit duidelijk in de tekst en inhoud van de eindverhandeling werd genotificeerd.

Universiteit Hasselt zal mij als auteur(s) van de eindverhandeling identificeren en zal geen wijzigingen aanbrengen aan de eindverhandeling, uitgezonderd deze toegelaten door deze overeenkomst.

Voor akkoord,

Drijkoningen, Daniel

Datum: **29/08/2014**